TÉCNICO LISBOA

Waste-to-Energy

Energy recovery from domestic wastewater

Eurico Yung Ferreira Moutinho

Thesis to obtain the Master of Science Degree in

Chemical Engineering

Supervisor: Dr. Diogo Miguel Franco dos Santos

Dr. Maria Margarida Pires dos Santos Mateus

Examination Committee

Chairperson: Prof. João Carlos Moura Bordado

Supervisor: Dr. Diogo Miguel Franco dos Santos

Members of the Committee: Dr. Luís Miguel de Almeida Amaral

Setembro de 2015

Acknowledgements

I would like to thank my supervisors, for the given opportunity to work on this internship, the contribution that helped to finish it and being able to write a paper from it.

To SIMTEJO, for providing the necessary effluent in order to proceed the study.

I am grateful to master David Cardoso for the helping he gave during this internship period.

" May the force be equal to
mass times acceleration, Harry
- Gandalf "
- Michael Scott

Abstract

This work focuses on water electrolysis studies, with ten different cathode materials, to find effective electrocatalysts to produce H_2 using an effluent from municipal wastewater treatment as a hydrogen source. Tests are done with or without the addition of electrolyte, being the electrolyte selected KOH. The study consists in applying cyclic voltammetry at different temperatures, ranging between 25 and 85 ºC and using the Tafel and Butler-Volmer scientific models to obtain the kinetic parameters. The electrodes used were the stainless steel 304 (SS304), platinum (Pt) and platinum-rare earth (Pt-RE) binary alloys, and nickel (Ni) and Ni-RE alloys, with the REs being cerium (Ce), samarium (Sm), dysprosium (Dy), and holmium (Ho). It was possible to conclude that, the addition of KOH improves considerably the efficiency of the electrochemical process. The activation energy obtained with a Ni electrode with KOH addition was 228kJ mol^{-1}. It was also made a study of the anodic reaction with Pt electrodes.

Cyclic voltammetry and chronoamperometry were also performed in a study involving electrolysis of synthetic urine, using Pt and Ni electrodes.

Keywords: Energy; Environment; Hydrogen; Wastewater.

Resumo

Este trabalho centra-se na aplicação da electrólise, com a utilização de dez cátodos de diferentes materiais de forma a encontrar electrocatalisadores eficientes na produção de H_2, sendo usado como fonte do hidrogénio o efluente proveniente de uma ETAR, com ou sem adição de um electrólito, sendo o electrólito escolhido o KOH. O estudo consiste na aplicação de voltametria cíclica a uma velocidade de varrimento de 0.5 mV/s, a diferentes temperaturas que variam entre 25 e 85ºC. Utilizaram-se os métodos de Tafel e de Butler-Volmer para obtenção dos parâmetros cinéticos. Os eléctrodos usados para este trabalho foram o aço-inox 304 (SS304), a platina (Pt) e platina-terra raras, e o níquel (Ni) e níquel-terras raras (Ni-RE), com as RE a serem o cério (Ce), samário (Sm), disprósio (Dy) e o hólmio (Ho). Verificou-se que a adição do KOH melhora consideravelmente a eficiência do processo electroquímico. A energia de activação obtida com o eléctrodo do Ni no efluente com adição de KOH foi de 228 kJ mol^{-1}. Foi feito também um pequeno estudo sobre a reacção anódica com o eléctrodo de Pt.

Analisou-se também a electrólise de uma solução de urina sintética, aplicando voltametria cíclica a várias velocidades de varrimento e cronoamperometria a diferentes potenciais, utilizando eléctrodos de Pt e Ni.

Palavras-chave: Energia; Ambiente; Hidrogénio; Águas residuais.

Table of Contents

List of figures

List of tables

Lists of symbols, abbreviations or other

α	- Charge transfer coefficient
η	- Overpotential
A	- Amperes
BDD	- Boron doped diamond
BOD	- Biochemical oxygen demand
CA	- Chronoamperometry
C_i^*	- Bulk concentration of species i
COD	- Chemical oxygen demand
CV	- Cyclic voltammetry
D_i	- Diffusion coefficient of species i in water
E	- Potential of an electrode (versus a reference)
E_a	- Activation energy
E_p	- Peak potential
$E_{p1/2}$	- Half-peak potential
E_0	- Standard potential of an electrode
F	- Faraday's constant
HER	- Hydrogen evolution reaction
ICE	- Instantaneous current efficiency
i	- Current
j	- Current density
j_0	- Exchange current density
mV/s	- millivolts per second
n	- Number of electrons involved in an electrode reaction
n_a	- Number of exchanged electrons in the rate determining step
OCP	- Open circuit potential
OER	- Oxygen evolution reaction
R	- Universal gas constant
RE	- Rare-earth
t	- Time
T	- Temperature
TOC	- Total organic compounds
ν	- Scan rate (mV/s)
V	- Volts

1. Introduction

In the last years, the clean water resources are scarce because of the increase of the industrial and agriculture activities caused by the world population growth and technology advances. In order to resolve this problem, there is some interest in developing the water treatments techniques for the possibility of reusing the domestic and industrial wastewaters. The organic compounds in wastewaters are the main pollutants. They are extremely toxic and constitute a serious problem to environment and human health. One of the solution for the water resource problem is a technology, invested by Bill Gates[1], which consists in obtaining water by boiling the sewer sludge in a chamber. The water vaporizes and the dry sludge goes to a furnace were will produce energy.

On this context, the electrochemical technology has been shown to be a good alternative to eliminate the organic pollutants present in the wastewaters. The electrochemical processes are being developed in order to treat the organic compounds in the wastewaters because of its advantages, such as environmental compatibility, versatility, energy efficiency, safety and cost. The organic compounds degradation process is basically based on the production of OH ions, from the electrolysis of water, which will oxide the organic molecules producing CO_2.

The most common technique, for this electrolysis process, is the Fenton reaction with the help of UV exposition and/or the use of electrolytes that increase the current density, such as NaCl and Na_2SO_4[2-4]. On this technique the hydroxide ions production can be described by the following processes.

$$Cl^- + H_2O \rightarrow HClO + H^+ + 2e^- \qquad \textit{Eq. 1}$$

$$HClO \leftrightarrow ClO^- + H^+ \qquad \textit{Eq. 2}$$

$$O_2 + 2H^+ + 2e^- \rightarrow H_2O_2 \qquad \textit{Eq. 3}$$

When the hydrogen peroxide is electrochemically produced on the cathode, the use of iron as anode can promote Fenton's reaction.

$$Fe^{2+} + H_2O_2 \rightarrow Fe^{3+} + OH^- + OH^* \qquad \textit{Eq. 4}$$

The use of iron anodes combined with the production of hydrogen peroxide, not only promotes the Fenton's reaction, but also promotes coagulation of soluble and insoluble iron complex. This makes the iron anode an electrode with a short lifespan.

Another interesting scientific topic that has been discussed in the last few years is the possibility to collect and store energy in a clean and safe form, and hydrogen is considered to be a strong candidate for that energy source. In this work, several electrochemical processes have been considered in a way that, with the degradation of the organic compounds, it would be possible to also produce hydrogen. This allows the energy costs be reduced and make more viable the wastewater treatment by electrolysis.

What will make possible to use this electrochemical process, is the choice of the electrode material that must have specific physical properties like chemical stability, corrosion resistance, good electrical conductivity, catalytic activity and a good cost/lifespan ratio.

A good hydrogen production efficiency from the chemical oxidation of the pollutants can be obtained by using an electrochemically active anode that has high oxygen evolution reaction (OER) rate. The anodic electrodes with high OER that are commonly used are based in SnO_2, PbO_2, RuO_2, IrO_2 and BDD (Boron Doped Diamond) [5-8]. They have high efficiency for the organic compound oxidation, combined with inert metals/metal oxides like Ti, Pt, TiO_2 and Ta_2O_5, which add a greater corrosion resistance and electrocatalytic activity. But since these materials have high costs, its commercial applications are very limited.

Cho et al. [6], tried to eliminate the organic compounds (in this case human urine) and at the same time produce hydrogen using BiO_X/TiO_2 anodes in NaCl electrolyte solution. A cell potential of 3V was applied and formation of foam was observed, caused by the liberation of oxygen and hydrogen with proteins. With this material it was possible to get a potential on the anode lower than that obtained with IrO_2 or RuO_2 based electrodes. On the other hand, there was formation of the chlorine complex because of the presence of the chloride ions. The values of chemical oxygen demand (COD) analysis did not change much before and after the treatment, because of the decomposition of the high molecular weight organic compounds into only small compounds. On the cathode side (stainless steel) it was observed a formation and precipitation of $CaCO_3$ and $Mg(OH)_2$.

Ma et al. [3], studied phenol as the organic pollutant, using Ti/IrO_2-RuO_2 as anode, and a potential of 3V, using Na_2SO_4 as the electrolyte and the hydrogen is formed mainly from the protons of the organic compound. Na_2SO_4 improves the hydrogen production better than NaCl and has the advantage of not producing the chlorate complex. During the degradation of phenol by electrochemical oxidation, three stages of the process were observed, and each stage represents different rates of phenol degradation and hydrogen production, showing different instantaneous current efficiency (ICE) for the COD removal. On the first stage, the ICE and the hydrogen production rate increased slightly; on the second stage the ICE raises and the hydrogen production rate fell dramatically; and on the third stage the ICE value fell and the hydrogen production rate increased indicating that the water started to have more participation on the hydrogen production. In this work the COD removal efficiency was about 90% and the degradation process can be better explained on Fig. 1. The protons released from the phenol and organic intermediates through electrochemical oxidation degradation process, can form hydrogen molecules in cathodic reactions.

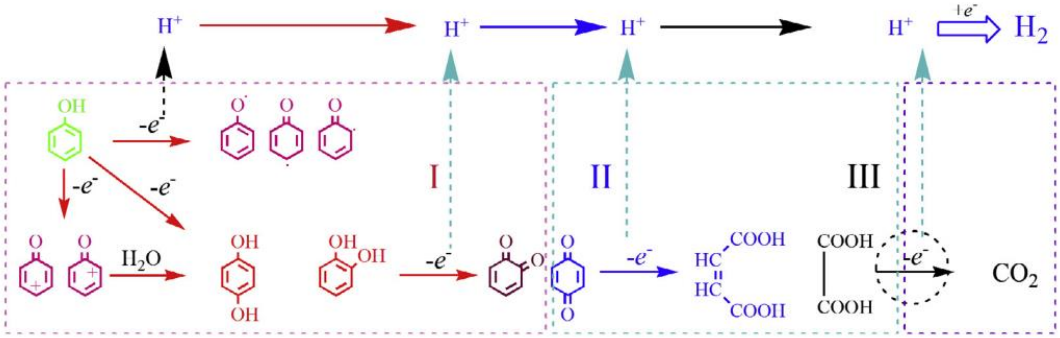

Fig. 1 - Example of hydrogen production mechanism from electrochemical oxidation of an organic compound (phenol)[3]

Considering the cathode, where the molecular hydrogen is formed, the materials that have been used are stainless steel, platinum, aluminium and nickel. The hydrogen production by electrolysis is known as hydrogen evolution reaction (HER) and can have a high or low efficiency depending on the electrocatalytic activity and the contact superficial area of the electrode. The reaction mechanism can be explained from Volmer's (Eq. 5), Heyrovsky's (Eq. 6) and Tafel's (Eq. 7) electrochemical reactions, were the hydrogen atoms are adsorbed by the electrode's metal and after that the molecular hydrogen are formed.

$$H^+ + e^- \rightarrow H_{ads} \qquad \textit{Eq. 5}$$

$$H_{ads} + H^+ + e^- \rightarrow H_2 \qquad \textit{Eq. 6}$$

$$2H_{ads} \rightarrow H_2 \qquad \textit{Eq. 7}$$

According to recent articles focused on the hydrogen production, there have been attempts to develop catalysts to improve the efficiency of HER, preferably with materials that are more abundant on earth. One of those materials is the nickel complex (Fig.2)[9], which was tested with water and acetic acid, and according to the literature this complex has been able to catalyse the proton reduction into H_2 in any pH range, making possible to produce about 547 mol of hydrogen per hour per mol of catalyst on pH 5 and 302 mol of hydrogen per hour per mol of catalyst on pH 8 and in any case it was not shown decomposition of the catalyst.

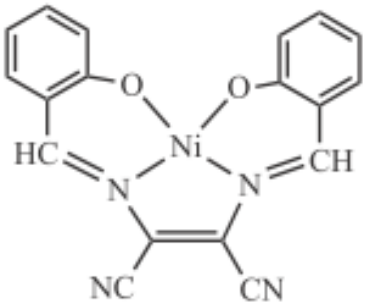

[NiL]

Fig. 2 - Schematic representation of the complex [NiL]

Another catalyst/mediator that was studied recently is the silicotungstic acid[10], which is able to produce hydrogen with a rate 30 times faster than if it was simply used with the platinum electrode. Its performance can be seen on Fig. 3.

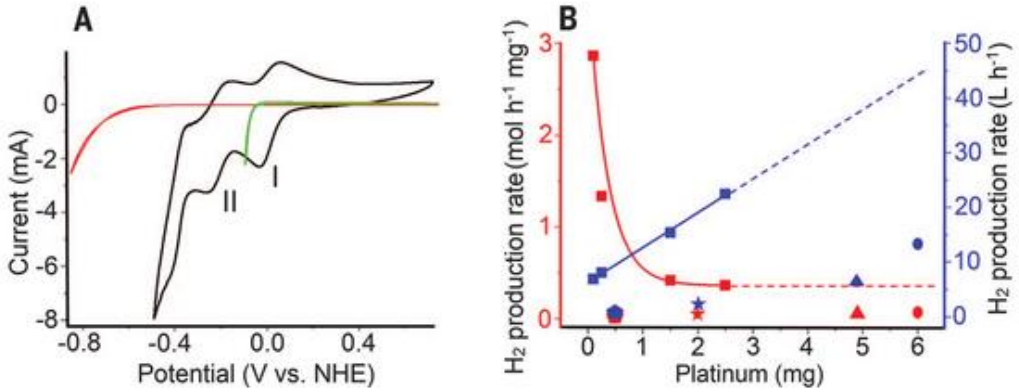

Fig. 3 - Performance of silicotungstic acid as electrochemical mediator[10]. (A) Reductive CVs: black, $H_4[SiW_{12}O_{40}]$ in water (0.5 M, pH 0.5); red, 1 M H_3PO_4 (pH = 1.0); green, 1 M H_3PO_4 (pH = 1.0) on a Pt disc working electrode. (B) Comparison of the rate of H_2 production. Square symbols indicate data obtained by silicotungstic acid. Red data (left-hand y axis): the rate of H_2 production per milligram of Pt. Blue data (right-hand y axis): the absolute rate of H_2 production determined for H_2 production from $H_6[SiW_{12}O_{40}]$.

1.1. Objectives

The main objectives are analysing the feasibility of electrochemical treatment of domestic wastewaters, by using cyclic voltammetry on effluents samples, with different electrodes at different temperatures. Several kinetic parameters are determined, such as transfer coefficient, α, and exchange current, j_0, on order to achieve a lower consumption of energy for hydrogen production, as compared with the electrolysis of pure water.

2. Introduction to electrochemistry

Electrochemistry is the study of electricity and its relation with chemical reactions that take place in the interface of an electrode and of an ionic conductor, the electrolyte. These reactions involve the transfer of electrons between the electrode and a species in the electrolyte creating a change on the oxidation state of such element. This type of reaction is called redox (reduction-oxidation) reaction. The

oxidation of a species is when one of its electrons is lost and the reduction is when a electron is gained.[11,13,14] For example, for the redox reaction given in Eq. 8:

$$H_2 + F_2 \rightarrow 2HF \qquad \textit{Eq. 8}$$

The partials equations for the oxidation and reduction are given by Eq. 9 and Eq. 10 respectively.

Oxidation: $H_2 \rightarrow 2H^+ + 2e^-$ *Eq. 9*

Reduction: $F_2 + 2e^- \rightarrow 2F^-$ *Eq. 10*

To understand electrochemistry, it is necessary to consider five important interrelated concepts:

- The electrode's potential determines the analyte's form at the electrode's surface;
- The concentration of analyte at the electrode's surface may not be the same as its concentration in bulk solution;
- In addition to the redox reaction, the analyte may participate in other reactions;
- Current is a measure of the rate of the analyte's oxidation or reduction;
- We cannot simultaneously control current and potential.

The measurements in electrochemistry are made in a device called electrochemical cell that consists in two conductive electrodes. The potential of one electrode is sensitive to analyte's concentration and is called the working electrode. The second electrode is the auxiliary electrode that completes the electric circuit. Another electrode is generally used called the reference electrode, which provides a reference potential against the working electrode's potential.

Since it is not possible to simultaneous control the current and the potential, there are two basic experimental designs that can be used:

- measure the potential while controlling the current;
- measure the current while controlling the potential. [12]

Some basic concepts in electrochemistry are defined in the next sections.

2.1. Potentiometer & Potentiostat

A potentiometer is an equipment used to measure the potential of an electrochemical cell. The potentiometer consists on a power supply, an electrochemical cell with a working, reference and auxiliary electrodes, an ampere-meter for measuring the current, a slide-wire resistor and a tap key for closing the circuit through the electrochemical cell.

A potentiostat is an equipment that makes possible to control the potential of the working electrode. The potential of the working electrode is measured relative to a reference electrode that is connected to the working electrode through a high-impedance potentiometer. It can also be used as a galvanostat, in which case it is used to control the current that passes through the circuit. Both equipments are represented on Fig. 4. [12]

Fig. 4 – Potentiostat/Galvanostat Princeton Applied Research/EG&G Model 273A (left) and Digital Potentiometer Dual Channel model DP002 (right).

2.2. Electrolytic cell

It is an electrochemical cell that consists on a recipient with the electrodes placed inside where an external supplied electric current is used to drive a chemical reaction that would not occur spontaneously.[12]

2.3. Reference electrodes

The ideal reference electrode is one that provides a stable and known potential so that any change in cell potential is attributed to analyte's effect on the potential of the working electrode. There are three common reference electrodes that are preferably used, because they are easy to make and to use.[12-14]

2.3.1. Standard hydrogen electrode

It is the reference electrode used to establish standard-state potentials. The value of the standard electrode potential is zero, which forms the basis one needs to calculate cell potentials using different electrodes or different concentrations. This electrode is composed of a platinum electrode immersed in a solution of 1 M H^+ in which the activity of hydrogen ions is 1 and the fugacity of the hydrogen gas is 1 (Fig. 5). This electrode starts with an initial discharge to allow electrons to fill into the highest occupied energy level of Pt. As this is done, some of the H+ ions form H_3O^+ ions with the water molecules in the solution. These hydrogen and hydronium ions then get close enough to the Pt electrode (on the platinized surface of this electrode) to where a hydrogen is attracted to the electrons in the metal and forms a hydrogen atom. Then these combine with other hydrogen atoms to create $H_2(g)$. This hydrogen gas is released from the system. In order to keep the reaction going, the electrode requires a constant flow of $H_2(g)$. [12-14]

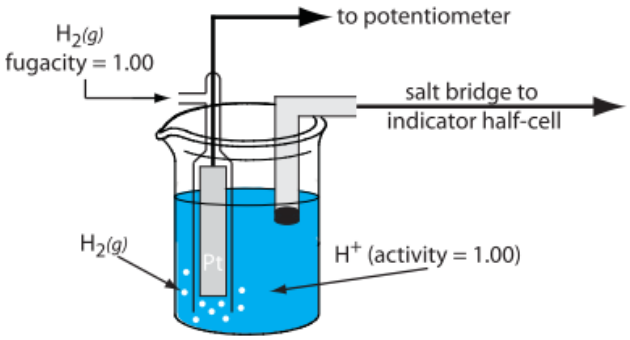

Fig. 5 - Schematic diagram showing the standard hydrogen electrode.

2.3.2. Calomel electrode

This reference electrode is based on the redox couple between Hg_2Cl_2 and Hg (Fig. 6).

$$Hg_2Cl_2(s) + 2e^- \leftrightarrow 2Hg(l) + 2Cl^-(aq) \qquad \textit{Eq. 11}$$

The potential of a calomel electrode is determined by the activity of Cl^- in equilibrium with Hg and Hg_2Cl_2. The concentration of Cl^- is determined by the solubility of KCl. Because the concentration of Cl^- is fixed by the solubility of KCl, the potential of the calomel electrode remains constant even if some of the solution is lost by evaporation. The main disadvantage of this electrode is that the solubility of the KCl is dependent with the temperature. At higher temperatures the solubility of KCl increases and the electrode's potential decreases. The potential can be less dependent with the temperature if the electrode contains an unsaturated solution of KCl, but it can change if the concentration increases due to evaporation. [12-14]

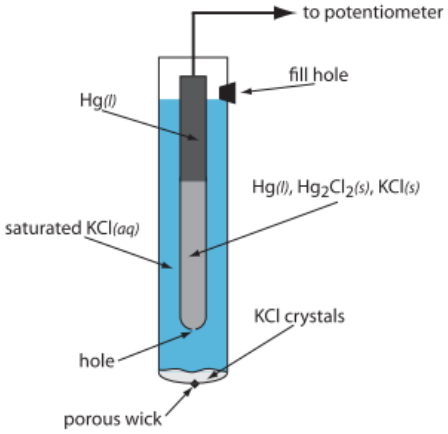

Fig. 6 - Schematic diagram showing the saturated calomel electrode.

2.3.3. Silver/silver chloride electrode

Another common reference is the silver/silver chloride electrode (Fig. 7) that is based on the redox couple between AgCl and Ag:

$$AgCl(s) + e^- \leftrightarrow Ag(s) + Cl^-(aq) \qquad \textit{Eq. 12}$$

Just like the case of the calomel, the activity of the Cl^- determines the potential of this electrode. This a widely used reference electrode because it is inexpensive and not as toxic as the calomel electrode which contains mercury. A silver/silver chloride electrode is made by taking a wire of solid silver and coating it in AgCl. Then it is placed in a tube of KCl and AgCl solution. [12-14]

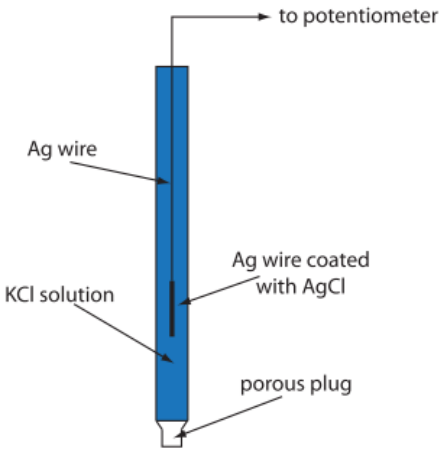

Fig. 7 - Schematic diagram showing an Ag/AgCl electrode

2.4. Open Circuit Potential

The open circuit potential (OCP) is the potential of the working electrode relative to the reference electrode when no potential or current is being applied to the cell. By measuring the OCP it is possible to determine the ratio of [O] to [R], considering the reaction $O + ne^- \rightarrow R$, through the use of the Nernst equation: [12-14]

$$E = E_0 - \frac{RT}{nF} ln\left(\frac{[R]}{[O]}\right) \qquad \textit{Eq. 13}$$

2.5. Cyclic voltammetry

CV is a measurement technique that applies a linear voltage scan in both positive and negative directions. One of the principal uses of cyclic voltammetry is to study the electrochemical behaviour of compounds. A current peak in the CV diagram means that a certain electrochemical process is triggered by passing the corresponding voltage. A peak shift between positive and negative scan is measure for the reversibility of the electrochemical process. On a CV it can be used different scan rates and each one can get a curve with the same form, but with the difference that the total current increases with increasing scan rate. This difference is explained with the size of the diffusion layer on the electrode surface, in slower rates the diffusion layer grows further from the electrode and consequently the flux to the electrode surface is considerably smaller in comparison with faster rates. Fig. 8 shows the cyclic voltammogram for the redox at both a faster and a slower scan rate. On reversible electron transfer reaction, peaks appear on the voltage whatever the scan rate, but for cases that is not reversible, there is a different behaviour where peaks vary as a function of the scan rate. By analysing the variation of peak position as a function of scan rate it is possible to gain an estimate for the electron transfer rate constants. [12-14]

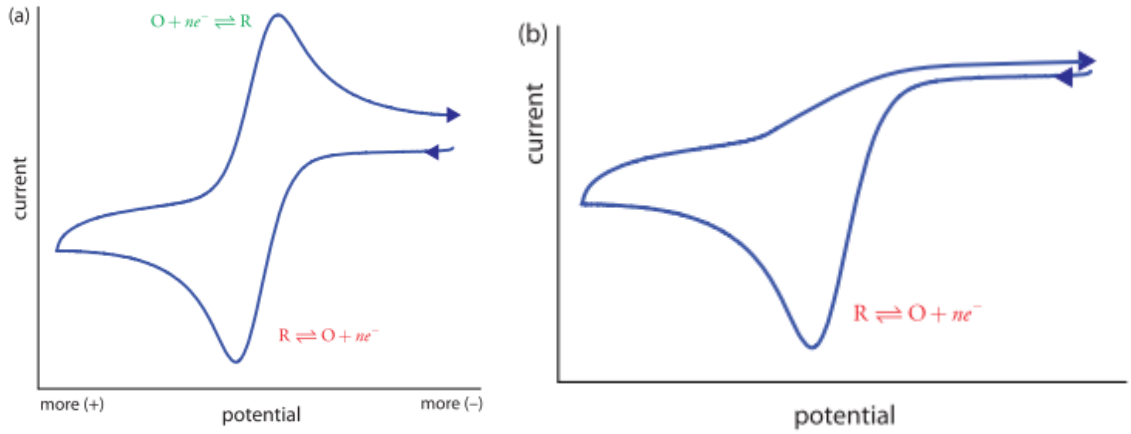

Fig. 8 - Cyclic voltammograms for R at (a) a faster scan rate and (b) a slower scan rate.

2.6. Chronoamperometry

Amperometry defines the whole of electrochemical techniques in which a current is measured as a function of an independent variable that is, typically, time or electrode potential. Chronoamperometry, is a technique in which the current-time behaviour of an electrochemical system is observed after a potential step in a still solution. On Fig. 9A, considering a system where species O is electrochemical inactive at E_i and the potential of the electrode is stepped to E_f, O is reduced in a simple charge transfer reaction. On Fig. 9B, the current is due to the diffusion of O toward the electrode.[12]

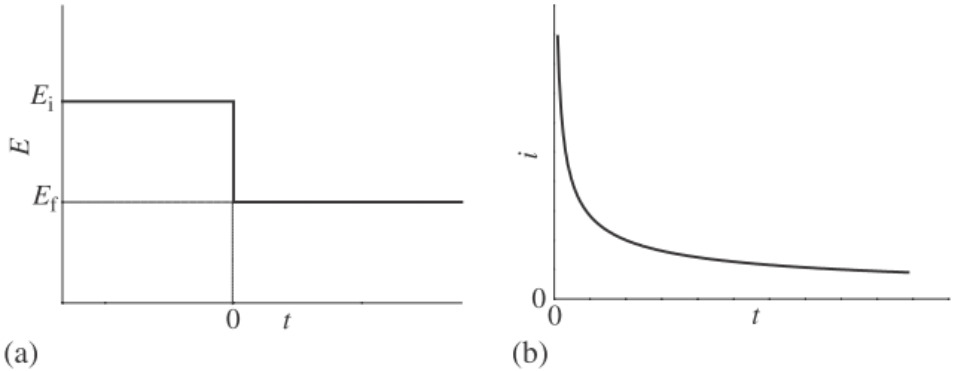

Fig. 9 - Potential step experiment to a planar electrode: (a) Potential waveform, (b) current response.

2.7. Exchange current density

A current density, j, is the electric current that passes the system, normally measured in amperes per unit area cross section.

The exchange current density, j_0, is an important parameter used, for example, in the Tafel equation and Butler-Volmer equation. It corresponds to the current where the forward and reverse reactions are at equilibrium state. Basically is a background current to which the net current observed at various overpotentials is normalized, being, for the present case, one of the most important variables that explain the large differences in the rate of hydrogen evolution reaction on metallic surfaces. Table 1 shows j_0 values for different metals in a 1M H_2SO_4 solution, where palladium shows to be the better metal for hydrogen evolution reaction, while the mercury is the worst. [11]

Table 1 - Comparison of j_0 for hydrogen evolution reaction in 1 M H_2SO_4[14]

Electrode material	$-\log_{10}(j_0\ (A/cm^2))$
Palladium	3.0
Platinum	3.1
Rhodium	3.6
Iridium	3.7
Nickel	5.2
Gold	5.4
Tungsten	5.9
Niobium	6.8
Titanium	8.2
Cadmium	10.8
Manganese	10.9
Lead	12.0
Mercury	12.3

2.8. Butler-Volmer equation

Butler-Volmer equation is an activation controlled reaction; it describes how the current on a given electrochemical cell depends on the electrode potential. This gives rise to electrode kinetics that are described by Eq. 14.

$$j = j_0 \left\{ e^{\frac{(1-\alpha)nF}{RT}\eta} - e^{-\frac{\alpha nF}{RT}\eta} \right\} \qquad \textit{Eq. 14}$$

While the Butler-Volmer equation is valid over the full potential range, simpler approximate solutions can be obtained over more restricted ranges of potential. As overpotentials, either positive or negative, become larger than about 0.05 V, the second or the first term of equation becomes negligible, respectively. Hence, simple exponential relationships between current and overpotential are obtained or can be considered as logarithmically dependent on the current density. This theoretical result is in agreement with the experimental findings of the German physical chemist Julius Tafel (1905), and the usual plots of overpotential versus log current density are known as Tafel lines.

Another simpler approximate solution can be obtained with a low overpotential region known as polarization resistance, where the η has a value inferior than 0.05 V making the product between this variable and F/RT inferior to 1 and since the exponentials can be simplified in the form of

$$e^x = 1 + x + \frac{x^2}{2!} + \cdots \qquad \textit{Eq. 15}$$

The equation becomes

$$j = j_0 \left\{ 1 + (1-\alpha)\frac{nF}{RT}\eta + \cdots \right\} \qquad \textit{Eq. 16}$$

And by simplifying and rearranging the equation we can get an approximate version in the form of

$$j = j_0 \frac{nF}{RT}\eta \qquad \textit{Eq. 17}$$

The points that are normally used for the calculation of this low overpotential form of the Butler-Volmer equation are the first 30-50 mV of η measured in the voltammetry, as can be shown in the example Fig. 10 where the points can be seen between the red marks. [11]

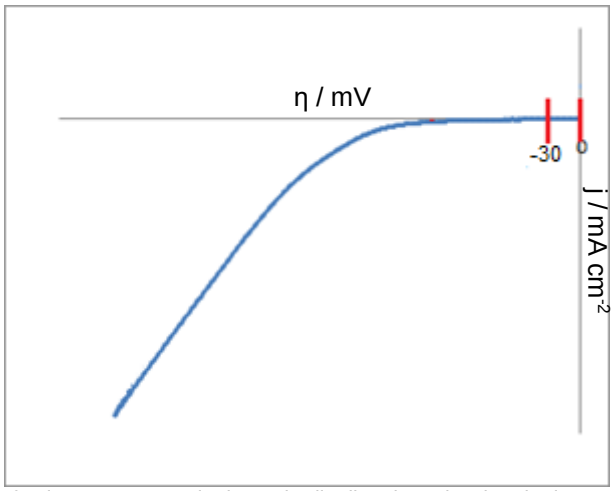

Fig. 10 - Example of voltammetry scan in the cathodic direction, showing the low overpotential region.

2.9. Tafel equation

It is an equation that relates the rate of an electrochemical reaction to the overpotential and it can be written in a very simple form as

$$\eta = a + b \times log|j| \qquad \textit{Eq. 18}$$

It is used for the kinetics of a "single electrode process" involving a generic number n_a of electrons in a single rate-determining step (rds) and the value of n_a is normally 1, Where *a* and *b* are constants that can be obtained from a graphic representation of η vs log | j | known as Tafel plot. This equation is normally used on high overpotential (typically between 100-300 mV) and the Tafel slope can be used to calculate the change transfer coefficient, α. Tafel plots can also be used to calculate the exchange current density, j_0, from the y-intercept of the Tafel regions.

$$b = \frac{2.3RT}{\alpha n_a F} \qquad a = \frac{2.3RT}{\alpha n_a F} log|j_0| \qquad \textit{Eq. 19}$$

For a reduction and oxidation process, the relevant equations for the calculation of the α and j_0 are given by Eq. 19 and Eq. 20.

$$b = \frac{2.3RT}{(1-\alpha) n_a F} \qquad a = \frac{2.3RT}{(1-\alpha) n_a F} log|j_0| \qquad \textit{Eq. 20}$$

The chosen region to use for the calculation of the Tafel plot is where the curve starts to in the graphic and where it ends, like in the Fig. 11. With this, it is possible to construct the graphic of η vs. log j similar to Fig. 12. [11]

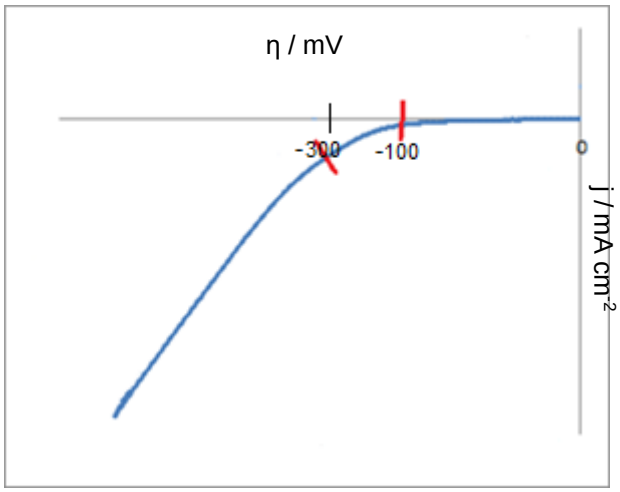

Fig. 11 - Example of reduction region of voltammetry showing Tafel region.

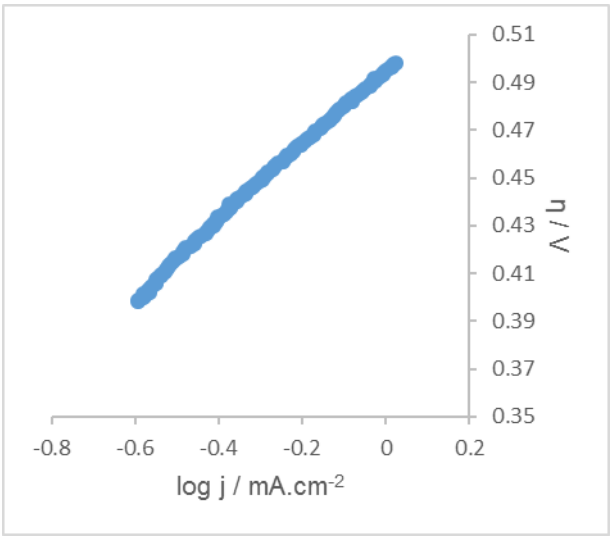

Fig. 12 - Example of Tafel plot (η vs. log j).

3. Municipal wastewater characterisation

It's impossible to avoid the production of waste originated by human activity and great part of it will end up in wastewaters. The quantity and quality of wastewater depends on many factors, since not all humans and industries produce the same amount of waste. The design of a sewer system also influences significantly the characteristics of the wastewater. Most developed countries use separate sewer systems and some countries combine different sewer systems mixing different types of wastewater. The daily or yearly polluting load may form a good basis for evaluating of the composition of a wastewater.

The composition of typical municipal wastewater is shown in Table 2. Like domestic houses, there are some industries that also produce wastewaters from their process and the Table 3.2 shows the

composition of two different wastewaters from different origins. A municipal wastewater normally consists of microorganisms such as bacteria and virus, biodegradable organic materials, detergents, pesticides, nutrients, inorganic materials, strong odour and even some radioactivity[0]. Organic matter is the major component in the wastewater and is measured as Chemical oxygen demand (COD) and Biochemical oxygen demand (BOD). On Table 4 and Table 5, it shows some physical characteristics of the wastewater and toxic matter that are normally in it.

Chemical oxygen demand, COD, is method that measures the amount of pollutant in water. This test is based on the amount of oxygen needed for the oxidation of the organic matter in water and is commonly expressed in milligrams of oxygen consumed per litre of sample.

Biochemical oxygen demand, BOD, is another method that measures the amount of pollutant in water. It shows the amount of oxygen needed for the aerobic organisms to break down organic matter in water and is commonly expressed in milligrams of oxygen consumed per litre of sample.

Table 2 - Typical composition of untreated domestic wastewater

		Concentration[a]		
Contaminants	**Unit**	**Low Strength**	**Medium Strength**	**High Strength**
Solids, total (TS)	mg/L	390	720	1230
Dissolved, total (TDS)	mg/L	270	500	860
Fixed	mg/L	160	300	520
Volatile	mg/L	110	200	340
Suspended solids, total (TSS)	mg/L	120	210	400
Fixed	mg/L	25	50	85
Volatile	mg/L	95	160	315
Settleable solids	mL/L	5	10	20
Biochemical oxygen demand, 5-d, 20ºC (BOD, 20ºC)	mg/L	110	190	350
Total organic carbon (TOC)	mg/L	80	140	260
Chemical oxygen demand (COD)	mg/L	250	430	800
Nitrogen (total as N)	mg/L	20	40	70
Organic	mg/L	8	15	25
Free ammonia	mg/L	12	25	45
Nitrites	mg/L	0	0	0
Nitrates	mg/L	0	0	0
Phosphorus (total as P)	mg/L	4	7	12
Organic	mg/L	1	2	4
Inorganic	mg/L	3	5	10
Chlorides[b]	mg/L	30	50	90
Sulfate[b]	mg/L	20	30	50
Oil and grease	mg/L	50	90	100
Volatile organic compounds (VOC)	mg/L	<100	100-400	>400
Total coliform	No./100 mL	10^{6}-10^{8}	10^{7}-10^{9}	10^{7}-10^{10}
Fecal coliform	No./100 mL	10^{3}-10^{5}	10^{4}-10^{6}	10^{5}-10^{8}
Cryptosporidium oocysts	No./100 mL	10^{-1}-10^{0}	10^{-1}-10^{1}	10^{-1}-10^{2}
Giardia lamblia cysts	No./100 mL	10^{-1}-10^{1}	10^{-1}-10^{2}	10^{-1}-10^{3}

[a] Low strength is based on an approximate wastewater flowrate of 750L/capita.d (200 gal/capita.d). Medium strength is based on an approximate wastewater flowrate of 460 L/capita.d (120 gal/capita.d).
[b] Values should be increased by amount of constituent present in domestic water supply.

Concentrated wastewater (high strength) represents cases with low water consumption and/or infiltration. Diluted wastewater (low strength) represents high water consumption and/or infiltration.

The COD analysis measures (through chemical oxidation by dichromate) the majority of the organic matter present in the sample. The COD content can be subdivided in fractions, useful for consideration in relation to the design of treatment process.

Table 3 - The effluent composition for two industrial activities

		Wool textile mill[a]		Tomato cannery[b]	
Constituent	**Unit**	**Annual average**	**Daily maximum**	**Peak season[c]**	**Off season[d]**
Flowrate	m^3/d	-	-	4364-22300	1140-6400
pH	-	5.92	-	7.2-8.0	7,2-8,0
BOD	mg/L	90.7	169	460-1100	29-56
COD	mg/L	529	1240	-	-
SS	mL/L	-	-	6-80	0.5-2.2
TSS	mg/L	93.4	860	270-760	69-120
TDS	mg/L	-	-	480-640	360-520
Nitrate-N	mg/L	-	-	0.4-5.6	0.1-2.2
Ammonia-N	mg/L	8.1	54	-	-
Phosphorus	mg/L	-	-	1.5-7.4	0.3-3.9
Sulphate	mg/L	-	-	15-23	7.1-9.9
DO	mg/L	-	-	0.9-3.8	1.6-9.8
Oil and grease	mg/L	27.4	45.2	-	-
Temperature	ºC	-	-	18-23	13-19

[a] Yohe and Rich (1995).
[b] Adapted from Crites and Tchobanoglous (1998).
[c] Peak season is from early July to late September, when fresh-harvest tomatoes are canned. Treatment consists of screening and brief sedimentation.
d Off season is from November to June, when canned tomatoes are remanufactured into tomato paste, tomato sauce, and other tomato product (e.g., salsa, ketchup, spaghetti sauce). Treatment typically consists of screening, aeration, and sedimentation.

The theoretical COD can be calculated from an oxidation equation. For example, theoretical COD of ethanol is calculated based on the Eq. 21.

$$C_2H_5OH + 3O_2 \rightarrow 2CO_2 + 3H_2O \qquad \textit{Eq. 21}$$

So if 46g of ethanol needs 96g of oxygen, the theoretical COD of ethanol is 96/46=2.09.

The BOD analysis measures the oxygen used for oxidation of part of the organic matter. BOD analysis has its origin in effluent control. The standard BOD analysis generally takes 5 days, it can take 1 day if speed is needed or 7 days if convenience is the main option. If all biodegradable material is required, it takes 25 days.

Most components in the wastewater are not the direct target for treatment, but they contribute to the toxicity of the wastewater, either in relation to the biological process or to the receiving waters.

Table 4 - Different parameters in municipal wastewater [15].

Parameter	High	Medium	Low	Unit
Absol. viscosity	0.001	0.001	0.001	kg/m.s
Surface tension	50	55	60	Dyn/cm^2
Conductivity	120	100	70	mS/m^1
pH	8.0	7.5	7.0	
Alkalinity	7	4	1	Eqv/m^3
Sulphide	10	0.5	0.1	gS/m^3
Cyanide	0.05	0.030	0.02	g/m^3
Chloride	600	400	200	gCl/m^3

Table 5 - Special parameters in wastewater, xenobiotics with toxic and other effects (in mg/l) [15].

Parameter	High	Medium	Low
Phenol	0.1	0.05	0.02
Phthalates, DEHP	0.3	0.2	0.1
Nonylphenols, NPE	0.08	0.05	0.01
PAHs	2.5	1.5	0.5
Methylene chloride	0.05	0.03	0.01
LAS	10,000	6,000	3,000
Chloroform	0.01	0.05	0.01

3.1. Wastewater treatment plant

The wastewater treatment technology has evolved over the years due to the civilization of human population and the increasing awareness and understanding of the interrelation of the spreading of diseases and sanitation, waste handling, and water treatment. The present wastewater treatment systems consist of a sequence of several processes that can be divided in stages, offering different levels of treatment (

Fig. 13). The main stages that compose the most common Sewage Treatment Plant, specifically those used for the treatment of domestic wastewater, are known as conventional methods which are divided in preliminary, primary, secondary and tertiary types of treatments.

The preliminary treatment consists in removing the solids bigger than 0.01 mm like debris, grit and grease. Removal of these materials is necessary to enhance the operation and maintenance of subsequent treatments units. The techniques used for this process are, for example, wet sieving, trituration, degritting and degreasing.

The primary treatment consists in removing the settle able organic and inorganic solids and the removal of materials that will float, typically achieved through chemical addition or filtration. Approximately 25 to 50% of the incoming biochemical oxygen demand (BOD_5), 50 to 70% of the total suspended solids, and 65% of the oil and grease are removed during primary treatment. The techniques used for this process are, for example, coagulation, flocculation, sedimentation, skimming and decantation.

The secondary treatment consists in removing the biodegradable organic matter (dissolved or suspended), suspended solids and nutrients like nitrogen and phosphorus. The removal of

biodegradable dissolved and colloidal organic matter is made by using aerobic biological treatment processes. Aerobic biological treatment is performed in the presence of oxygen by aerobic microorganisms that metabolize the organic matter in the wastewater. The microorganisms must be separated from the treated wastewater by sedimentation to produce clarified secondary effluent.

The tertiary treatment consists in removing the left-over dissolved and suspended materials after normal biological treatment, often by granular medium filtration or microscreens. Disinfection and nutrient removal are also included on this stage. Disinfection normally involves the injection of a chlorine solution at the head end of a chlorine contact basin. The chlorine dosage depends upon the strength of the wastewater and other factors, but dosages of 5 to 15 mg/l are common. Ozone and ultra violet (UV) irradiation can also be used for disinfection, although these methods are not of common use.

All the organic and inorganic solid obtained from the primary and secondary stages, which are separated from the wastewater, are mixed together creating a heterogeneous mix of hazardous materials called sewage sludge. The sludge normally has a lot of water. In order to be transported, the volume must be reduced by removing most of the water. Common dewatering processes include lagooning in drying beds, pressing (where sludge is mechanically filtered, often through cloth screens to produce a firm cake) and centrifugation. The majority of sewage sludge produced in wastewater treatment plants is disposed of on land, primarily agricultural land.

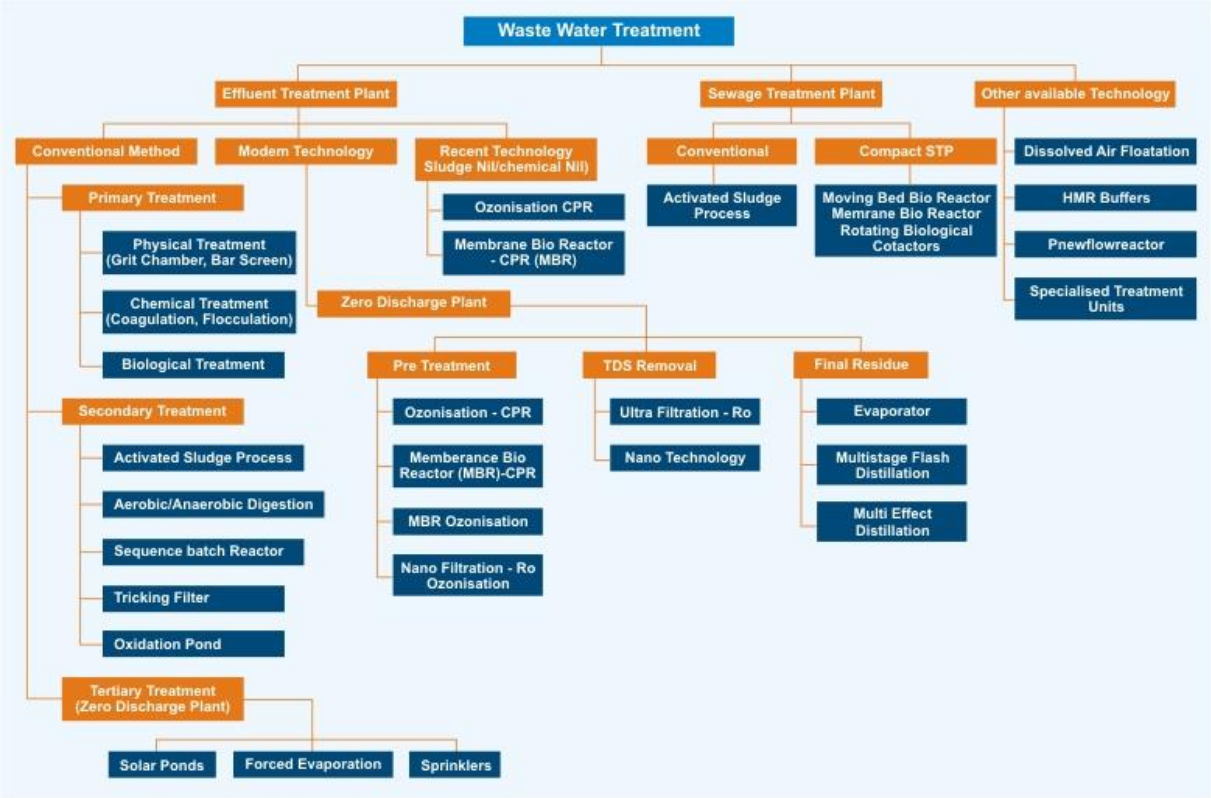

Fig. 13 – Types of Wastewater Treatment Processes.

4. Experimental Analysis

4.1. Materials

For this work, it was studied the electrochemical behaviour of the urine, one of the components of the domestic wastewater, because it was noticed during the study of the wastewater, that the current density at a given voltage was low compared to other works with the same electrodes materials[16-19] (ex: 2.5 mA cm^{-2} vs 50 mA cm^{-2} with Pt-Dy) and that the HER was also low. So to get a better understand of that, it was prepared a solution of synthetic urine with composition reported in the literature [20], and the quantity is measured as shown in Table 6 for a volume of 250 ml with a pH of 6.0 ± 0.1 at 25ºC (the solution initial pH was 5.0, and NaOH (≥99%) was used to reach that value) with a conductivity of 1594 ± 10 mS m^{-1} which is more than the wastewater (as can be seen on the characterisation of wastewater).

Table 6 - Overview of synthetic urine composition

Compound and purity	Supplier	Added mass (g)
NaCl (100%)	V.Reis	0.7418
KCl (100%)	Panreac	0.3965
$CaCl_2$	V.P.	0.2765
Na_2SO_4	-	0.5516
KH_2PO_4 (≥97%)	May & Baker Ldt	0.3551
NH_4Cl (≥99.5%)	Sigma-Aldrich	0.2808
Urea (≥99.5%)	Merck	6.2305

4.1.1. Sampling and characterisation of wastewater

The wastewater used throughout this study was an effluent provided by SIMTEJO, a company that provide an urban wastewater treatment service. The effluents were sampled at the outlet of the primary decantation process. The samples were collected and stored in polyethylene terephthalate bottles and kept in a fridge at the temperature of about 4ºC until use. The wastewater has a pH of 7.0 ± 0.1 and a conductivity of 131 ± 10 mS m^{-1}, which is similar to the common domestic wastewater seen on Table 4.

4.1.2. Experimental setup

The tests were carried out on a cylindrical electrolytic cell made of glass material with a capacity of about 125 ml. The electrochemical experiments were performed using potentiostat/galvanostat Princeton Applied Research/EG&G Model 273A. The cell temperature was controlled by using a thermostat (Brand Model). The material used as auxiliary electrode was a platinum mesh and as reference electrode saturated calomel electrode (SCE) (HANNA HI5412). As working electrode, for the synthetic urine it was only used platinum and for the wastewater platinum and platinum-rare earth, stainless steel 304 and nickel and nickel-rare earth (being RE the Ce, Sm, Dy and Ho) were used (Table 7).

Table 7 – Geometric area of the electrodes

Electrode	SS 304	Pt	Ni	Pt-Ce (50%)	Ni-Ce (10%)	Pt-Sm (50%)	Ni-Sm (10%)	Pt-Dy (50%)	Ni-Dy (10%)	Pt-Ho (50%)
Area (cm^2)	8	1	0.79	0.135	0.4	0.092	0.53	0.23	0.39	0.23

4.2. Methods

The electrochemical reduction process was performed in the electrochemical cell containing the sample with about 125 ml of volume. The electrodes were placed vertically in the recipient in order they don't touch each other.

The study of the electrolysis of the synthetic urine was made by making a voltammetry scan on the negative potential side from the OCP to a potential of -1.2/-1.3 V at several rates. Those rates were 0.5, 1.0, 1.5, 2.5, 5.0, 10, 15, 25, 50, 100, 150, 250, 500, 1000 mV s^{-1} at 25ºC and each scan gave a voltammogram that shows two cathodic current peaks on the reduction side. The appearance of these peaks shows there are species in the solution that are being reduced instead of just water, which means it is possible that this kind of reduction can give a possibility of producing hydrogen at a lower voltage than from water electrolysis. The peaks were analysed by registering their values at the corresponding scan rate. With those values it is possible to construct two graphs, by making η vs. ln ν, and j vs. $\nu^{1/2}$ which gives us a linear correlation by using Eq. 22 and Eq. 23 to get value of *n* and α. [11]

$$j = 2.99 \times 10^5 \alpha^{1/2} n C_O^* D_O^{1/2} \nu^{1/2} \qquad \textit{Eq. 22}$$

$$\eta = -\frac{1}{2}\frac{RT}{\alpha n_a F} ln(\nu) - \frac{RT}{\alpha n_a F}\left[0.780 + ln\left(\frac{D_O^{1/2}}{k^o}\left(\frac{\alpha F}{RT}\right)^{1/2}\right)\right] \qquad \textit{Eq. 23}$$

Where α is the charge transfer coefficient, the η is the overpotential, C_i^* is the bulk concentration of specie i, D_i is the diffusion coefficient of specie i in water, F is the Faraday's constant, j is the current density, n is the stoichiometric number of electrons involved in an electrode reaction, n_a is the number of exchanged electrons in the rate determining step, R is the universal gas constant, T is the Temperature, ν is the scan rate.

As for the study of water electrolysis in synthetic urine the method that was used to calculate α and j_0, were through the chronoamperometry (CA) measurements upon application of a given potential at several applied potential values. The technique consists on recording the current density on the system after it becomes stable, after some period of time, not inferior to 20 seconds. The potentials that were used to apply the CA were 0.0, -0.2, -0.3, -0.4, -0.5, -0.55, -0.6, -0.65, -0.7, -0.75, -0.8, -0.85, -0.9, -0.95, -1.0, -1.05, -1.1, -1.15, -1.2, -1.25, -1.3, -1.35, -1.4, -1.45 and -1.5 V. With these values it is possible to construct graphics like j vs. η and η vs. log j and by using the Tafel equation, α and j_0 can be obtained.

The study of the electrolysis of the wastewater was made by making a voltammetry scan from the OCP to a potential of -1.5 V using different solution: just using the effluent without the support of additional electrolytes and with the addition to the effluent of potassium hydroxide (KOH). This procedure followed that previously reported [21] for a study involving urea solution. Despite the wastewater has lower concentration of urea it has a high concentration of other organic compounds that may also react with KOH. For that reason, about 39g of KOH (90% Sigma-Aldrich) was added to each 125 ml of effluent sample in order to have 5M KOH concentration. CV measurements were made, in our case, two different rates: 50 and 0.5 mV s^{-1} with temperatures at 25, 35, 45, 55, 65, 75 and 85ºC for each cathodes chosen for this experimental, except for the rare-earth alloys that, because of technical problems, it was not possible to do all the temperatures. The scan at 50 mV s^{-1} rate is used to obtain a quick characterisation

of the system. The scan at 0.5 mV/s is used for the analysis of the Tafel behaviour. Once the curves are obtained, the α and j_0 where then calculated from the Tafel plot by using Tafel equation, the j_0 was also calculated from low overpotential by using the Butler-Volmer equation.

It was also applied to each situation, a complete CV scan between -1.4V and 0.5V (for just the effluent) or 0.4V (for the others types of solution) at 50 mV/s rate with a temperature of 25ºC, in order to compare not only their electro-reduction behaviour but also their electrooxidation. The results on the reduction part were similar with the rest of the experiment except for the synthetic urine, which had no reduction peaks. On the oxidation part it did not show any significant activity except for the nickel in KOH solution, where it shows what seems to be the oxidation and subsequent reduction of the electrode.
An anodic voltammetry scan was made from OCP to 0.5V, with Pt electrode at 25ºC with the same scan rates used in synthetic urine, on the effluent, before and after KOH, and water with KOH. There were peaks potential with effluent+KOH, and those peaks were analysed to make the η vs ln ν plot to calculate the α and *n*. The results can be seen in Table 17 and Table 18. Since is not possible to know the concentration and the diffusion coefficient, the Eq. 24 was used to get the α and Eq. 25 was used to get the n.[11] E_p is the peak potential and $E_{p1/2}$ is the half-peak potential.

$$\eta = -\frac{1}{2}\frac{RT}{(1-\alpha)n_a F}ln(\nu) - \frac{RT}{(1-\alpha)n_a F}\left[0.780 + ln\left(\frac{D_O^{1/2}}{k^o}\left(\frac{\alpha F}{RT}\right)^{1/2}\right)\right] \qquad \textit{Eq. 24}$$

$$\left|E_p - E_{p/2}\right| = \frac{1.857RT}{n\alpha F} \qquad \textit{Eq. 25}$$

5. Results and discussions

5.1. Synthetic urine

On all the CV analysis on the synthetic urine made at 25ºC, with platinum as working electrode, has formed two reduction peaks currents and the current density increased with the scan rate, as it can be seen on Fig. 14. At higher temperature like 55ºC the solution started to form precipitate, it was not possible to analyse to see what formed those solids but, it is possible to be calcium phosphate.

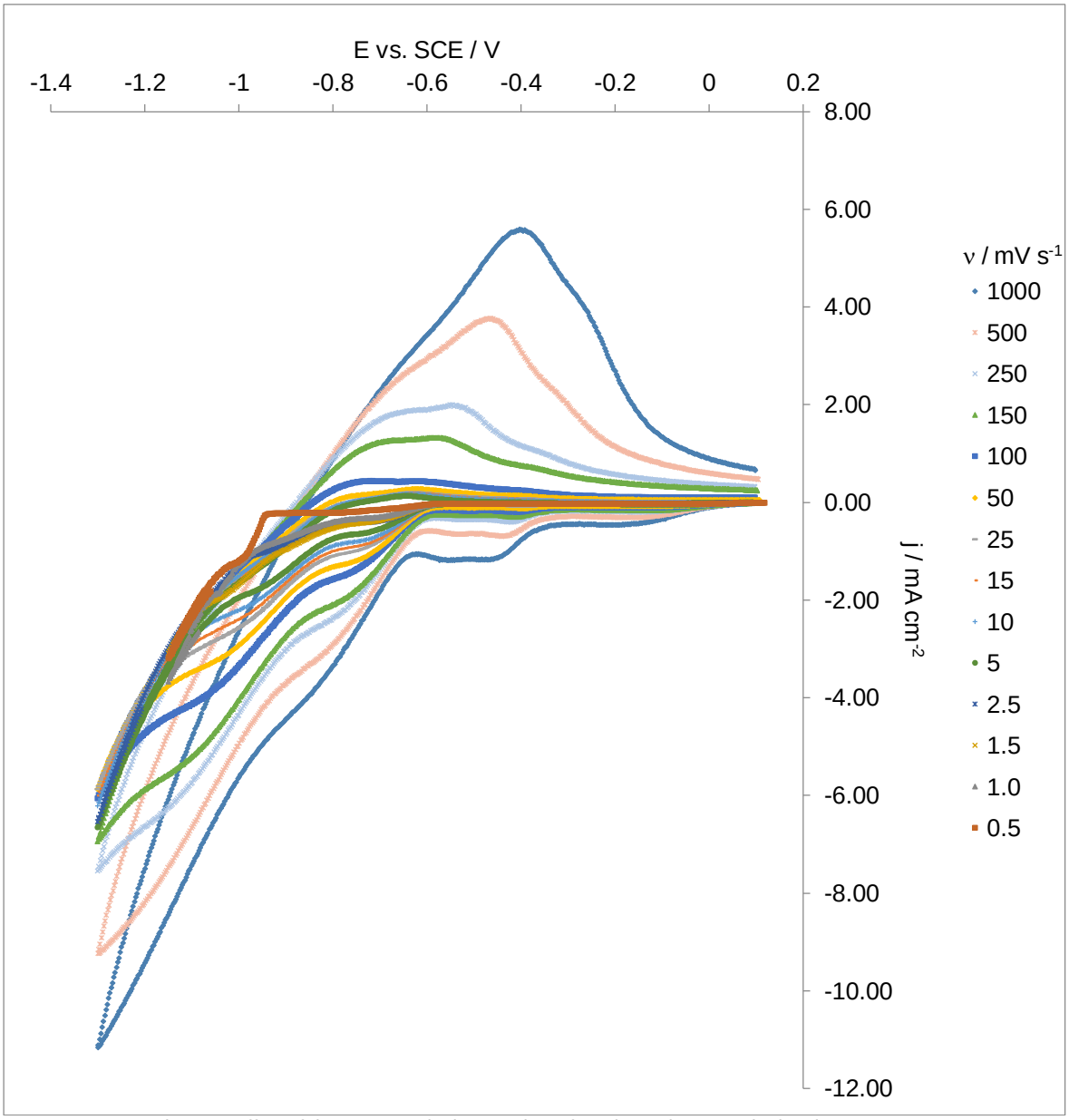

Fig. 14 – Effect of the scan rate in the CV plots of Pt electrode on synthetic urine at 25ºC.

The peaks values were registered, being the peak on the right the first peak and the peak on the left the second peak.

From here the linear regressions from those points are made, in order to calculate the desired parameters, and the graphic representation of the points can be seen in the Fig. 15 and Fig. 16.

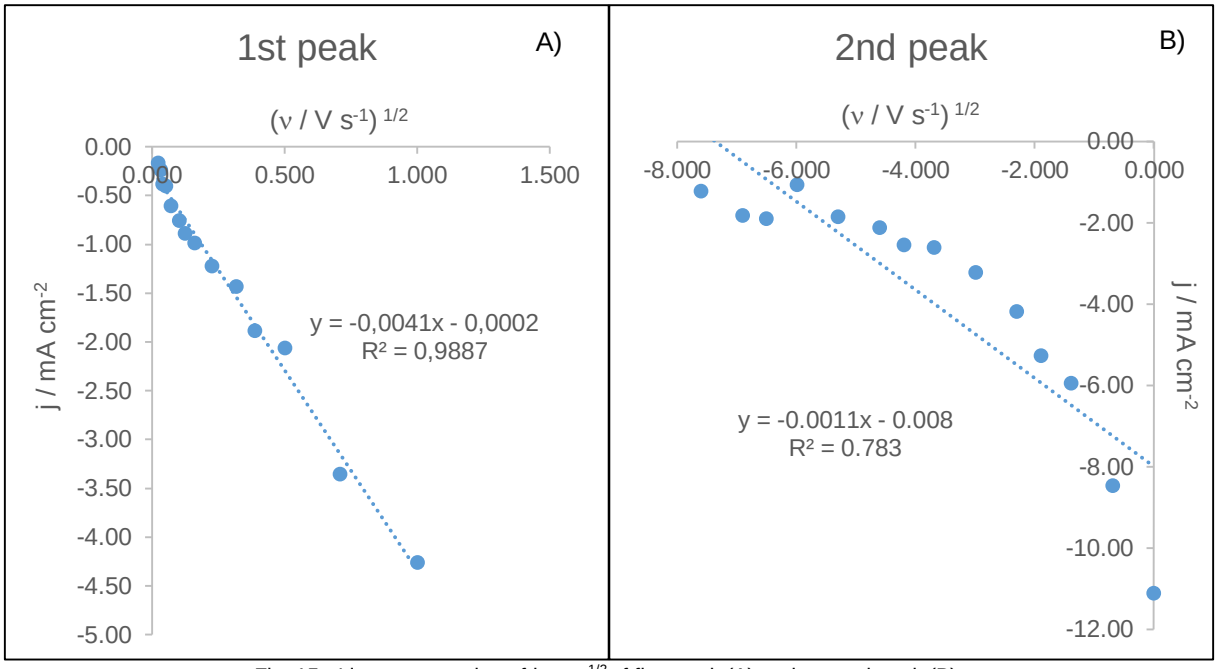

Fig. 15 - Linear regression of j vs. $\nu^{1/2}$ of first peak (A) and second peak (B).

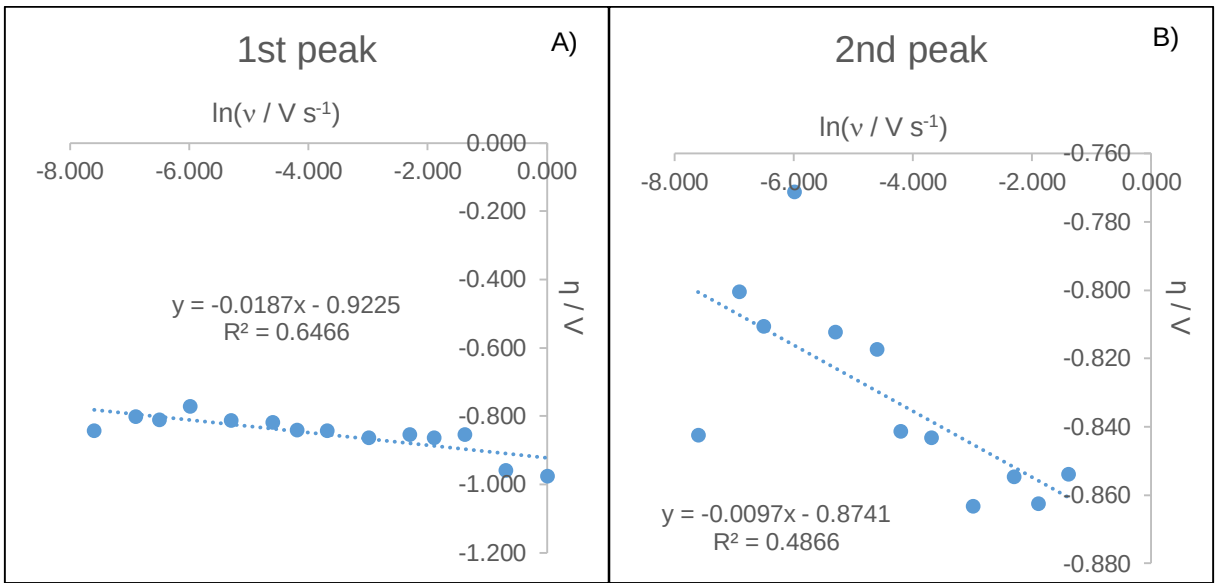

Fig. 16 - Linear regression of η vs. ln ν of first peak (A) and second peak (B).

Table 8 - Parameters needed for potential scan methods.

R (J/mol.K)	8.314
F (c/mol)	96485
n	1
T (K)	298,15
D_{urea} ($cm.s^{-2}$)	1.38E-05 [22]
Area (cm^2)	1
C^*_{urea} (mol/cm^3)	0.000416

Table 9 - α and n values.

	m(η)	α	m(j)	n
1st peak	0.0187	0.69	0.0041	0.01
2nd peak	0.0097	1.32	0.0011	0.00

By using the Eq. 21 and Eq. 22 it is possible to get the results for *α* and *n* in which are represented in the Table 9, looking at this results the first thing that pops up in mind is that the values does not match with the reality, that's because the α is a parameter that can only have values between 0 and 1 and yet the 2nd peak has a value of 1.32, the *n* is a parameter that represents the stoichiometric electrons transfer which means it can only have integer numbers between 0 and up, but in this case the values obtained are 0.01 and 0, which makes no sense, since there's peaks on the CV representation and was noticed a formation of bubbles during the experimentation, meaning that a number of electrons were exchanged and so the *n* should have a value greater than 0. Even excluding of some lagged points to increase the R-squared, the result did not get any significant better.

Meanwhile, before proceeding of the calculation with the CV scan, it was made an analysis with the CA method to calculate the parameters and see if the results of both methods are similar. The obtained points with this method (Table 20) were used to construct a graphic similar to a CV scan and a Tafel plot, as can be seen in Fig. 17 and Fig. 18, to get the parameters by using the Eq. 19.

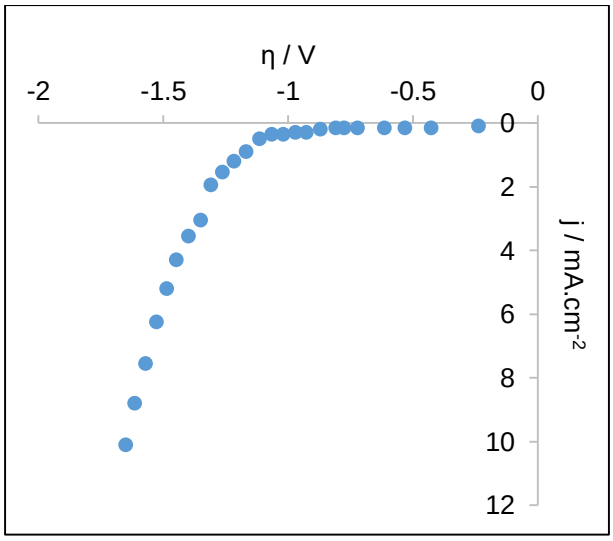

Fig. 17 - j vs. η plot from the CA scan.

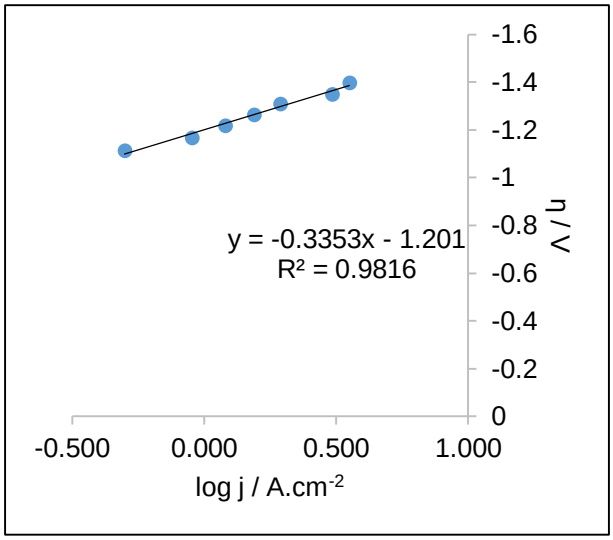

Fig. 18 - Tafel plot of the synthetic urine.

Table 10 - Results with the CA scan.

n	α	b (mV dec^{-1})	j_0 (A cm^{-2})	-log(j_0)
1	0.18	335	2.59E-07	6.6

With the linear equation obtained from the linear regression on the Tafel plot, the results are presented in the Table 10, the value of the exchange current density calculated is an acceptable value considering the current intensity of OCP of each test.

Because of the CV scan results, that were not very conclusive and unreal, it was tried to redo the experiment all over, but it did not go well, while making the CV scan the peaks disappeared and even by doing a new solution the peaks current still did not appeared and the reason of why that happens are still unknown, since it was not possible to analyse the chemistry changes of the solution.

5.2. Wastewater effluent without electrolyte addition

With just the wastewater effluent, all ten electrodes materials were used for the CV scan with a rate of 0.5 mV s^{-1}, from the OCP to a potential of -1.5V vs SCE. The polarization curves from the CV scan, showed that the temperature affects the current density at a given voltage, being the difference between the 25ºC and 85ºC, of same material, were around double. In Fig. 19, represents the different results from the electrodes at 25ºC. From those polarization curves, the nickel and nickel-rare earth have similar behaviour between them, almost without any difference. The platinum and platinum-rare earth are the ones that shows the best performance of all electrodes, especially the rare earth that, not only got better current density than nickel alloys at a given voltage, it also got better values than the pure platinum. As for the SS304 electrode, it shows to have the lowest performance.

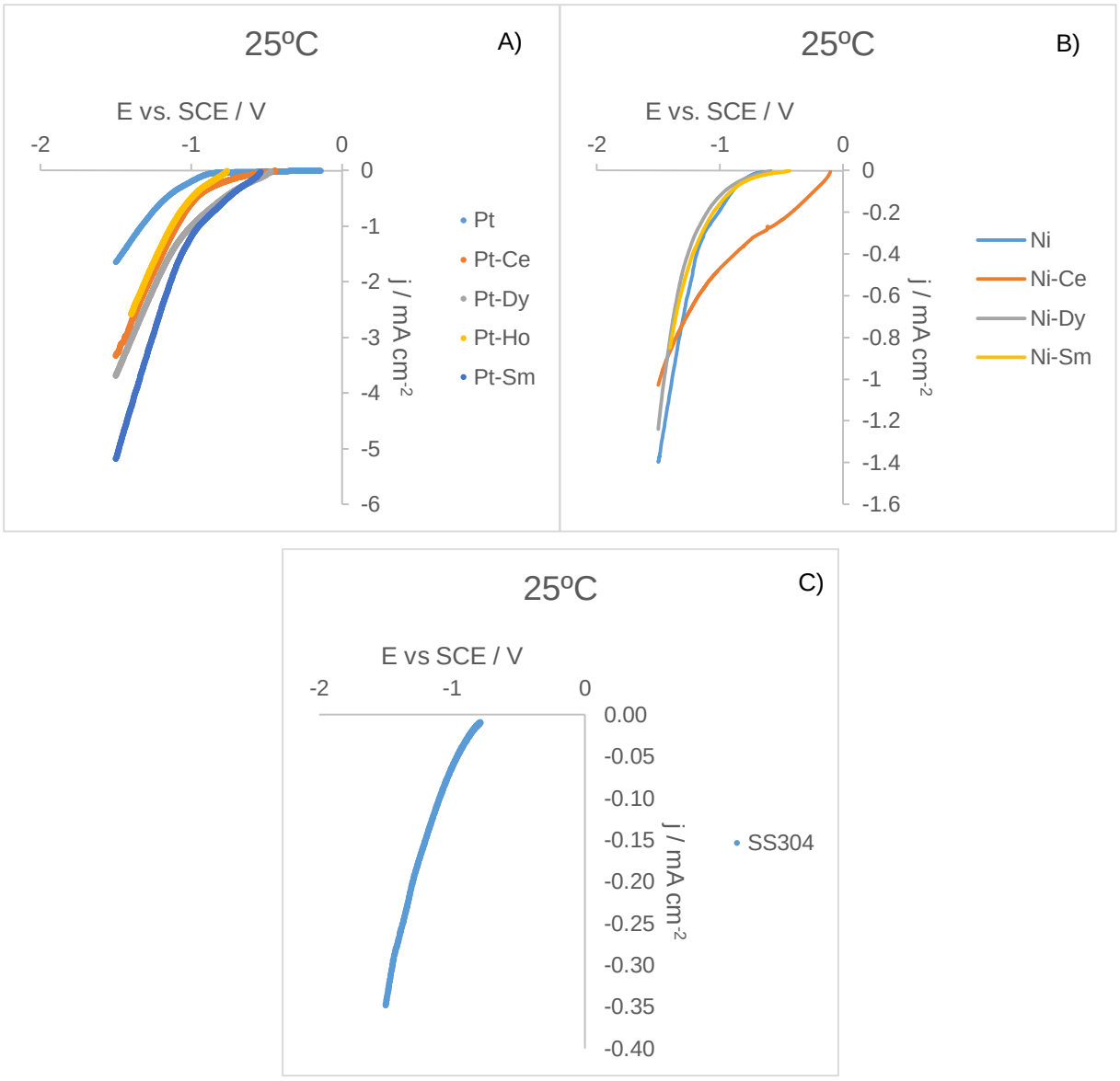

Fig. 19 - Polarization curves at 25 ºC of Pt and Pt alloys (A), Ni and Ni alloys (B) and SS304 (C) of the domestic wastewater.

The Table 11 and Table 12 represents the results calculated from the Tafel and Butler-Volmer methods respectively. The results of j_0 differ significantly between the Tafel and Butler-Volmer methods and they oscillates with the temperature, mostly because of the "noise" that happened during the experiments that affected the current stability, especially at the low overpotential zone. The α have values between 0 and 0.5 (closer to 0 than 0.5), which shows that the redox reaction is quasi-reversible making it difficult for the HER to happen. The Tafel slope (b) have values superior to 120 mV dec^{-1} in all of the electrodes, suggesting that the Volmer reaction is the rate determining step for HER on the wastewater effluent.[11,20]

Table 11 - Parameters calculated from Tafel equation of the domestic wastewater.

	T (ºC)	25	35	45	55	65	75	85
Pt	α	0.25	0.36	0.23	0.26	0.22	0.21	0.24
	b(mV dec^{-1})	237	171	278	253	309	326	292
	j_0(mA/cm^2)	$4.66x10^{-05}$	$5.94x10^{-03}$	$2.32x10^{-04}$	$2.55x10^{-04}$	$1.03x10^{-03}$	$1.38x10^{-03}$	$1.01x10^{-03}$
Ni	α	0.19	0.22	0.24	0.24	0.22	0.20	0.19
	b(mV dec^{-1})	311	283	259	271	311	337	376
	j_0(mA/cm^2)	$1.04x10^{-02}$	$6.89x10^{-03}$	$6.64x10^{-03}$	$4.43x10^{-03}$	$3.21x10^{-03}$	$3.52x10^{-02}$	$7.59x10^{-03}$
Pt-Ce	α	0.14	0.16	0.13	0.13	0.13	0.15	0.23
	b(mV dec^{-1})	415	387	493	492	522	466	309
	j_0(mA/cm^2)	$2.73x10^{-02}$	$1.04x10^{-01}$	$2.66x10^{-01}$	$2.69x10^{-01}$	$2.78x10^{-01}$	$2,40x10^{-01}$	$1.95x10^{-01}$
Pt-Sm	α	0.10	0.07					
	b(mV dec^{-1})	617	741					
	j_0(mA/cm^2)	$2.14x10^{-01}$	$5.90x10^{-01}$					
Pt-Dy	α	0.07						
	b(mV dec^{-1})	791						
	j_0(mA/cm^2)	$2.15x10^{-01}$						
Pt-Ho	α	0.11	0.11					
	b(mV dec^{-1})	380	545					
	j_0(mA/cm^2)	$1.17x10^{-01}$	$2.61x10^{-01}$					
Ni-Ce	α	0.04	0.04	0.07	0.07	0.08	0.08	
	b(mV dec^{-1})	1717	1470	939	908	839	874	
	j_0(mA/cm^2)	$1.14x10^{-01}$	$1.40x10^{-01}$	$9.34x10^{-02}$	$1.18x10^{-01}$	$1.32x10^{-01}$	$1.62x10^{-01}$	
Ni-Sm	α	0.15	0.11					
	b(mV dec^{-1})	398	546					
	j_0(mA/cm^2)	$6.33x10^{-03}$	$4.21x10^{-02}$					
Ni-Dy	α	0.13	0.13					
	b(mV dec^{-1})	436	468					
	j_0(mA/cm^2)	$1.48x10^{-02}$	$1.81x10^{-02}$					
SS304	α	0.11	0.15	0.14	0.16	0.18	0.18	0.16
	b(mV dec^{-1})	518	402	439	416	369	379	432
	j_0(mA/cm^2)	$2.51x10^{-02}$	$2.37x10^{-02}$	$3.01x10^{-02}$	$3.13x10^{-02}$	$1.65x10^{-02}$	$2.21x10^{-02}$	$3.47x10^{-02}$

Table 12 - Parameters calculated from Butler-Volmer equation of the domestic wastewater.

j_0(mA/cm^2)	25ºC	35ºC	45ºC	55ºC	65ºC	75ºC	85ºC
Pt	$4.42x10^{-4}$	$1.38x10^{-3}$	$3.75x10^{-3}$	$5.66x10^{-6}$	$2.67x10^{-3}$	$2.88x10^{-3}$	$2.70x10^{-3}$
Ni	$4.29x10^{-4}$	$8.39x10^{-4}$	$2.30x10^{-3}$	$1.92x10^{-4}$	$6.06x10^{-3}$	$1.11x10^{-2}$	$2.93x10^{-3}$
Pt-Ce	$1.82x10^{-2}$	$4.21x10^{-2}$	$1.23x10^{-1}$	$1.22x10^{-1}$	$1.27x10^{-1}$	$1.01x10^{-1}$	$1.50x10^{-1}$
Pt-Sm	$7.90x10^{-2}$	$1.98x10^{-1}$					
Pt-Dy	$1.28x10^{-5}$						
Pt-Ho	$5.63x10^{-2}$	$8.75x10^{-2}$					
Ni-Ce	$2.57x10^{-2}$	$2.80x10^{-2}$	$2.78x10^{-2}$	$3.28x10^{-2}$	$4.23x10^{-2}$	$5.77x10^{-2}$	
Ni-Sm	$3.56x10^{-3}$	$8.48x10^{-3}$					
Ni-Dy	$4.88x10^{-3}$	$7.96x10^{-3}$					
SS304	$3.68x10^{-3}$	$4.89x10^{-3}$	$6.25x10^{-3}$	$7.98x10^{-3}$	$6.89x10^{-3}$	$6.80x10^{-3}$	$1.38x10^{-2}$

5.3. Wastewater effluent with addition of KOH as electrolyte

The addition of the KOH on the wastewater, improved the performance on all the electrodes considerably, the conductivity got a value of 77300 mS m^{-1} and gave a higher current density at a given voltage. Like before, it was applied an CV scan with a rate of 0.5 mV s^{-1}, but for the rare earths alloys it started from the OCP to a potential of -1.4V vs SCE, because more than that, would make the electrodes unusable (which is what happened with Pt-Ce). In Fig. 20 represents the polarization curves of the electrodes at 25ºC, that also shows nickel and nickel alloys have the same behaviour with almost no difference. The Pt-RE are the ones with better performance with a higher difference in current density with the other materials than before the addition of the KOH. The SS304 electrode, despite the improvement, still has the lowest current density at a given voltage.

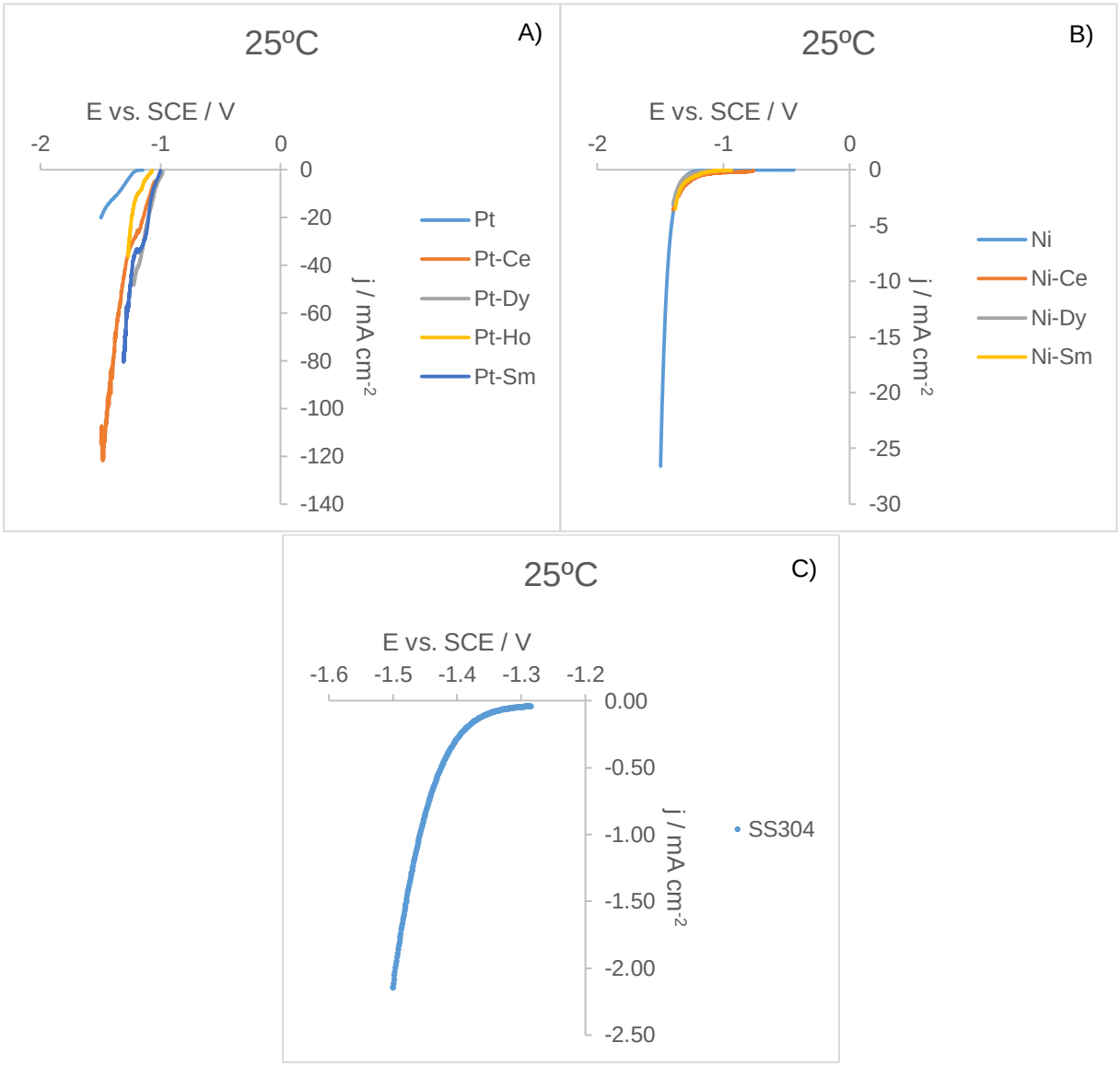

Fig. 20 - Polarization curves at 25 ºC of Pt and Pt alloys (A), Ni and Ni alloys (B) and SS304 (C) of the domestic wastewater effluent after KOH addition.

The results calculated from the Tafel and Butler-Volmer methods are shown in Table 13 and Table 14 respectively. In general, the α have values around 0.5, the ideal value for an electrolysis reaction, indicating a reversible redox reaction. The b values are closer to 120 mV dec^{-1}, indicating once more that the Volmer reaction is the rate determining step for HER mechanism.[11,20]

In the Pt case the α got unreal values, all superior to 1, probably caused by the "noises" at the time that deviated the Tafel plot to this extent, or it is possible that with this electrode there's a two-step electrode reaction (similar to what happens in Eq. 26 and Eq. 27). The b values range around 40 mV dec^{-1}, which suggests hydrogen production via the Volmer–Heyrovsky mechanism. So the number of electrons in a single rate-determining step, n_a, is equal to 2, making α having half of the original value falling to the 0-1 range, which is supposed to be.

$$Ox^{(p+2)+} + e^- \rightarrow Int^{(p+1)+} \quad \textit{Eq. 26}$$

$$Int^{(p+1)+} + e^- \rightarrow Red^{p+} \quad \textit{Eq. 27}$$

Table 13 - Parameters calculated from Tafel equation of the domestic wastewater after KOH addition.

	T (ºC)	25	35	45	55	65	75	85
Pt	α	1.28	1.16	1.38	1.42	1.51	1.54	1.54
	b(mV dec^{-1})	38	40	38	39	40	41	42
	j_0(mA/cm^2)	1.86x10^{-2}	2.37x10^{-2}	1.69x10^{-2}	1.86x10^{-2}	1.86x10^{-2}	1.85x10^{-2}	8.26x10^{-3}
Ni	α	0.51	0.56	0.39	0.36	0.33	0.35	0.33
	b(mV dec^{-1})	115	109	160	181	204	198	215
	j_0(mA/cm^2)	1.90x10^{-08}	1.84x10^{-06}	7.95x10^{-04}	3.86x10^{-03}	3.47x10^{-02}	4,02x10^{-02}	1,21x10^{-01}
Pt-Ce	α	0.32						
	b(mV dec^{-1})	182						
	j_0(mA/cm^2)	6.15						
Pt-Sm	α	0.51	0.42					
	b(mV dec^{-1})	115	145					
	j_0(mA/cm^2)	2.47	5.12					
Pt-Dy	α	0.59						
	b(mV dec^{-1})	100						
	j_0(mA/cm^2)	1.81						
Pt-Ho	α	0.55	0.39					
	b(mV dec^{-1})	108	156					
	j_0(mA/cm^2)	1.20	2.42					
Ni-Ce	α	0.22	0.08					
	b(mV dec^{-1})	274	758					
	j_0(mA/cm^2)	1.38x10^{-2}	4.72x10^{-1}					
Ni-Sm	α	0.31	0.26					
	b(mV dec^{-1})	188	230					
	j_0(mA/cm^2)	4.20x10^{-2}	2.81x10^{-2}					
Ni-Dy	α	0.31	0.25					
	b(mV dec^{-1})	192	247					
	j_0(mA/cm^2)	5.26x10^{-2}	3.92x10^{-2}					
SS304	α	0.57	0.58	0.56	0.51	0.56	0.55	0.55
	b(mV dec^{-1})	103	106	113	129	120	126	130
	j_0(mA/cm^2)	2.14x10^{-2}	3.55x10^{-2}	2.33x10^{-2}	1.38x10^{-2}	2.66x10^{-2}	4.21x10^{-2}	3.72x10^{-2}

Table 14 - Parameters calculated from Butler-Volmer equation of the domestic wastewater after KOH addition.

j_0(mA/cm^2)	25ºC	35ºC	45ºC	55ºC	65ºC	75ºC	85ºC
Pt	$5.62x10^{-2}$	$3.98x10^{-2}$	$4.73x10^{-2}$	$6.65x10^{-2}$	$6.63x10^{-2}$	$6.74x10^{-2}$	$2.53x10^{-2}$
Ni	$8.12x10^{-4}$	$2.28x10^{-3}$	$1.01x10^{-3}$	$2.54x10^{-3}$	$9.62x10^{-3}$	$2.28x10^{-2}$	$3.95x10^{-2}$
Pt-Ce	$5.19x10^{-2}$						
Pt-Sm	3.34	6.56					
Pt-Dy	2.47						
Pt-Ho	1.58	2.62					
Ni-Ce	$5.26x10^{-2}$	$1.62x10^{-1}$					
Ni-Sm	$1.46x10^{-2}$	$2.12x10^{-2}$					
Ni-Dy	$2.15x10^{-2}$	$2.52x10^{-2}$					
SS304	$1.19x10^{-2}$	$2.34x10^{-2}$	$1.48x10^{-2}$	$6.87x10^{-3}$	$1.78x10^{-2}$	$2.94x10^{-2}$	$2.47x10^{-2}$

As can be noticed, it was not possible for all electrodes to be studied at all the temperatures. For the ones that were able to do all the temperatures, the results overall, on both types of electrolytes, were not consistent. It was expected that the exchange current density increased consistently with temperature, instead the values oscillated. This can probably be explained from the “noises” that happened during the experiments which affected the voltammetry sweep, especially at low voltage, and the nature of the effluent, with the change of temperature and/or KOH, the composition may have altered through time, causing a Tafel plot deviation. Either way, one can thing can be concluded overall, from the results at 25ºC, is the fact that the difference of the kinetics parameters with and without KOH, indicates that with the addition, the α and j_0, on both methods, increase and b decrease on all the electrodes, which indicates that the HER process is more favourable with KOH.

The Table 15 and Table 16 shows a comparison, at 25ºC, between the kinetics parameters with and without KOH from both methods used. From the Tafel it shows that with the addition, the α and j_0 increase while b decrease on all the electrodes, which indicates that the HER process is more favourable with KOH. The Butler-Volmer shows the same thing about the j_0.

Table 15 - Comparison of the Tafel results between before and after KOH addition @25ºC.

		SS304	Pt	Ni	Pt-Ce	Ni-Ce	Pt-Sm	Ni-Sm	Pt-Dy	Ni-Dy	Pt-Ho
Without 5M KOH	α	0.11	0.25	0.19	0.14	0.04	0.10	0.15	0.07	0.13	0.11
	b (mV dec^{-1})	518	237	311	417	1616	617	398	791	458	380
	j_0 (mA cm^{-2})	2.51 x10^{-2}	4.66 x10^{-5}	1.04 x10^{-2}	2.73 x10^{-2}	1.14 x10^{-1}	2.14 x10^{-1}	6.33 x10^{-3}	2.15 x10^{-1}	1.48 x10^{-2}	1.17 x10^{-1}
With 5M KOH	α	0.57	1.28	0.51	0.32	0.22	0.51	0.31	0.59	0.31	0.55
	b (mV dec^{-1})	103	38.5	115	182	274	115	188	100	192	108
	j_0 (mA cm^{-2})	2.14 x10^{-2}	1.32 x10^{-2}	1.90 x10^{-8}	6.15	1.38 x10^{-2}	2.47	4.20 x10^{-2}	1.81	5.26 x10^{-2}	1.20

Table 16 - Comparison of the Butler-Volmer results between before and after KOH addition @25ºC.

		SS304	Pt	Ni	Pt-Ce	Ni-Ce	Pt-Sm	Ni-Sm	Pt-Dy	Ni-Dy	Pt-Ho
Without 5 M KOH	j_0 (mA cm^{-2})	3.68 x10^{-3}	4.42 x10^{-4}	4.29 x10^{-4}	1.82 x10^{-2}	2.57 x10^{-2}	7.90 x10^{-2}	3.56 x10^{-3}	1.28 x10^{-5}	4.88 x10^{-3}	5.63 x10^{-2}
With 5 M KOH	j_0 (mA cm^{-2})	1.19 x10^{-2}	5.62 x10^{-2}	8.12 x10^{-4}	5.19 x10^{-2}	5.26 x10^{-2}	3.34	1.46 x10^{-2}	2.47	2.15 x10^{-2}	1.58

As can be seen in Fig. 21, the evolution of the Tafel slope, with the increase of the temperature, shows some improvement of the performance of the electrodes, having more current density at the same voltage variation. The addition of the KOH increase the electrocatalytic activity for HER.

In the Fig. 22, we have the comparison of the Tafel plot from 3 electrodes before and after adding the KOH on the effluent at 25ºC. From this graph, is possible to see that the platinum electrode has the best performance of HER, while the SS304 has the worst performance at the same voltage variation.

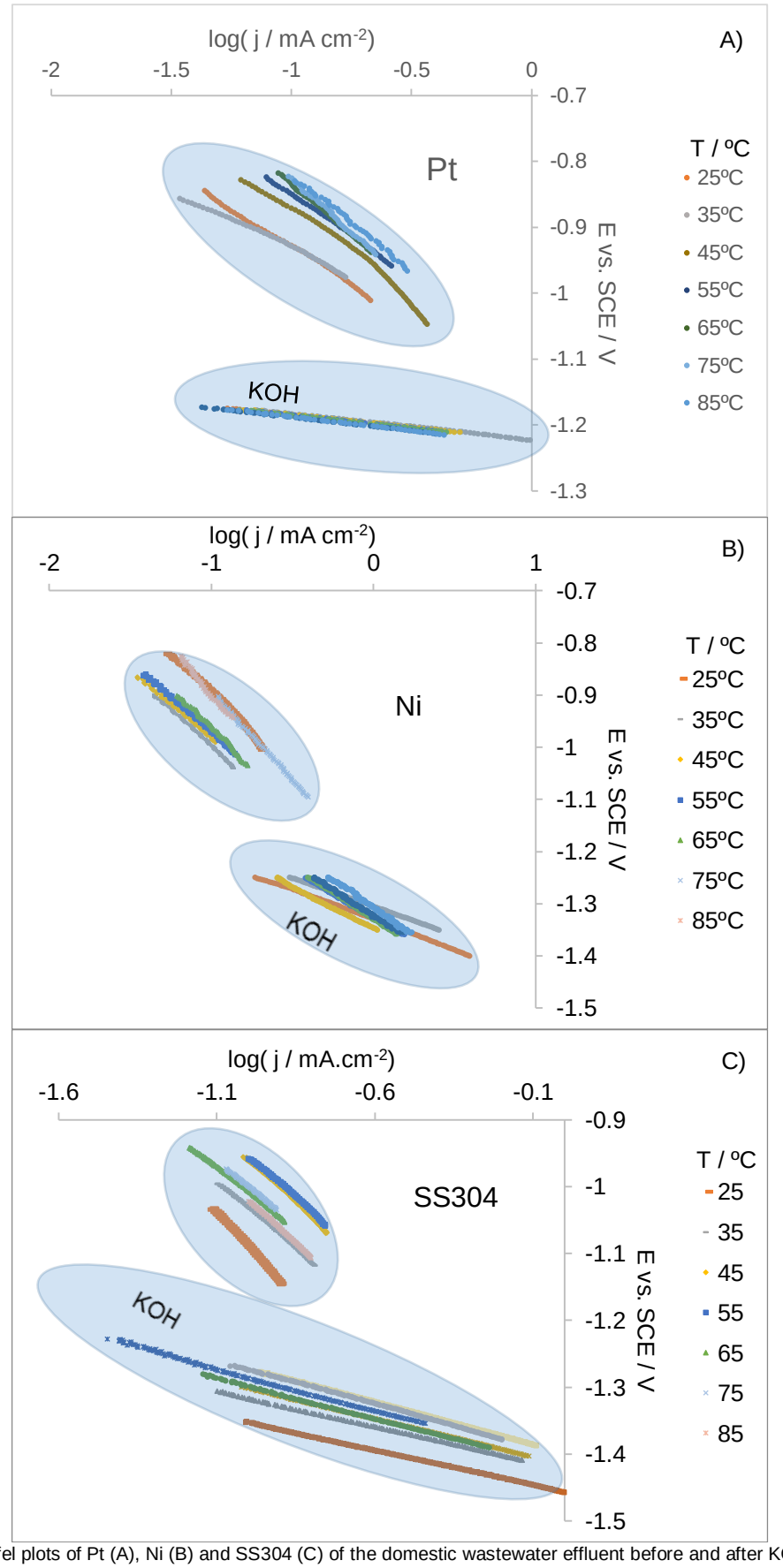

Fig. 21 – Tafel plots of Pt (A), Ni (B) and SS304 (C) of the domestic wastewater effluent before and after KOH addition.

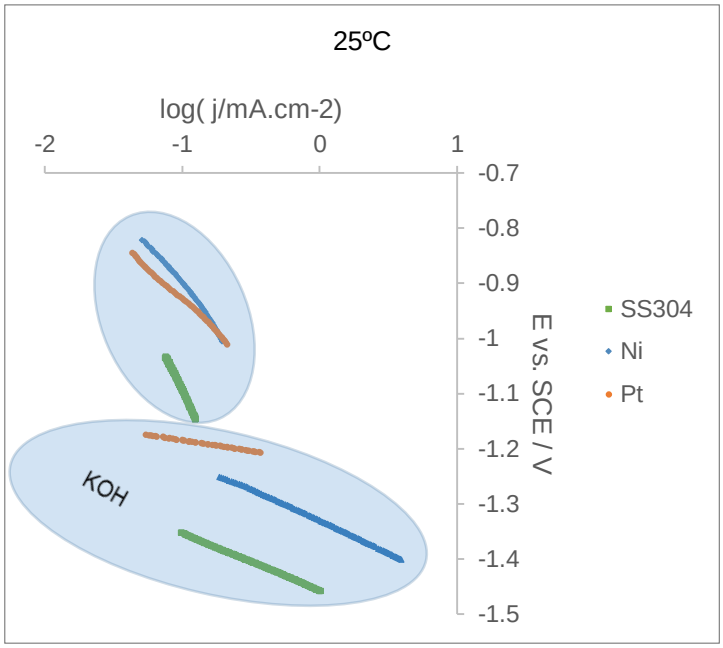

Fig. 22 – Comparison of Tafel plots at 25ºC of Pt (A), Ni (B) and SS304 (C) of the domestic wastewater effluent before and after KOH addition.

5.4. Activation energy

Because of the oscillation of all the results, it is not possible to apply the concept of the Arrhenius plot, in order to calculate the apparent activation energy using the Arrhenius equation (Eq. 28), except for the Ni electrode after KOH addition with Tafel method, which is the only one that has consistent results to do that.

$$\log j_0 = \log A - E_a/(2.3RT) \qquad \textit{Eq. 28}$$

Where A is the Arrhenius pre-exponential factor, E_a the activation energy. The Fig. 23 represents the plot of the logarithm of the exchange current density as a function of the reciprocal temperature and from the slope the E_a is obtained with a value of 228 kJ mol^{-1}. This kind of E_a value is high compared to other works with similar electrode material (46-71 kJ mol^{-1}).[16]

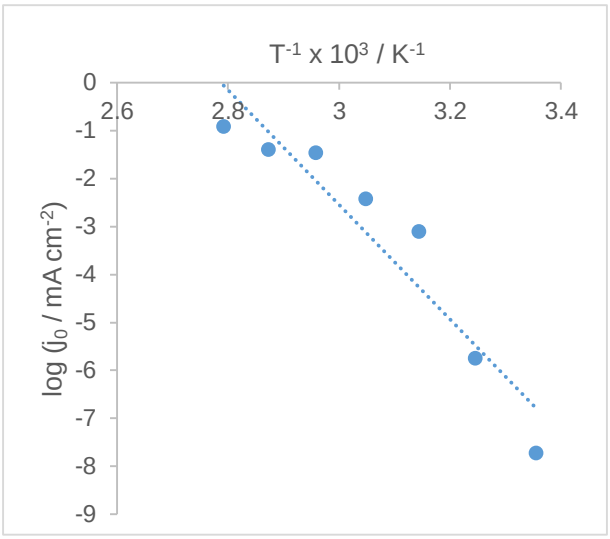

Fig. 23 - Arrhenius plot for Ni electrode with KOH

5.5. Anodic voltammetry scan of the wastewater

After the cathodic process, it comes the anodic process of the wastewater effluent before and after adding the KOH, and a 5M KOH solution with a platinum electrode. As would be expected, the KOH increased the current density of the solution and the presence of the OH^-, increased the electrochemical activity of the organic oxidation forming an anodic peak on each scan rate. The Fig. 24, represents the polarization curves from the OCP to 0.5 V vs SCE at different scan rates, of the domestic wastewater after adding the KOH, where it shows an increase of the current density with the scan rate. The peaks potential, from the anodic scan rate of the effluent with 5M, were then measured and from it, the α and the n values were calculated (Table 17).

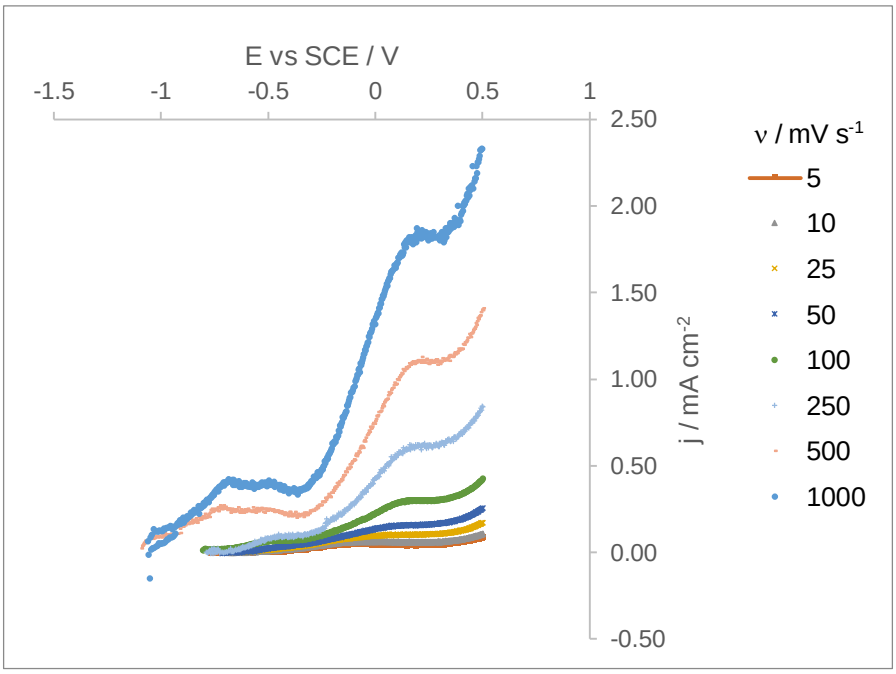

Fig. 24 – Anodic polarization curves of Pt of the domestic wastewater effluent after KOH addition.

Table 17 – Parameters of anodic peaks potential of effluent with KOH with Pt electrode.

ν (mV s^{-1})	E_p (V)	i (A)	Scan rate (V s^{-1})	ln ν	η	$E_{p/2}$	n	α
5	-0.0315	5.09E-05	0.005	-5.298	0.7420	-0.300	0.20	0.89
10	-0.064	6.57E-05	0.01	-4.605	0.6347	-0.295	0.23	
25	0.0265	9.85E-05	0.025	-3.688	0.7292	-0.300	0.16	
50	0.0787	1.52E-04	0.05	-2.995	0.7942	-0.153	0.23	
100	0.1529	2.96E-04	0.1	-2.302	0.9585	-0.125	0.19	
250	0.1612	6.03E-04	0.25	-1.386	0.9514	-0.080	0.22	
500	0.1692	1.09E-03	0.5	-0.693	1.2644	-0.090	0.21	
1000	0.1778	1.78E-03	1	0	1.2385	-0.130	0.17	

It was also analysed, the effluent+KOH subtracted with the water+KOH, which was not possible to calculate the *n* (Table 18), because it was impossible to retrieve the half-peak potential.

Table 18 – Parameters of anodic peaks potential of the difference between effluent with KOH and water with KOH with Pt electrode.

ν(mV s^{-1})	E (V)	i (A)	Scan rate (V s^{-1})	ln ν	η (V)	α
5	-0.0715	4.77E-05	0.005	-5.298	0.654	0.88
10	0.0517	5.82E-05	0.01	-4.605	0.705	
25	0.0525	7.16E-05	0.025	-3.688	0.710	
50	0.0932	1.50E-04	0.05	-2.995	0.763	
100	0.1454	2.79E-04	0.1	-2.302	0.899	
250	0.1612	4.04E-04	0.25	-1.386	0.892	
500	0.1692	7.91E-04	0.5	-0.693	1.204	
1000	0.1778	1.38E-03	1	0	1.176	

6. Conclusions

On both kind of used electrolyte, before and after the KOH, there is an oscillation on the results of j_0 with the increase of the temperature. Since that during the voltammetry scan there was some “noise” and the fact that the effluent has many different species in, it might have triggered some reaction with the change of temperatures especially with the addition of the KOH, which means that all this might have affected the behaviour of the polarisation curves during the process.

The addition of KOH in the effluent had produced more current density and produced more hydrogen bubbles than before it. The charge transfer coefficient also increases very significantly with its presence, indicating the influence of KOH, not only in the conductivity but also on the possibility that might have triggered some reaction with some species present in the effluent, causing more water molecules to get electrochemically reduced.

In comparison, in terms of kinetics of HER, after the addition of KOH the catalytic activity improves considerably in all the electrodes, as evaluated for both Tafel and Butler-Volmer methods. The activation energy given from the Arrhenius plot of Ni electrode with KOH, has a value of 228 kJ mol^{-1}.

Despite some inconsistency in the results, according to the CV diagrams, the Platine-rare earth electrodes have shown overall to be the electrodes that get the highest current densities at a given voltage. The curves from Platine, nickel and nickel-rare earth electrodes have similar behaviour compared with each other, when using just the effluent. After adding the KOH, the Pt gets bigger current

densities at higher temperatures at a given voltage than Ni and Ni-RE. The SS304 electrode, compared to all, is the one that shows the lowest current density at a given voltage.

From the information obtained from the anodic scan with Pt electrode on the effluent+KOH, there is an oxidation of the organic compounds present in the wastewater and the α and n values were around 0.89 and 0.20 respectively.

As for the synthetic urine, despite of not having stable results, it shows the possibility to produce hydrogen from an organic matter solution and with an electric conductivity about 10 times higher than the wastewater. It got a reasonable current density during the experiment and a formation of hydrogen bubbles.

7. Bibliography

[1] *"That Bill Gates Shit-Water Machine Might Actually Change the World"*, VICE Media LLC, January 8, 2015

[2] WANG, Qian, JIN, Tao, HU, Zhongxin, ZHOU, Lei, ZHOU, Minghua (2013) *"TiO2-NTs/SnO2-Sb anode for efficient electrocatalytic degradation of organic pollutants: Effect of TiO2-NTs architecture"*, Separation and Purification Technology 102.

[3] MA, Wei, CHENG, Zihong, GAO, Zhanxian, WANG, Ren, WANG, Baodong, SUN, Xi (2014) *"Study of hydrogen gas production coupled with phenol electrochemical oxidation degradation at different stages"*, Chemical Engineering Journal 241.

[4] ZAYAS, Teresa, PICAZO, Mario (2011) *"Removal of Organic Matter from Paper Mill Effluent by Electrochemical Oxidation"*, Journal of Water Resource Protection, 3, 32-40.

[5] DAGHRIR, Rimeh, DROGUI, Patrick, TSHIBAGU, Joel (2014) *"Efficient treatment of domestic wastewater by electrochemical oxidation process using bored doped diamond anode"*, Separation and Purification Technology 131.

[6] CHO, Kangwoo, KWON, Daejong, HOFFMAN, Michael R. (2014) *"Electrochemical treatment of human waste coupled with molecular hydrogen production"*, RSC Advances.

[7] NIU, Jungfeng, MAHARANA, Dusmant, XU, Jiale, CHAI, Zhen, BAO, Yueping (2013) *"A high activity of Ti/SnO2-Sb electrode in the electrochemical degradation of 2,4-dichlorophenol in aqueous solution"*, Journal of Environmental Sciences 25(7) 1424–1430.

[8] YOON, Jang-Hee, SHIM, Yoon-Bo, LEE, Byoung-Seob, CHOI, Se Yong, WON, Mi-Sook (2012) *"Electrochemical Degradation of Phenol and 2-Chlorophenol Using Pt/Ti and Boron-Doped Diamond Electrodes"*, Bull. Korean Chem. Soc. Vol. 33, No. 7

[9] CAO, Jie-Ping, FANG, Ting, FU, Ling-Zhi, ZHOU, Ling-Ling, ZHAN, Shuzhong (2014) *"A nickel molecular electro-catalyst for generating hydrogen from acetic acid or water"*, International Journal of Hydrogen Energy.

[10] RAUSCH, Benjamin, SYMES, Mark D., CHISHOLM, Greig, CRONIN, Leroy (2014) *"Decoupled catalytic hydrogen evolution from a molecular metal oxide redox mediator in water splitting"*, Science 345, 1326.

[11] BARD, Allen J., FAULKER, Larry R. (2001) *"Electrochemical Methods: Fundamentals and Applications 2nd Edition"*, John Wiley & Sons, Inc.

[12] http://chemwiki.ucdavis.edu/Analytical_Chemistry/Analytical_Chemistry_2.0/11_Electrochemical_Methods

[13] ZOSKI, Cynthia (2007) *"Handbook of Electrochemistry"*, Elsevier.

[14] SOBKOWIAK, Andrzej, SAWYER, Donald T., ROBERTS, Julian L. (1995) *"Electrochemistry for Chemists"*, Wiley-Interscience.

[15] HENZE, Mogens, LOOSDRECHT, Mark van, EKAMA, George, BRDJANOVIC, Damir (2008) *"Biological Wastewater Treatment: Principles, Modelling and Design"*, IWA Publishing.

[16] SANTOS, D.M.F., AMARAL, L., ŠLJUKIĆ, B., MACCIÒ, D., SACCONE, A., SEQUEIRA, C.A.C. (2014) *"Electrocatalytic activity of nickel-cerium alloys for hydrogen evolution in alkaline water electrolysis"*, Journal of The Electrochemical Society 161/4 F386-F390.

[17] CARDOSO, D.S.P., SANTOS, D.M.F., AMARAL, L., ŠLJUKIĆ, B., MACCIÒ, D., SACCONE, A., SEQUEIRA, C.A.C. (2015) *"Enhancement of hydrogen evolution in alkaline water electrolysis by using nickel-rare earth alloys"*. International Journal of Hydrogen Energy 40 (2015) 4295-4302.

[18] SANTOS, D.M.F., FIGUEIREDO, J.L., MACCIÒ, D., SACCONE, A., SEQUEIRA, C.A.C. (2013) *"Platinum-rare earth electrodes for hydrogen evolution in alkaline water electrolysis"*. International Journal of Hydrogen Energy 38 (2013) 3137-3145.

[19] SANTOS, D.M.F., ŠLJUKIĆ, B., SEQUEIRA, C.A.C., MACCIÒ, D., SACCONE, A., FIGUEIREDO, J.L. (2013) *"Electrocatalytic approach for the efficiency increase of electrolytic hydrogen production: proof-of-concept using Pt-Dy"*. Energy 50 486-492.

[20] LAUBE, Norbert, MOHR, Bernhard, HESSE, Albrecht (2001) *"Laser-probe-based investigation of the evolution of particle size distributions of calcium oxalate particles formed in artificial urines"*, Journal of Crystal Growth. 233, 367–374.

[21] BOGGS, Bryan K., KING, Rebecca L., BOTTE, Gerardine G. (2009) *"Urea electrolysis: direct hydrogen production from urine"*, The Royal Society of Chemistry.

[22] CUSSLER, E. L. (1984) *"Diffusion - mass transfer in fluid systems"*, Cambridge University Press, Cambridge, United Kingdom.

[23] LIAO, Lei, ZHU, Zie, BIAN, Xiaojun, ZHU, Lina, SCANLON, Michéal D., GIRAULT, Hubert H., LIU, Baohung (2013) *"MoS_2 Formed on Mesoporous Graphene as a Highly Active Catalyst for Hydrogen Evolution"*, Adv. Funct. Mater. 23, 5326-5333.

[24] PULKKA, Susanna, MARTIKAINEN, Mika, BHATNAGAR, Amit, SILLANPÄÄ, Mika (2014) *"Electrochemical methods for the removal of anionic contaminants from water – A review"*, Separation and Purification Technology 132.

[25] MENG, Yao, ALDOUS, Leigh, BELDING, Stephen R., COMPTON, Richard G. (2012) *"The hydrogen evolution reaction in a room temperature ionic liquid: mechanism and electrocatalyst trends"*, RSC PCCP.

[26] GUNASEKARA, Saman Nimali (2011) *"Improvements on Municipal Wastewater Treatment by: Chemical precipitation with Ca^{2+} & Mg^{2+} and acid hydrolysis of toilet paper"*, Royal Institute of Technology.

[27] SELEMBO, Priscila A., MERRIL, Mathew D., LOGAN, Bruce E. (2009) *"The use of stainless steel and nickel alloys as low-cost cathodes in microbial electrolysis cells"*, Journal of Power Sources, 190, 271–278.

[28] KOMORSKY-LOVRIĆ, Šebojka, LOVRIĆ, Milivoj (2014) *"Square-wave Voltammetry of Two-step Electrode Reaction"*, International Journal of Electrochemical Science 9, 435 – 444.

8. Appendix

8.1. Wastewater effluent without electrolyte addition

8.1.1. Platinum electrode

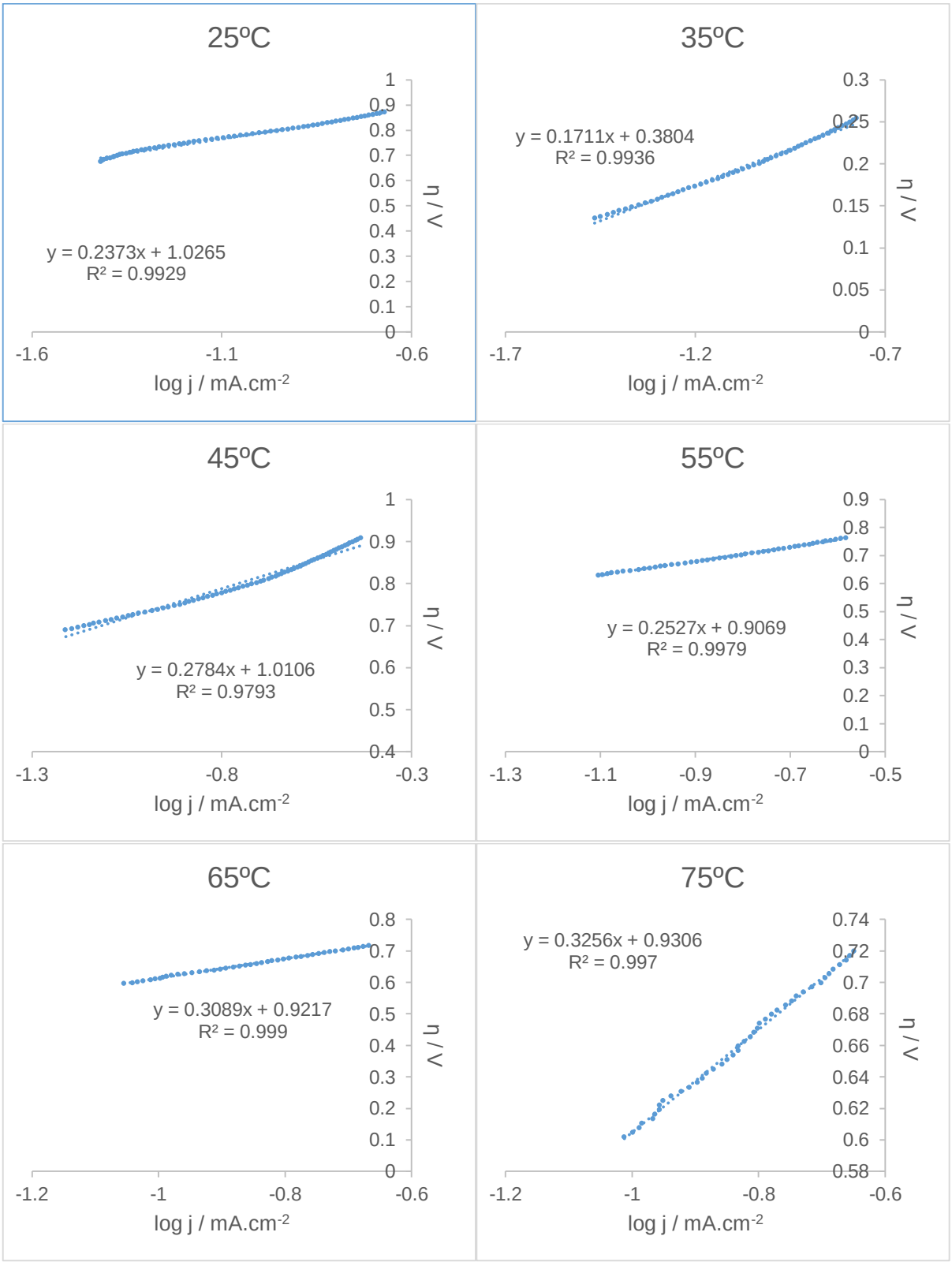

Fig. 25 - Tafel plots for different temperatures with Pt electrode of the domestic wastewater effluent.

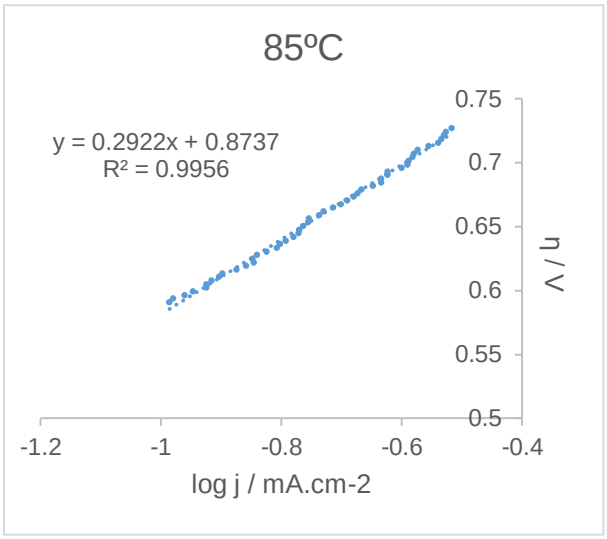

(cont.) Fig. 25 - Tafel plots for different temperatures with Pt electrode of the domestic wastewater effluent.

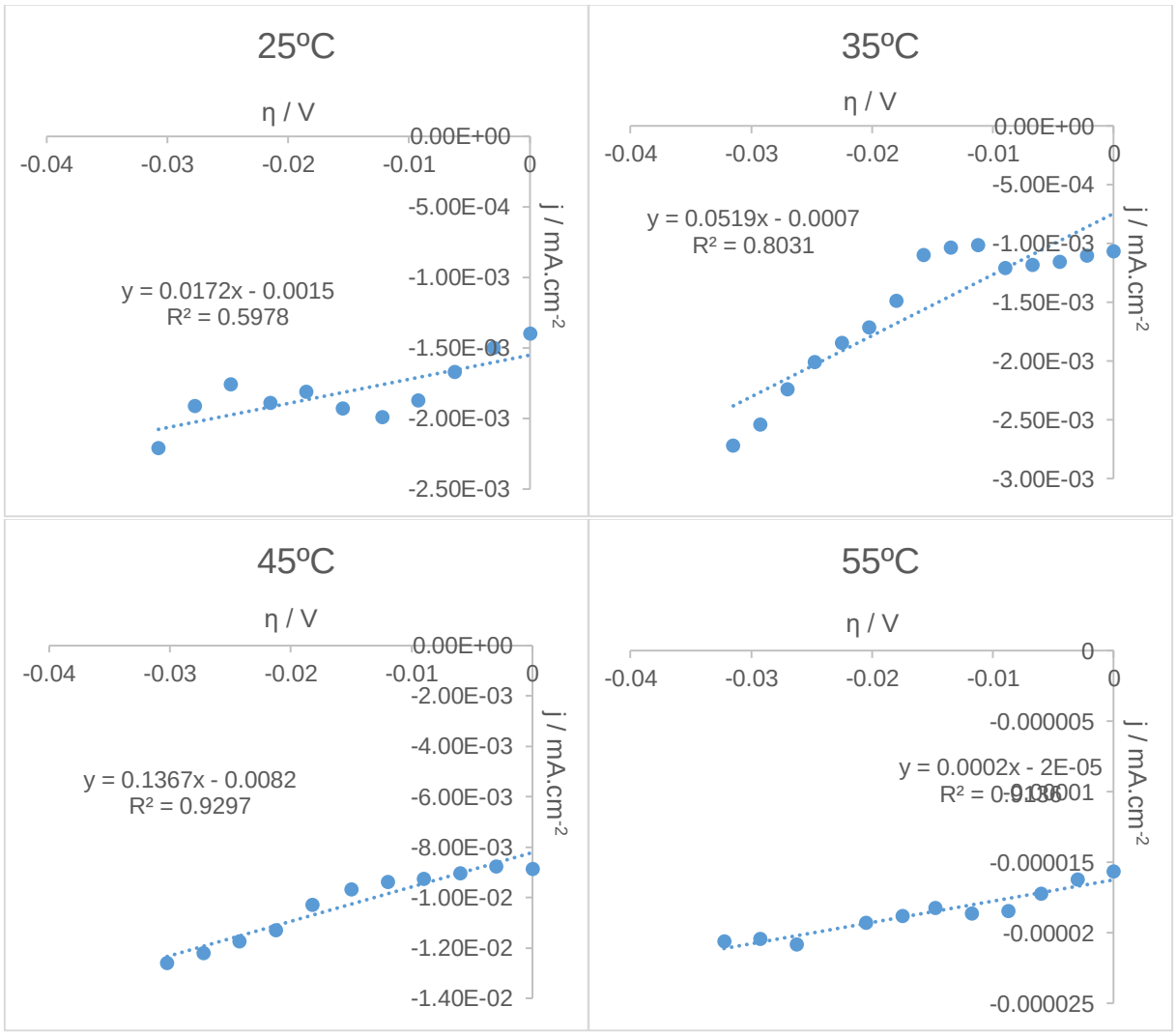

Fig. 26 - Low overvoltage representation with Pt electrode for Butler-Volmer equation of the domestic wastewater effluent.

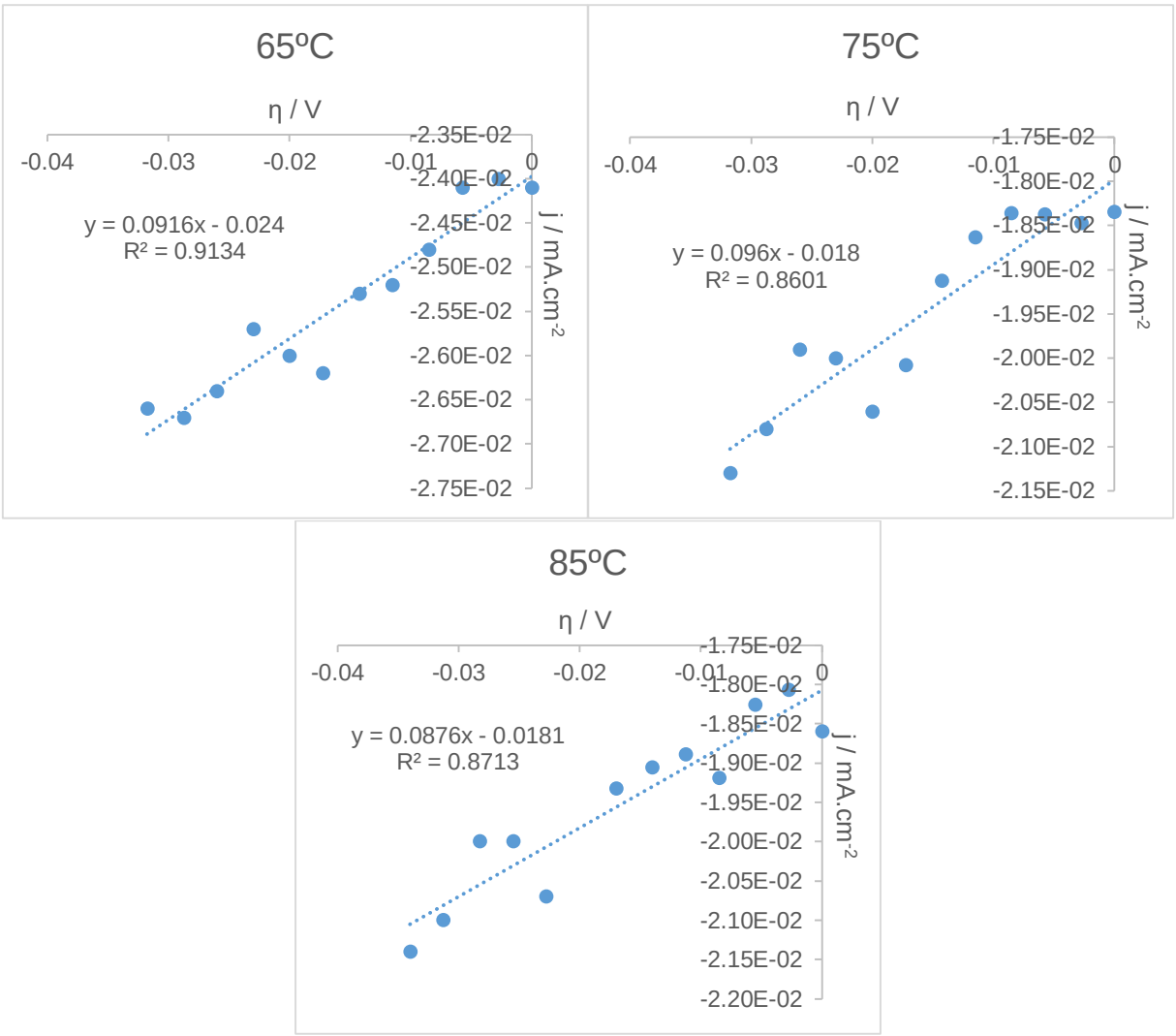

(cont.) Fig. 26 - Low overvoltage representation with Pt electrode for Butler-Volmer equation of the domestic wastewater effluent.

8.1.2. Nickel electrode

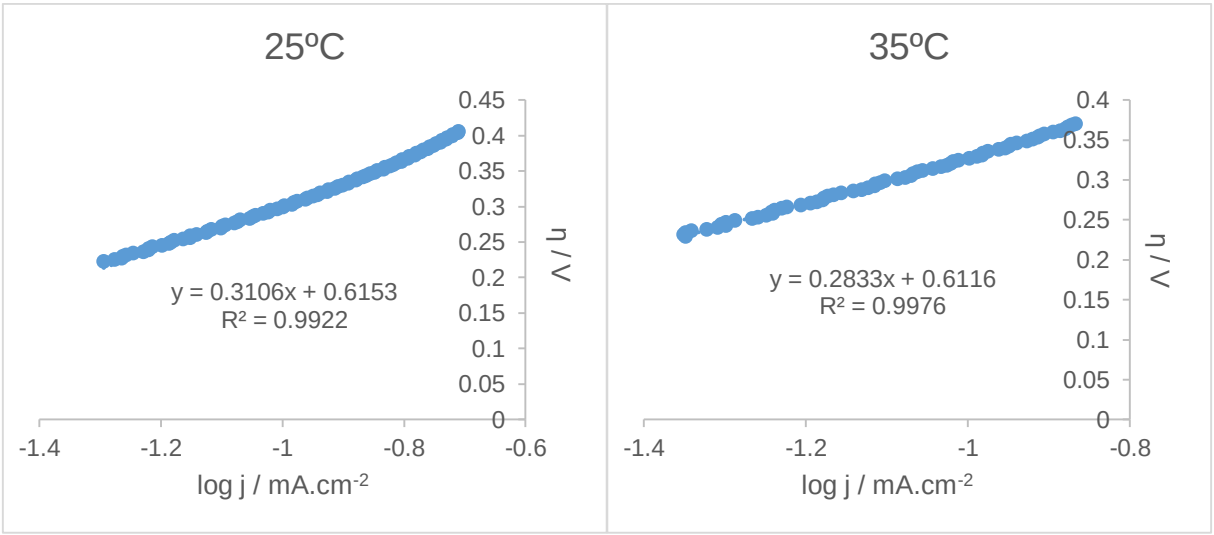

Fig. 27 - Tafel plots for different temperatures with Ni electrode of the domestic wastewater effluent.

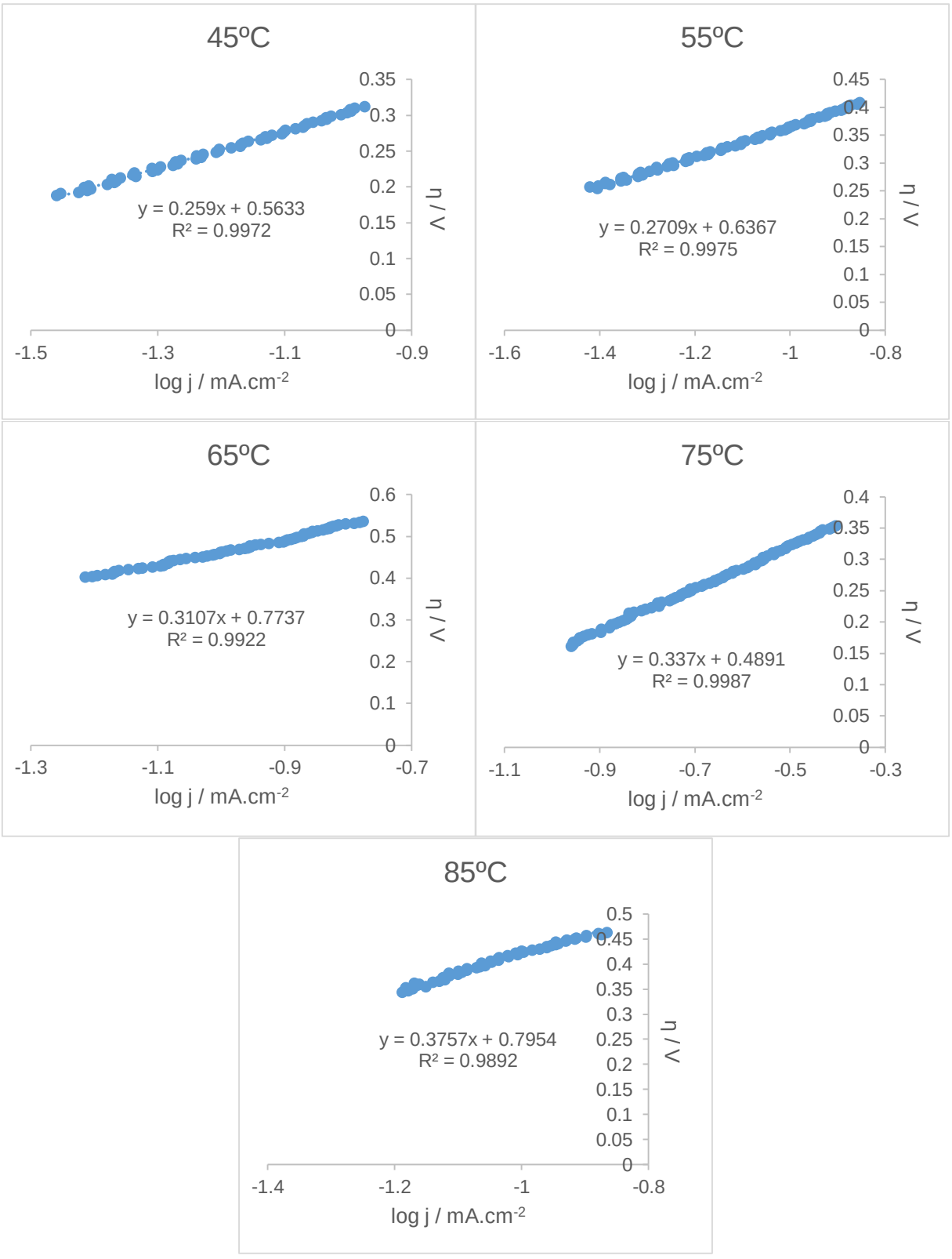

(cont.) Fig. 27 - Tafel plots for different temperatures with Ni electrode of the domestic wastewater effluent.

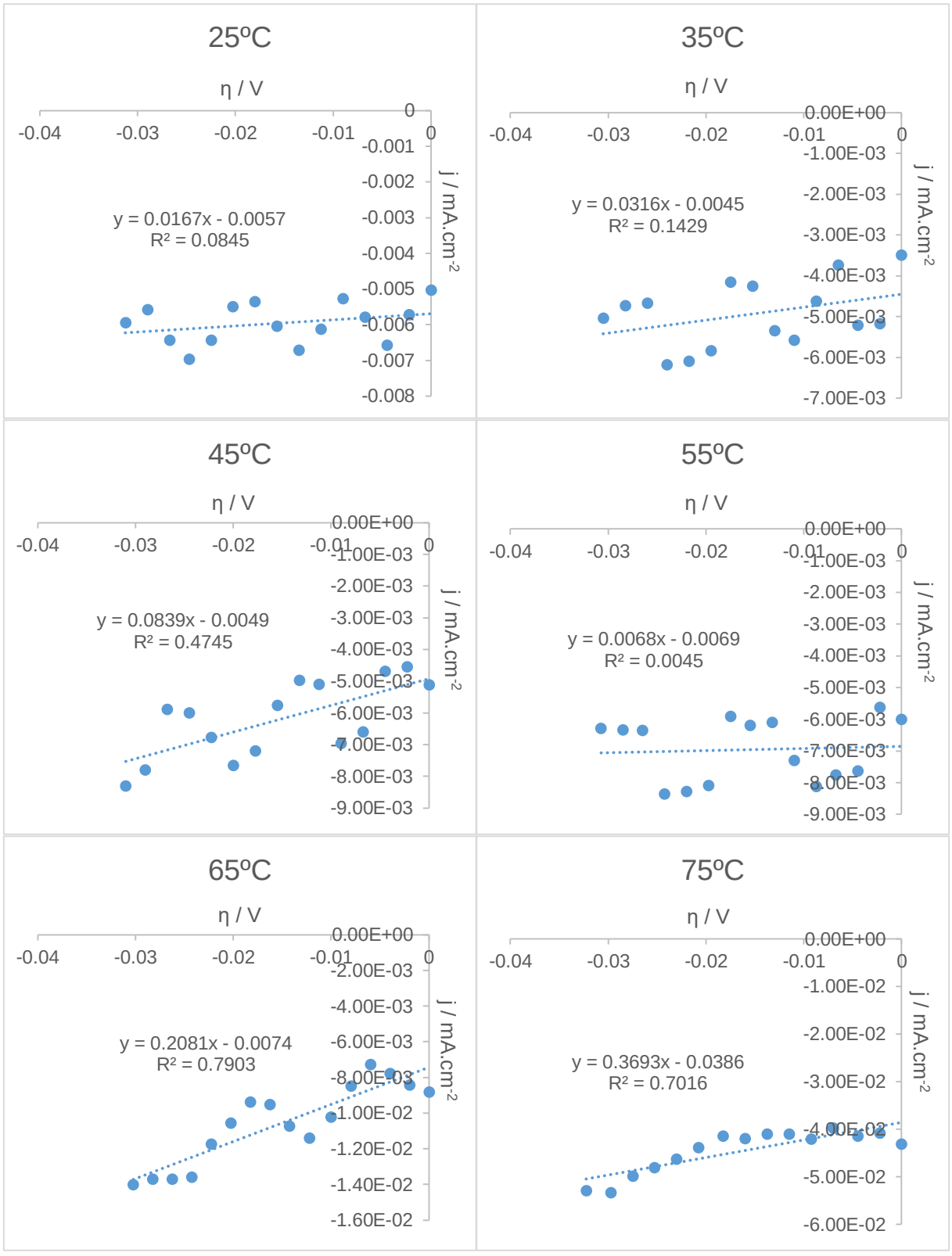

Fig. 28 - Low overvoltage representation with Ni electrode for Butler-Volmer equation of the domestic wastewater effluent.

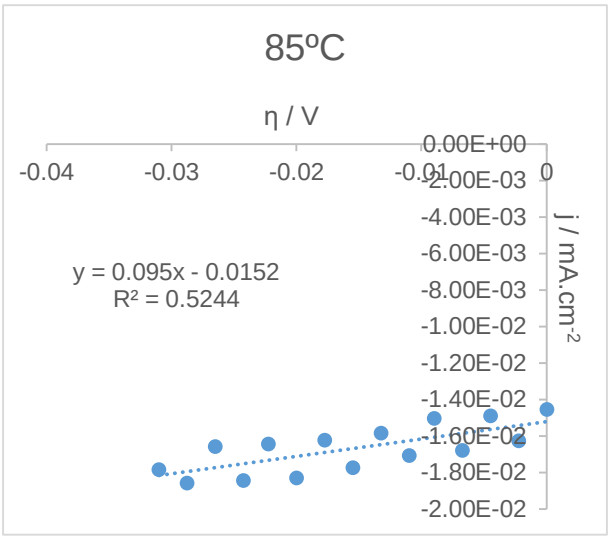

(cont.) Fig. 28 - Low overvoltage representation with Ni electrode for Butler-Volmer equation of the domestic wastewater effluent.

8.1.3. Stainless steel 304 electrode

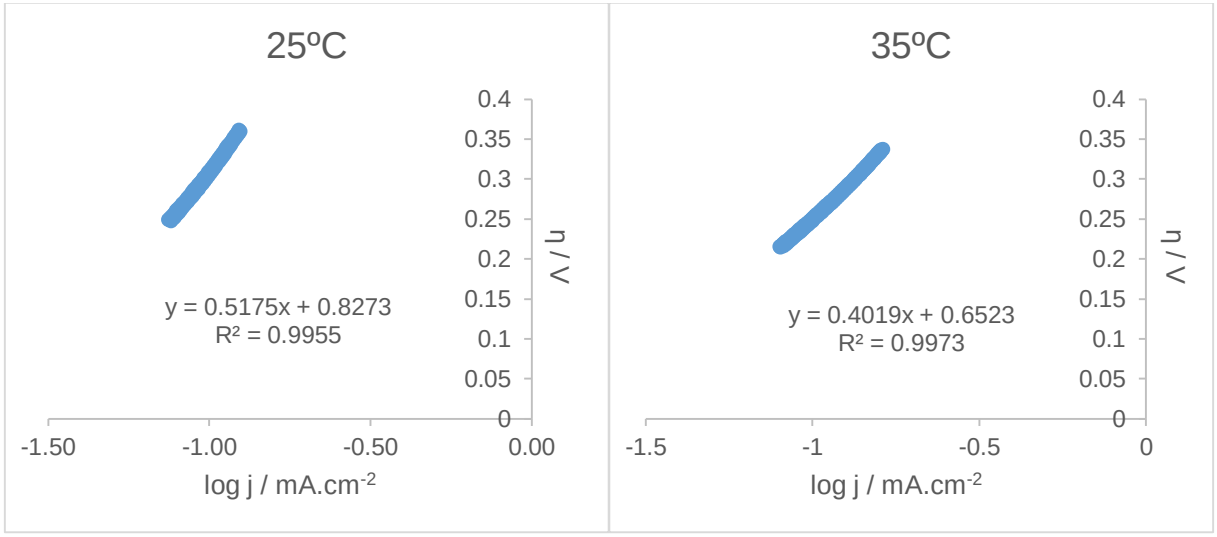

Fig. 29 - Tafel plots for different temperatures with SS304 electrode of the domestic wastewater effluent.

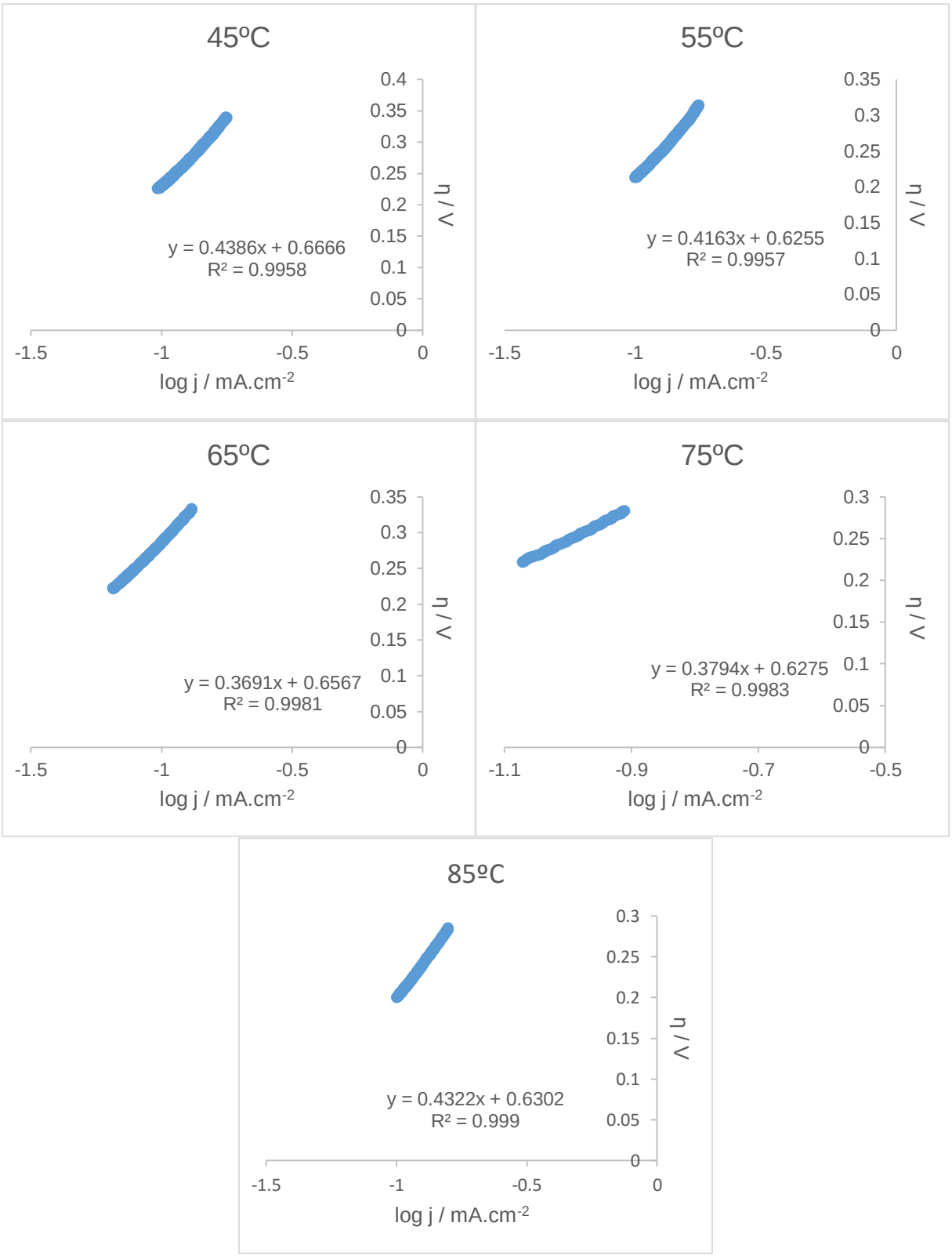

(cont.) Fig. 29 - Tafel plots for different temperatures with SS304 electrode of the domestic wastewater effluent.

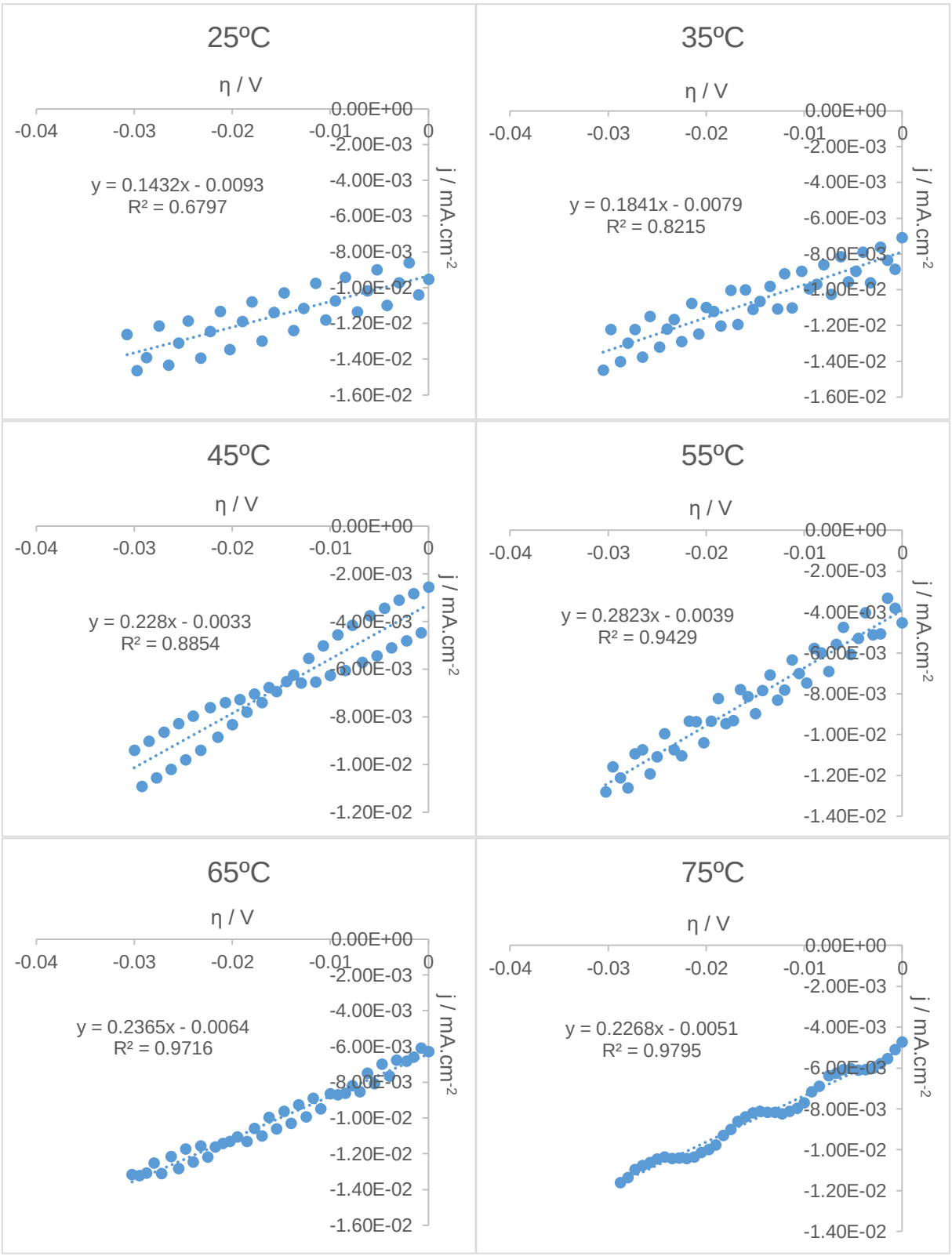

Fig. 30 - Low overvoltage representation with SS304 electrode for Butler-Volmer equation of the domestic wastewater effluent.

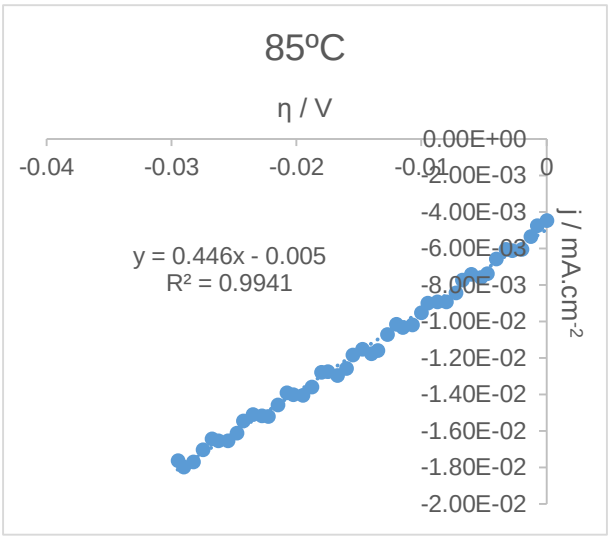

(cont.) Fig. 30 - Low overvoltage representation with SS304 electrode for Butler-Volmer equation of the domestic wastewater effluent.

8.1.4. Pt-Ce electrode

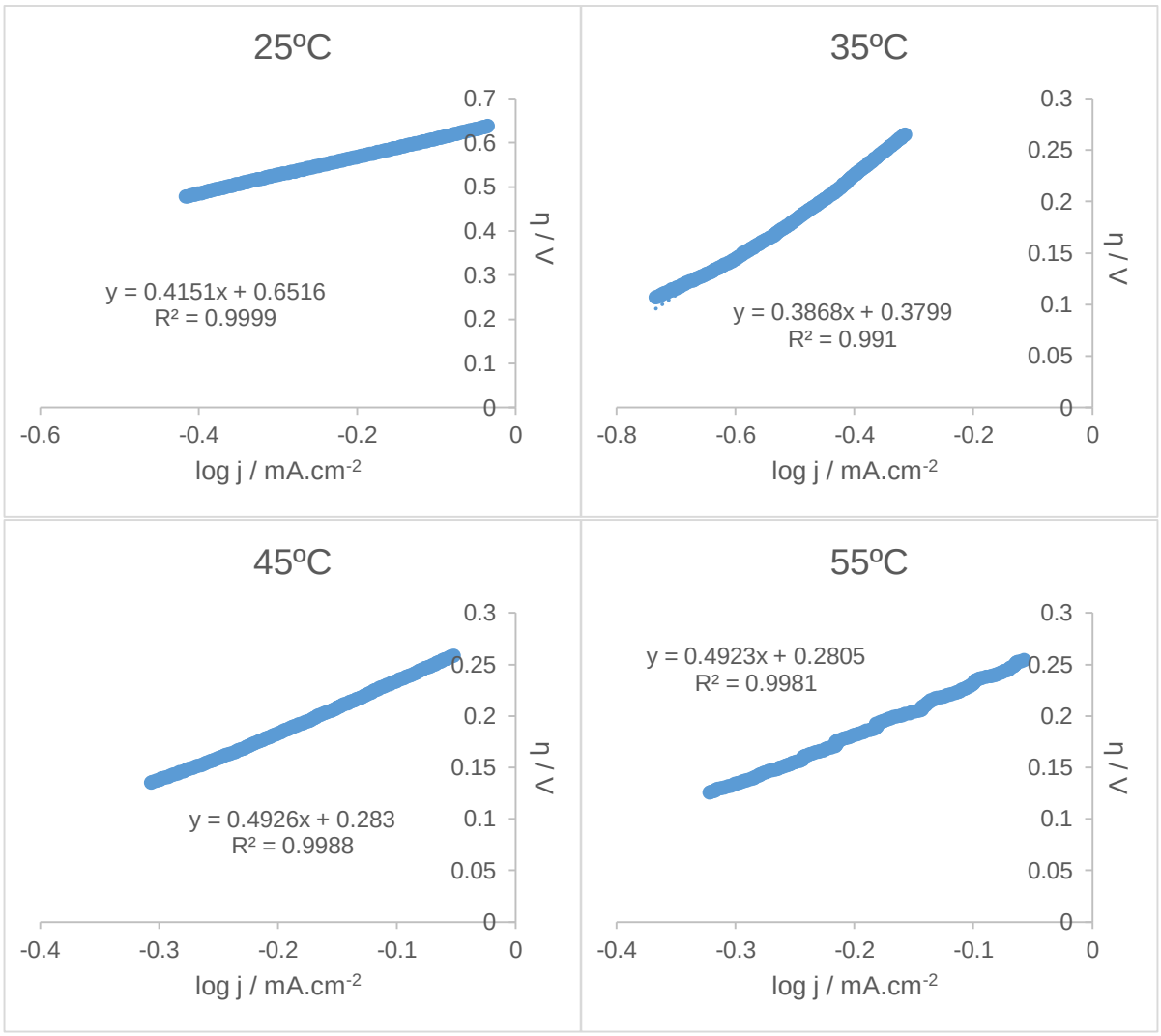

Fig. 31 - Tafel plots for different temperatures with Pt-Ce electrode of the domestic wastewater effluent.

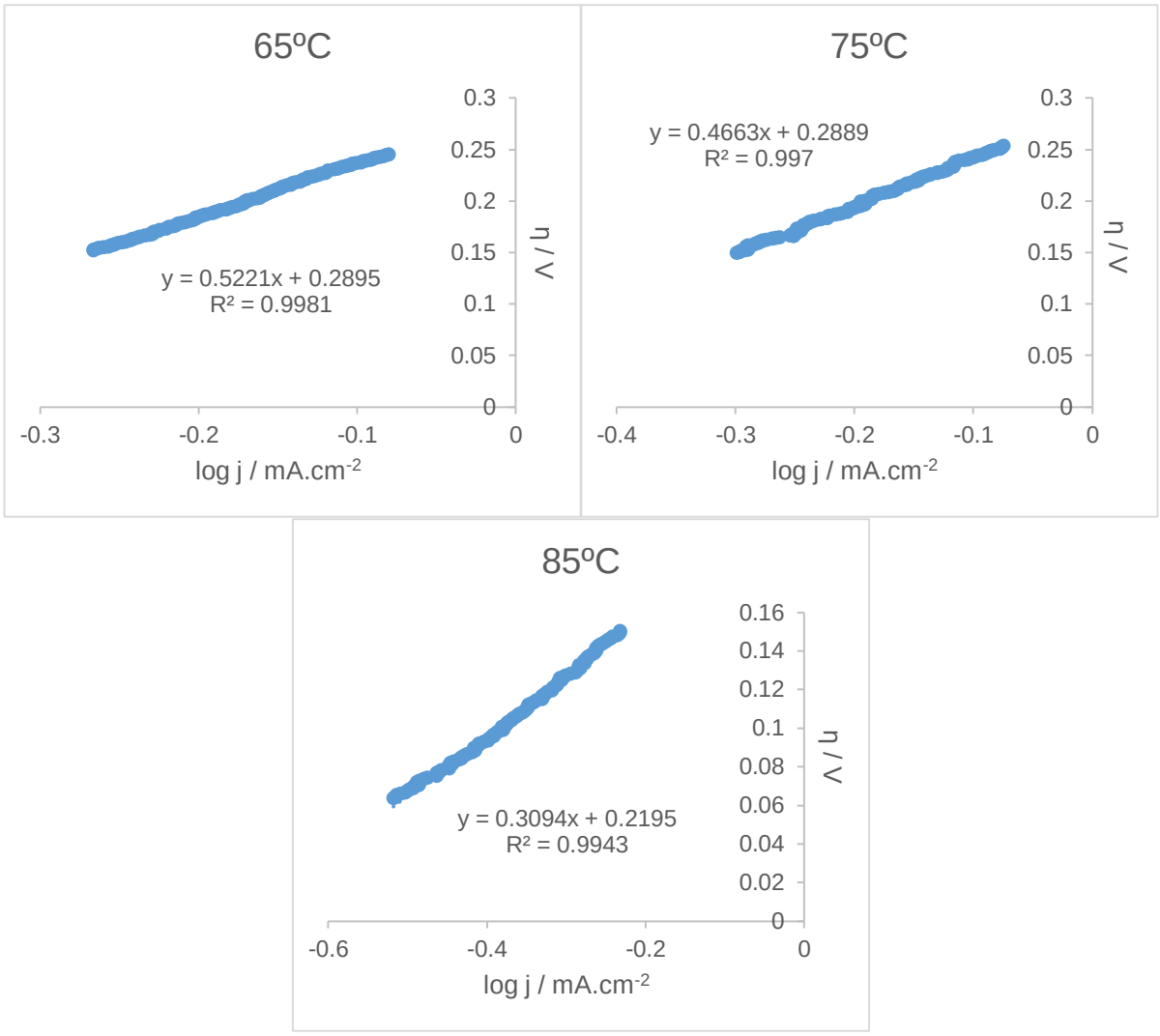

(cont.) Fig. 31 - Tafel plots for different temperatures with Pt-Ce electrode of the domestic wastewater effluent.

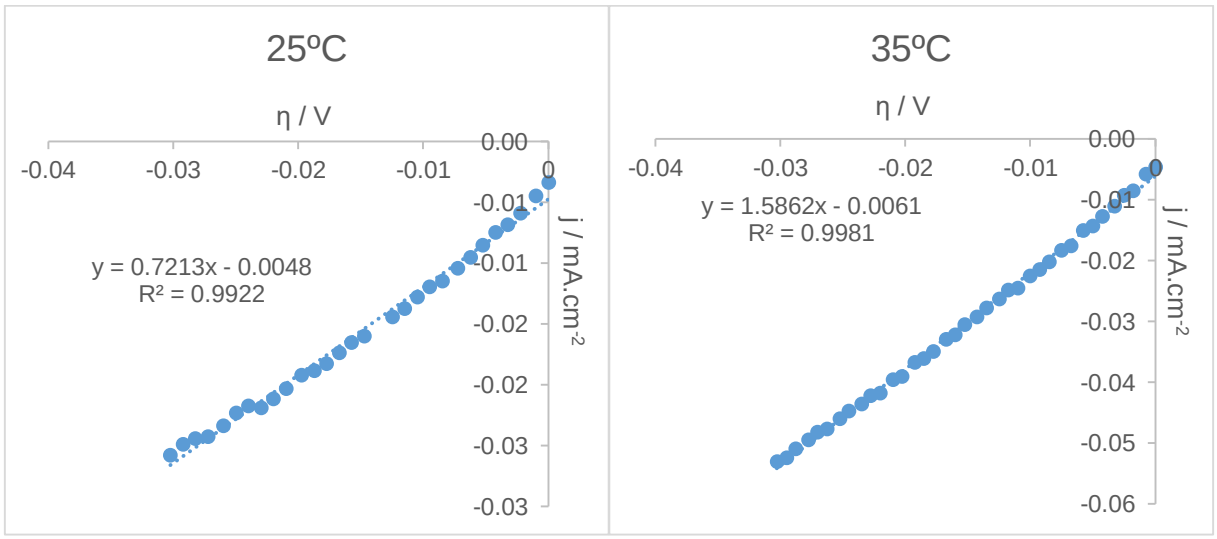

Fig. 32 - Low overvoltage representation with Pt-Ce electrode for Butler-Volmer equation of the domestic wastewater effluent.

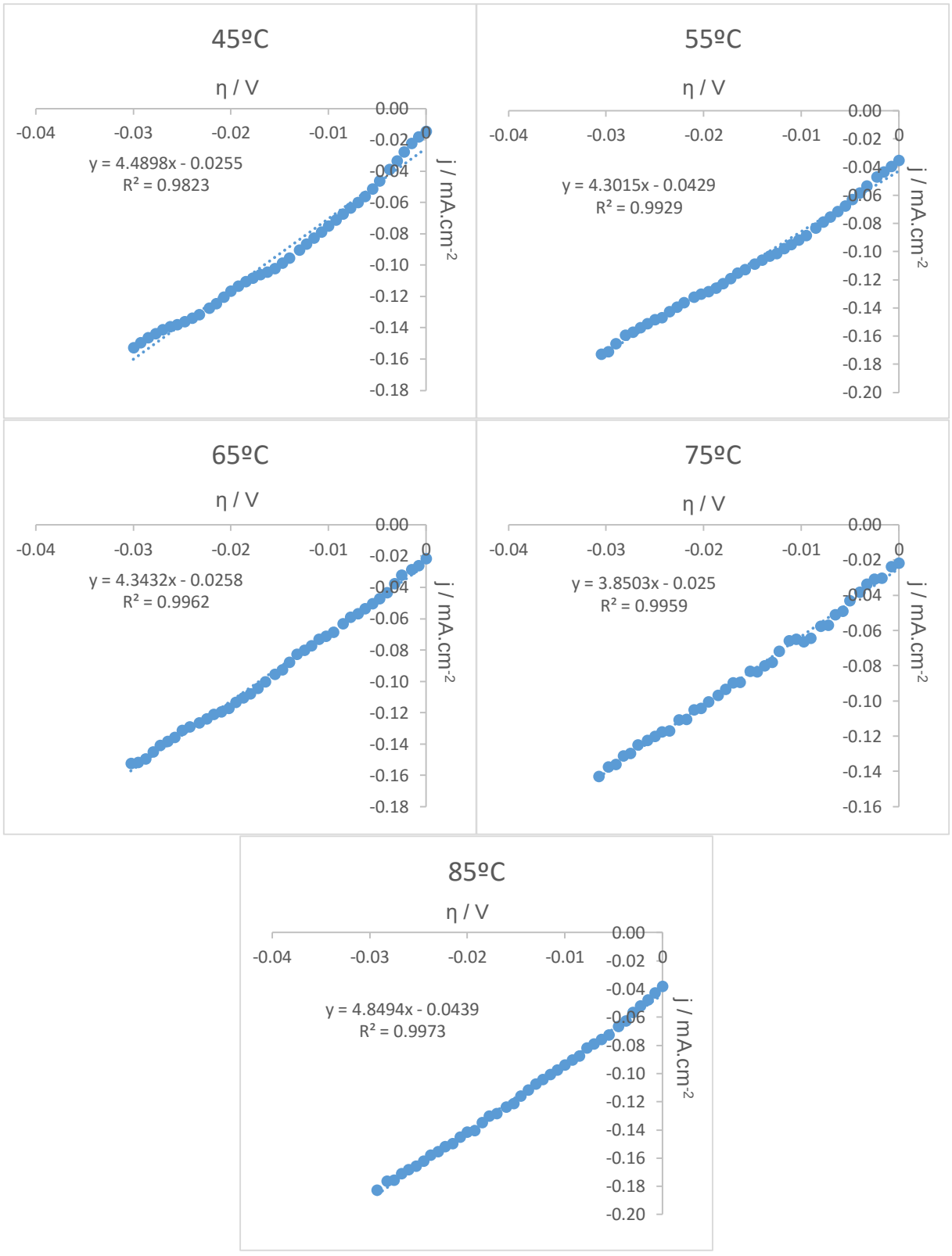

Fig. 32 - Low overvoltage representation with Pt-Ce electrode for Butler-Volmer equation of the domestic wastewater effluent.

8.1.5. Pt-Dy electrode

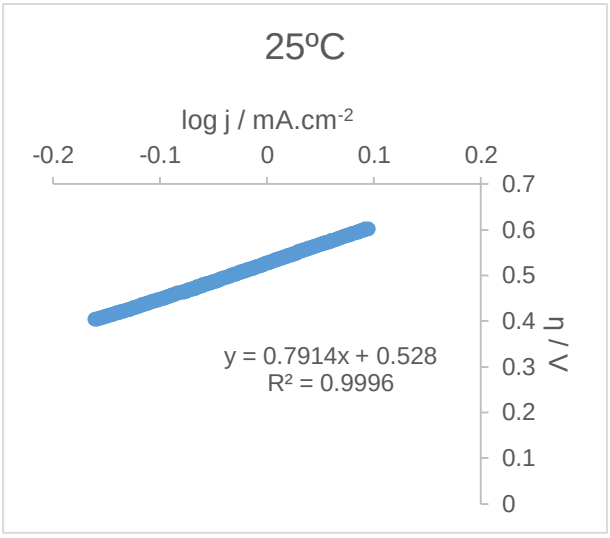

Fig. 33 - Tafel plots for different temperatures with Pt-Dy electrode

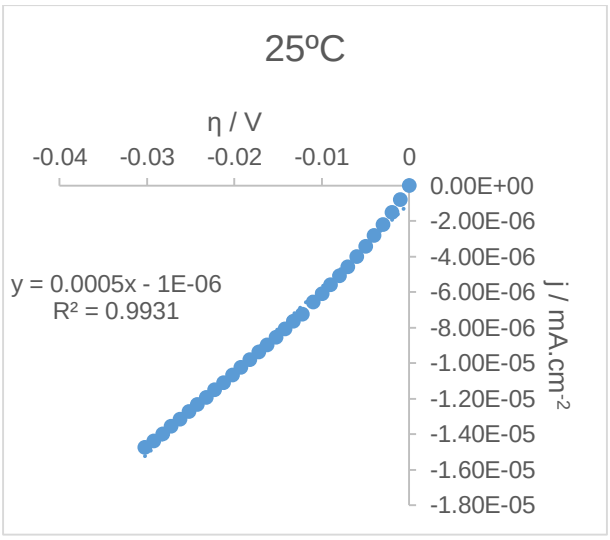

Fig. 34 - Low overvoltage representation with Pt-Dy electrode for Butler-Volmer equation of the domestic wastewater effluent.

8.1.6. Pt-Ho electrode

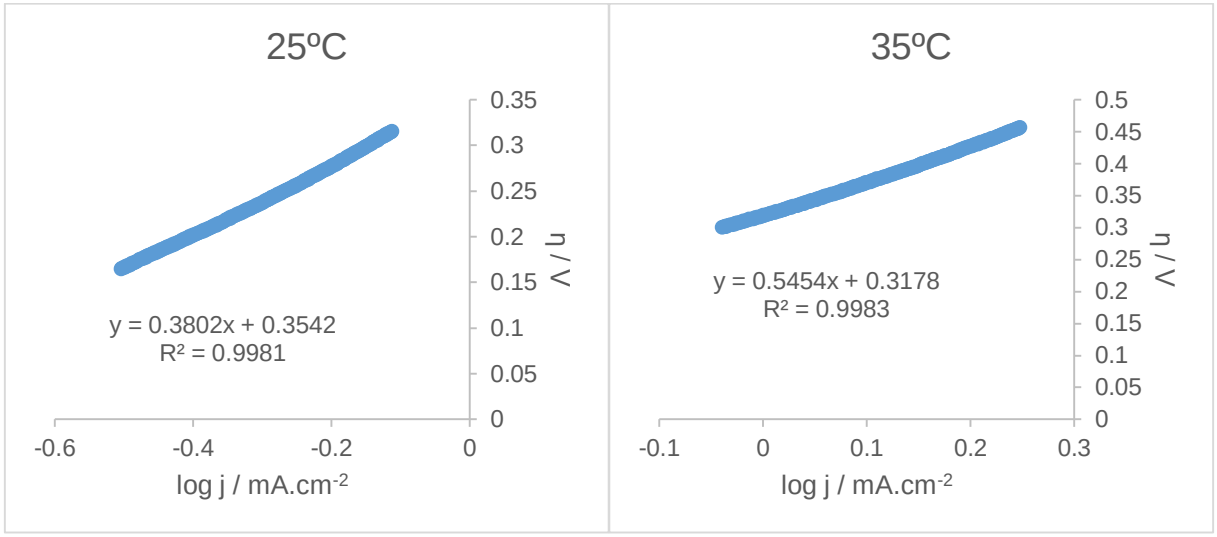

Fig. 35 - Tafel plots for different temperatures with Pt-Ho electrode of the domestic wastewater effluent.

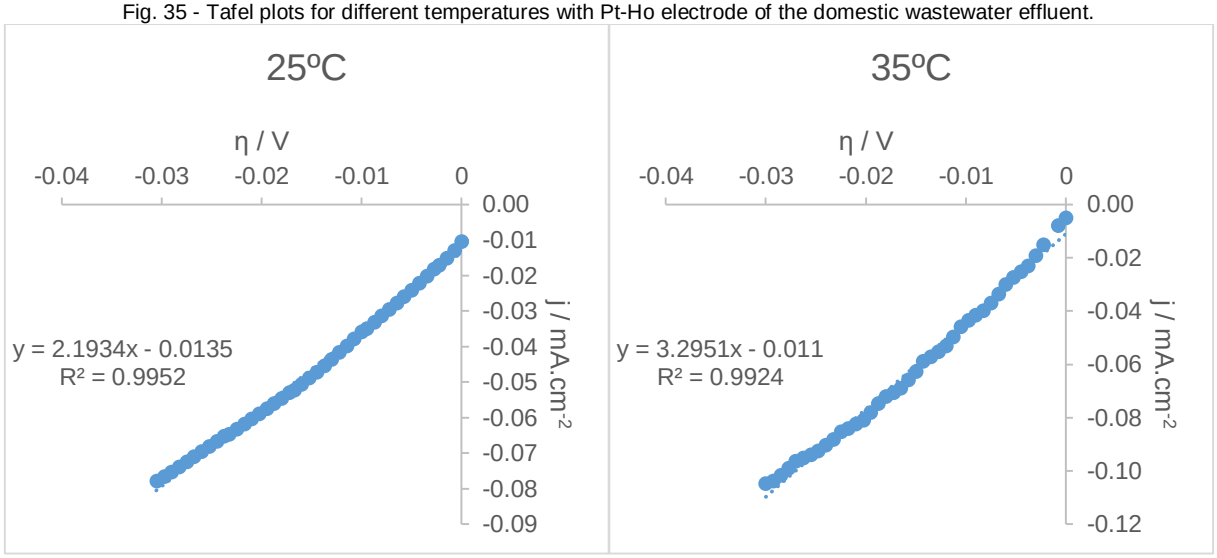

Fig. 36 - Low overvoltage representation with Pt-Ho electrode for Butler-Volmer equation of the domestic wastewater effluent.

8.1.7. Pt-Sm electrode

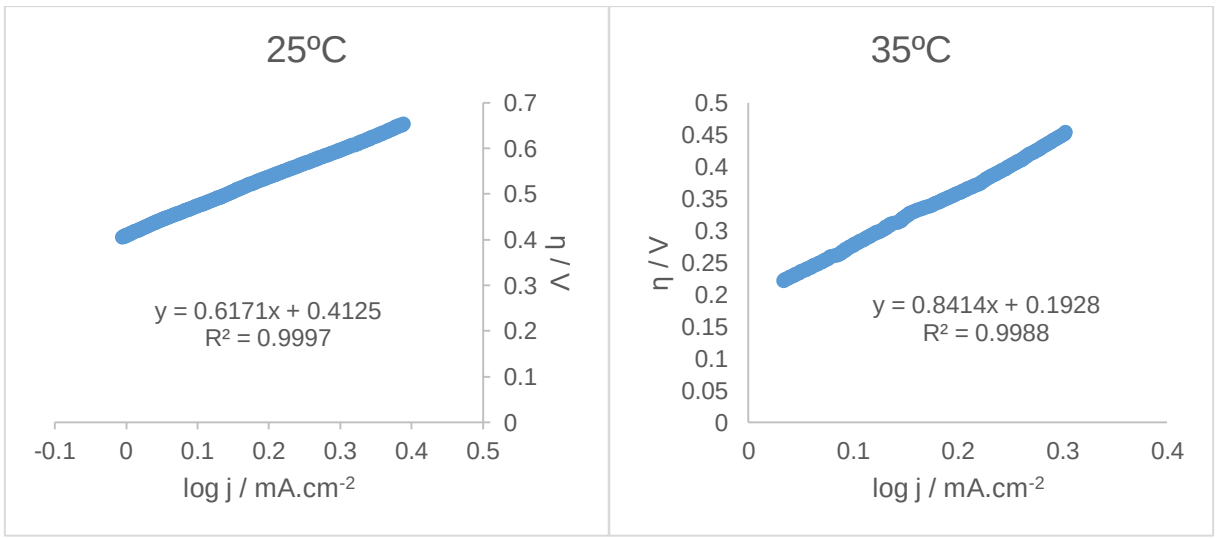

Fig. 37 - Tafel plots for different temperatures with Pt-Sm electrode of the domestic wastewater effluent.

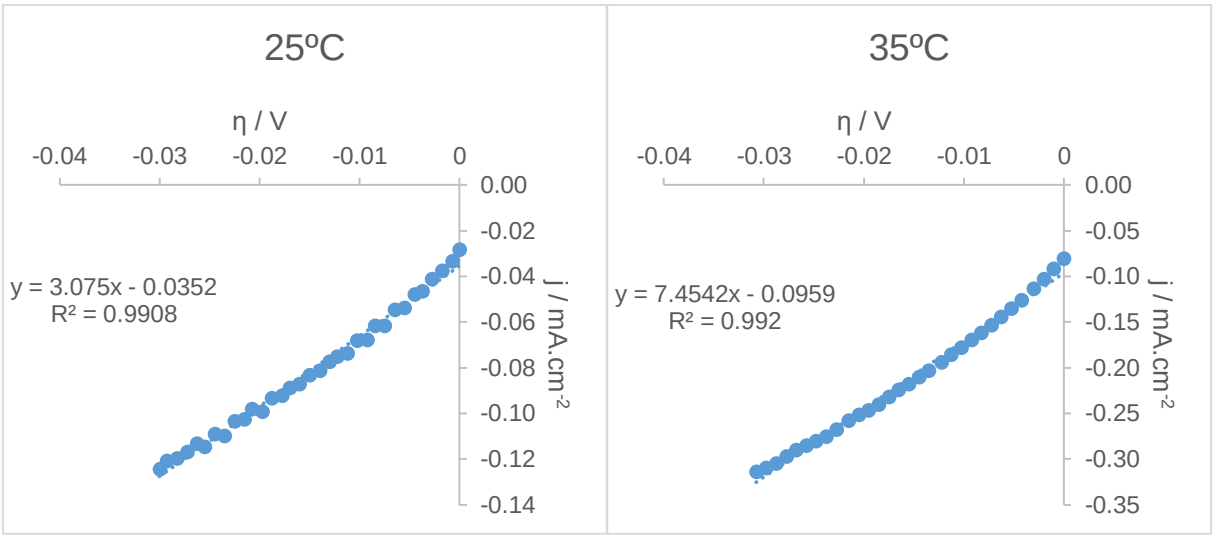

Fig. 38 - Low overvoltage representation with Pt-Sm electrode for Butler-Volmer equation of the domestic wastewater effluent.

8.1.8. Ni-Ce electrode

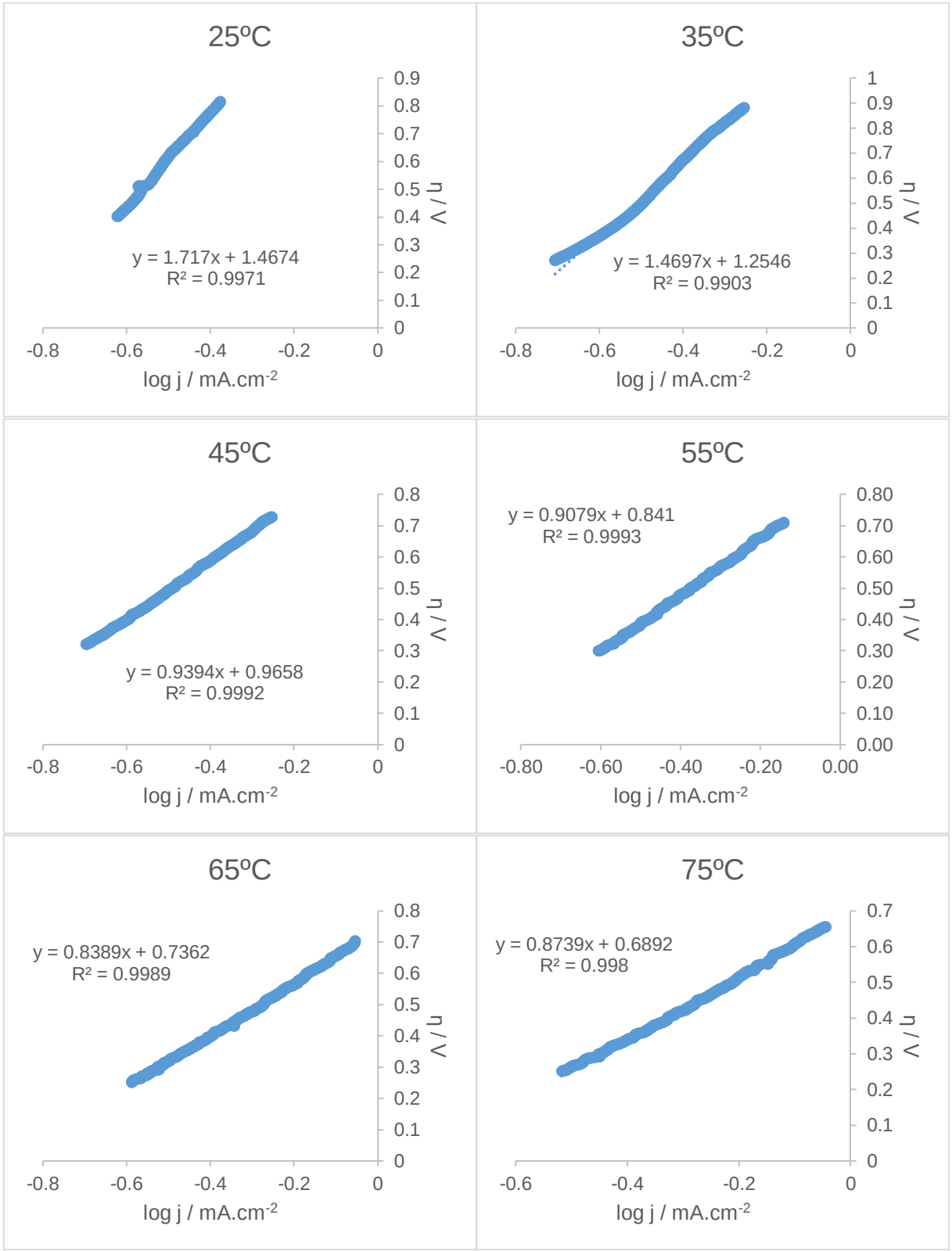

Fig. 39 - Tafel plots for different temperatures with Ni-Ce electrode of the domestic wastewater effluent.

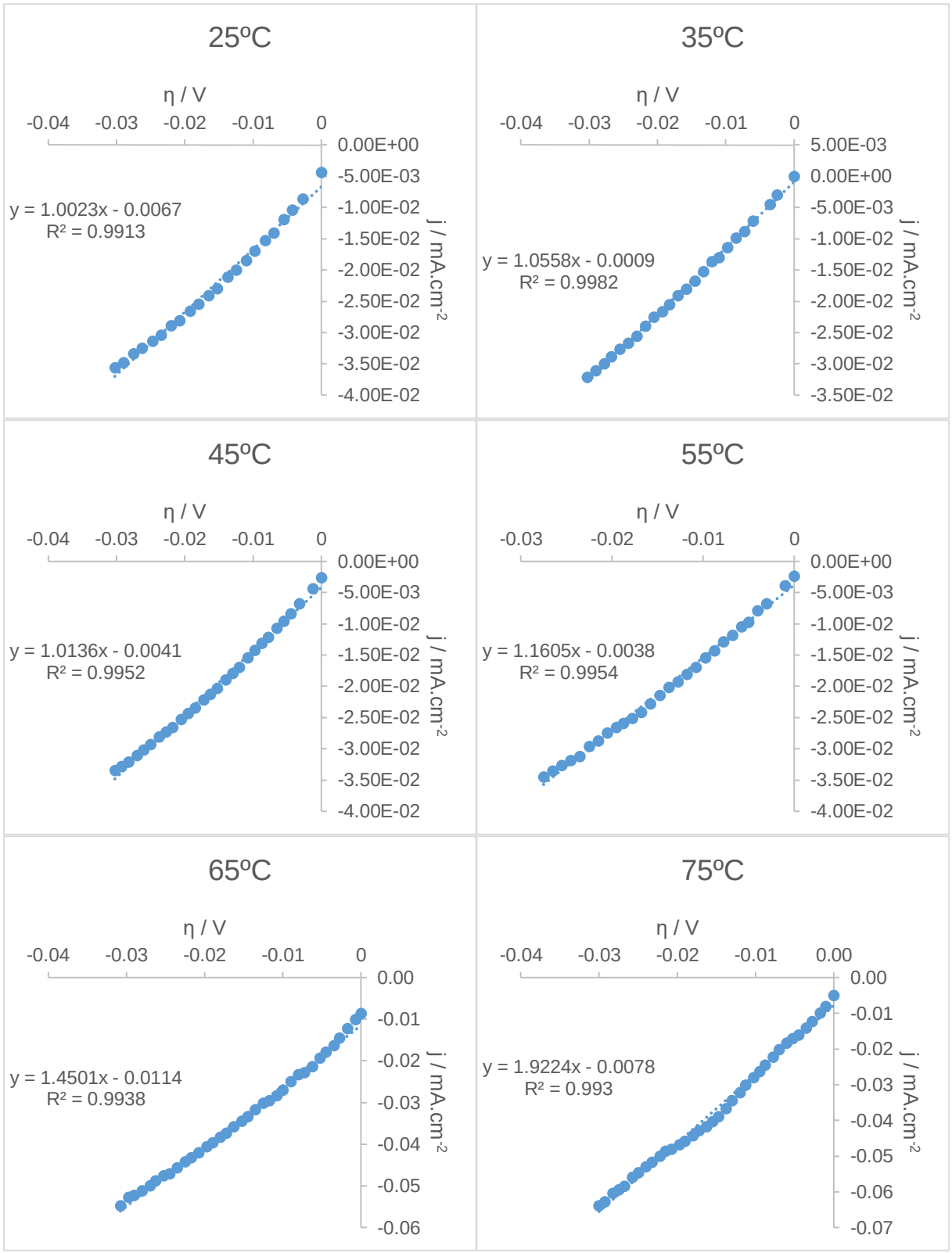

Fig. 40 - Low overvoltage representation with Ni-Ce electrode for Butler-Volmer equation of the domestic wastewater effluent.

8.1.9. Ni-Dy electrode

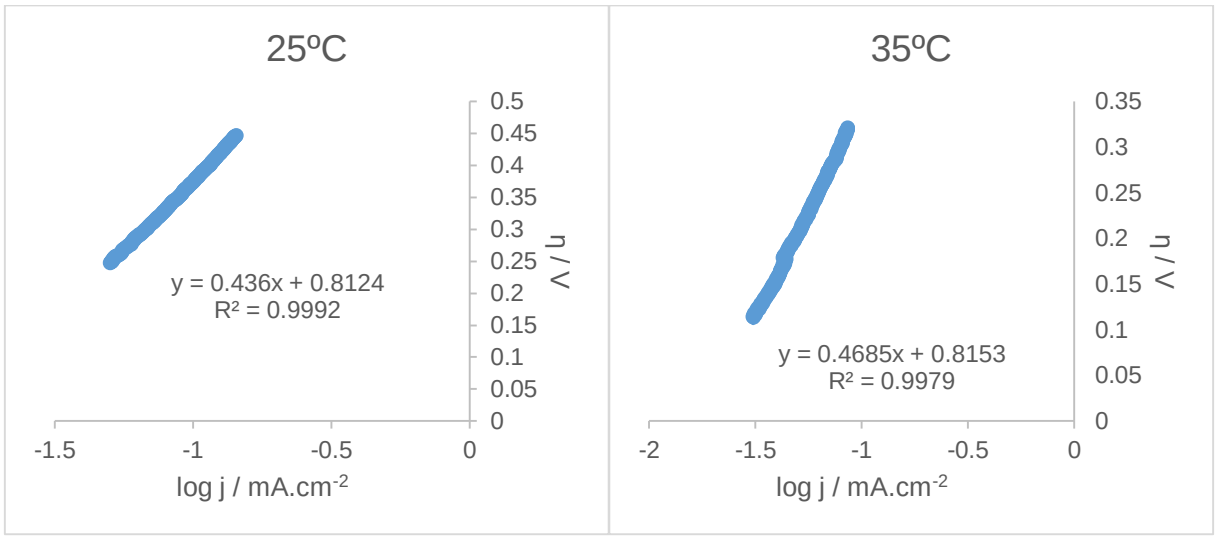

Fig. 41 - Tafel plots for different temperatures with Ni-Dy electrode of the domestic wastewater effluent.

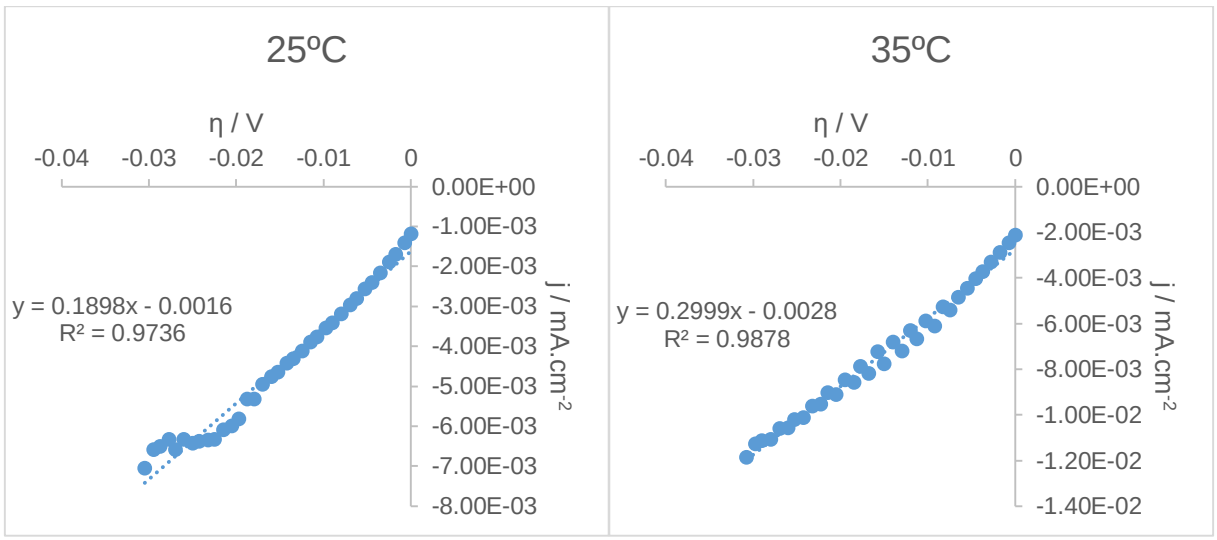

Fig. 42 - Low overvoltage representation with Ni-Dy electrode for Butler-Volmer equation of the domestic wastewater effluent.

8.1.10. Ni-Sm electrode

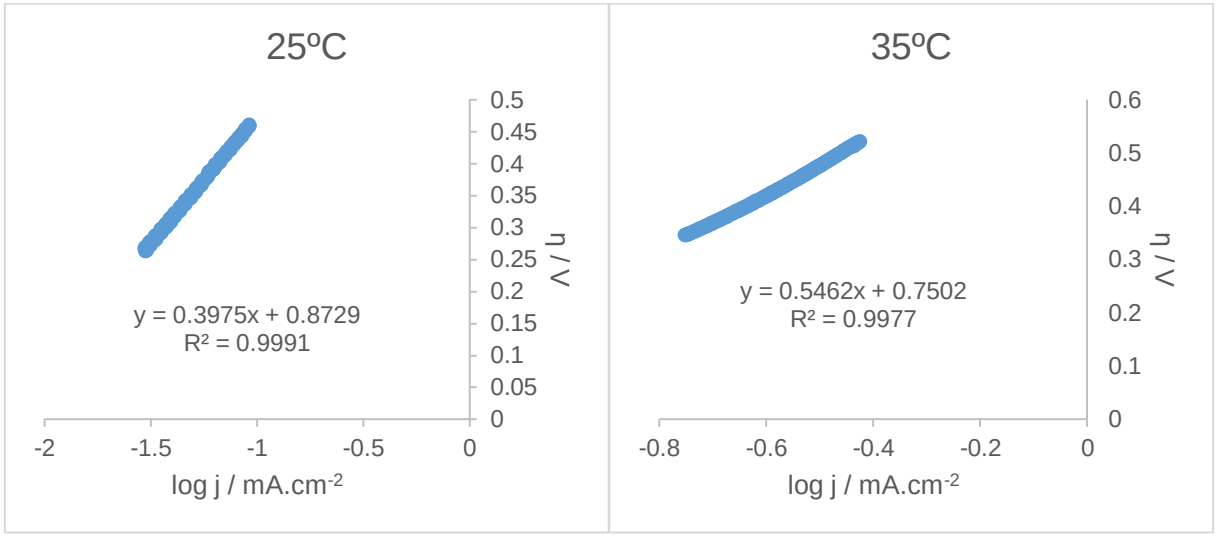

Fig. 43 - Tafel plots for different temperatures with Ni-Sm electrode

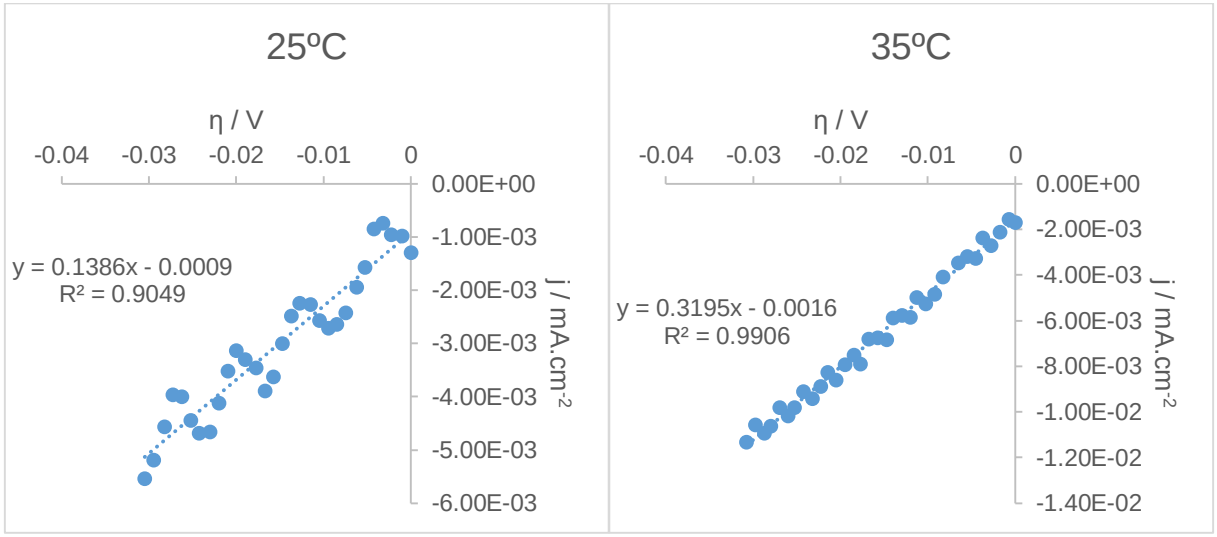

Fig. 44 - Low overvoltage representation with Ni-Sm electrode for Butler-Volmer equation of the domestic wastewater effluent.

8.2. Wastewater effluent with addition of KOH as electrolyte

8.2.1. Platinum electrode

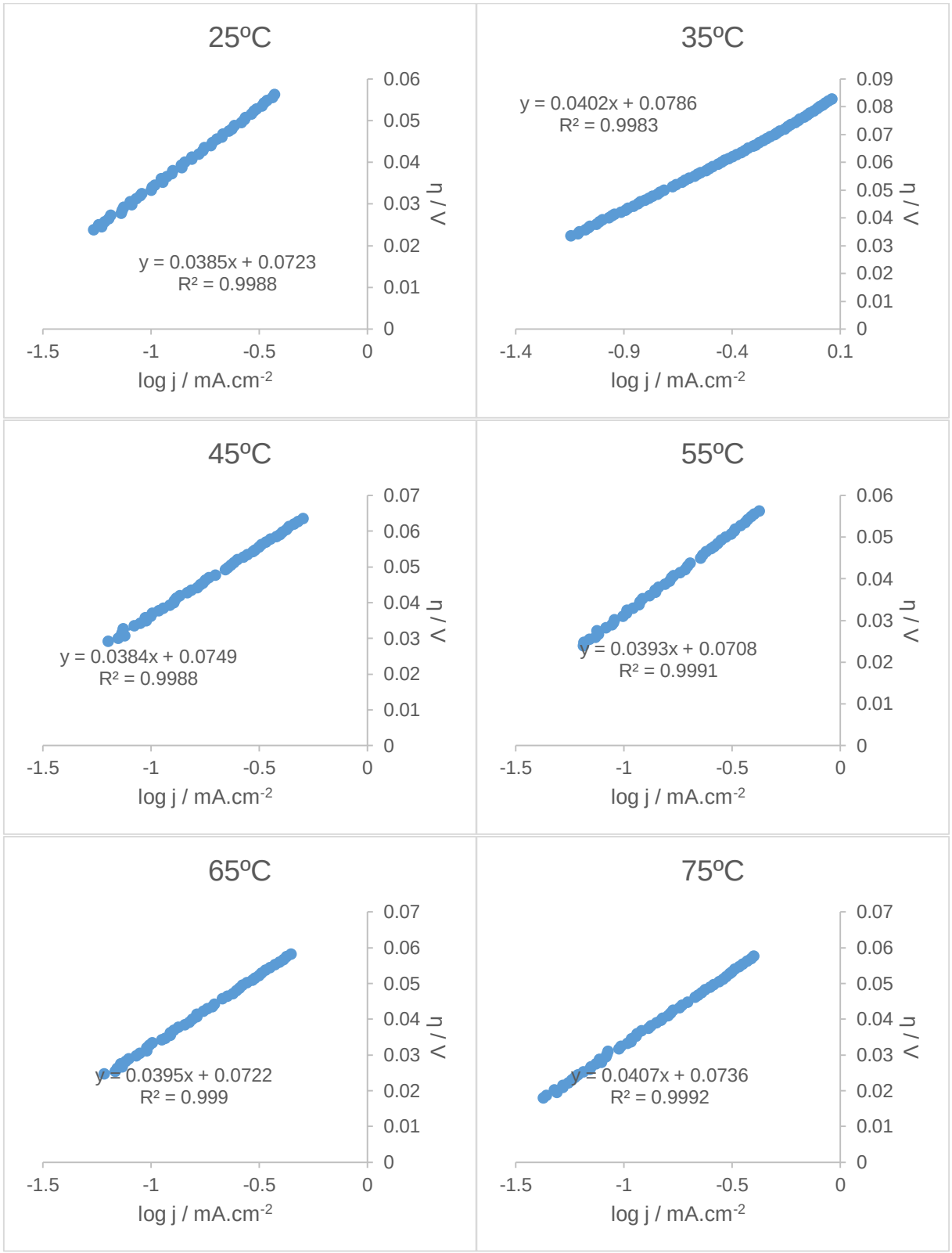

Fig. 45 - Tafel plots at different temperatures with Pt electrode of the domestic wastewater effluent after KOH addition.

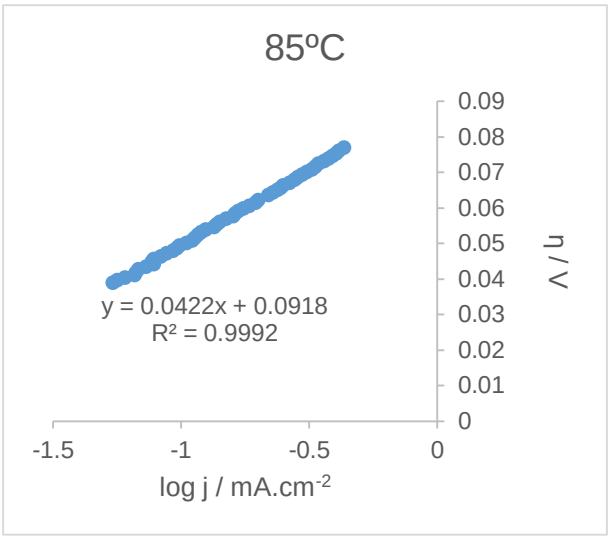

(cont.) Fig. 45 - Tafel plots at different temperatures with Pt electrode of the domestic wastewater effluent after KOH addition.

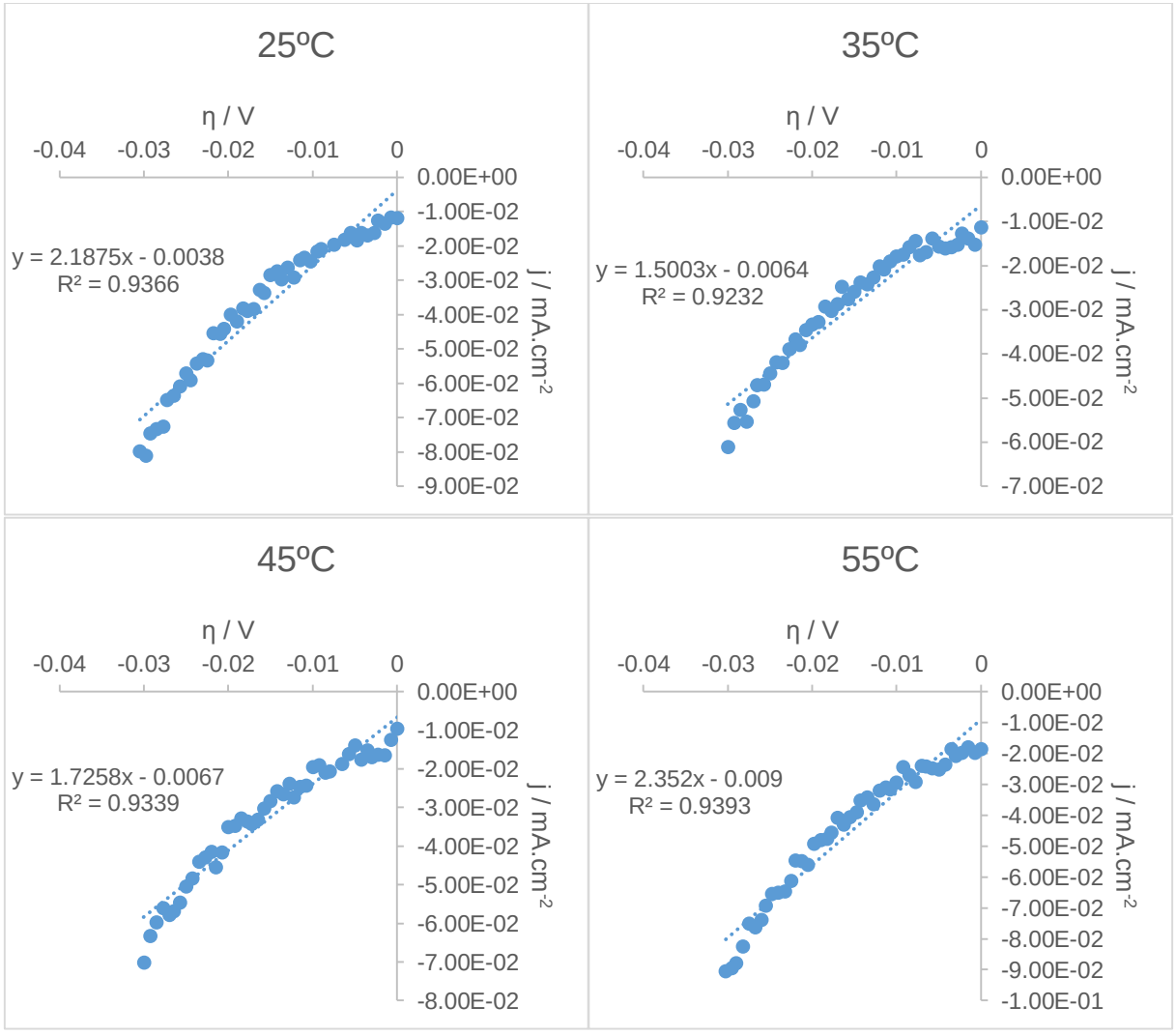

Fig. 46 - Low overvoltage representation with Pt electrode for Butler-Volmer equation of the domestic wastewater effluent after KOH addition.

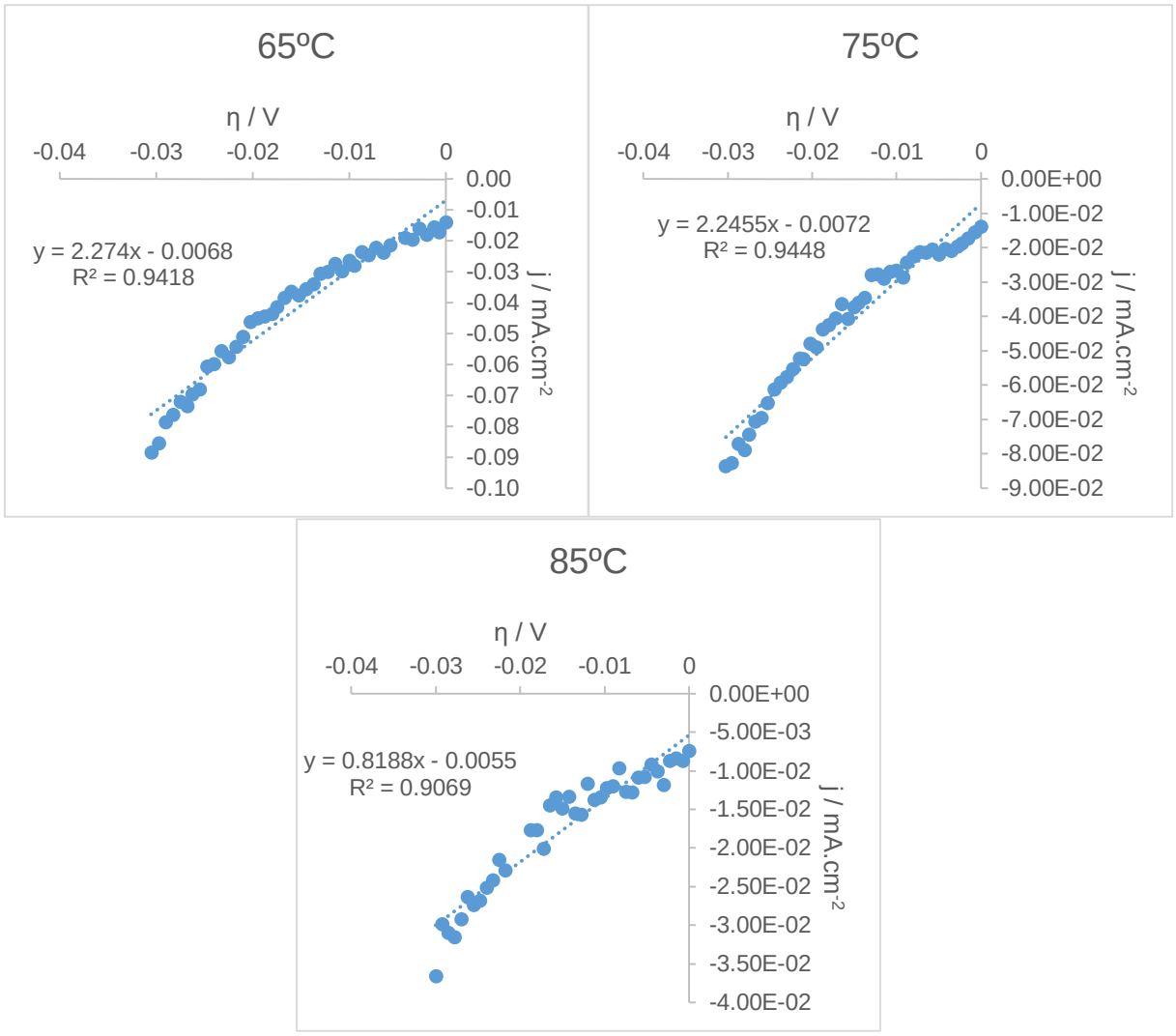

(cont.) Fig. 46 - Low overvoltage representation with Pt electrode for Butler-Volmer equation of the domestic wastewater effluent after KOH addition.

8.2.2.Nickel electrode

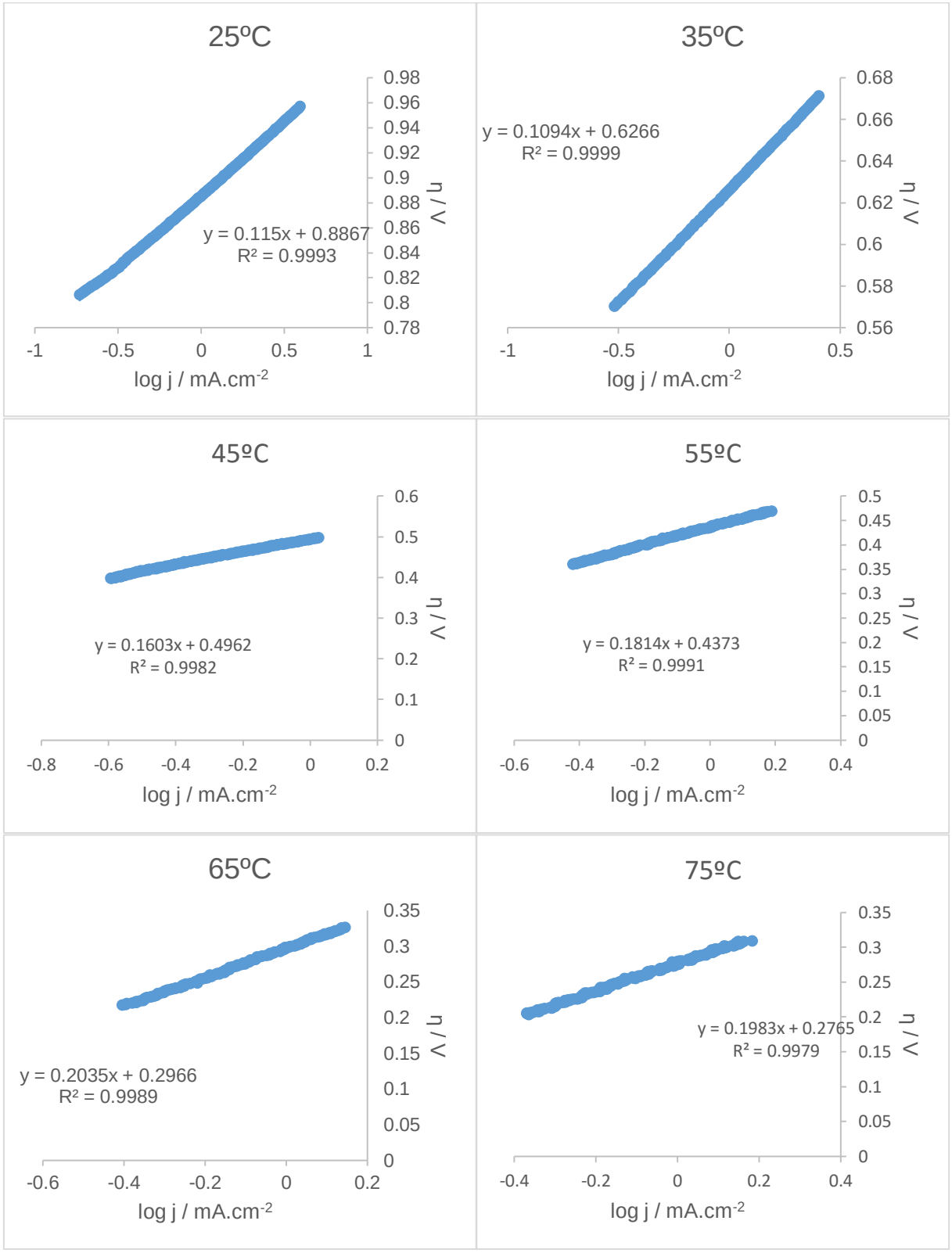

Fig. 47 - Tafel plots at different temperatures with Ni electrode of the domestic wastewater effluent after KOH addition.

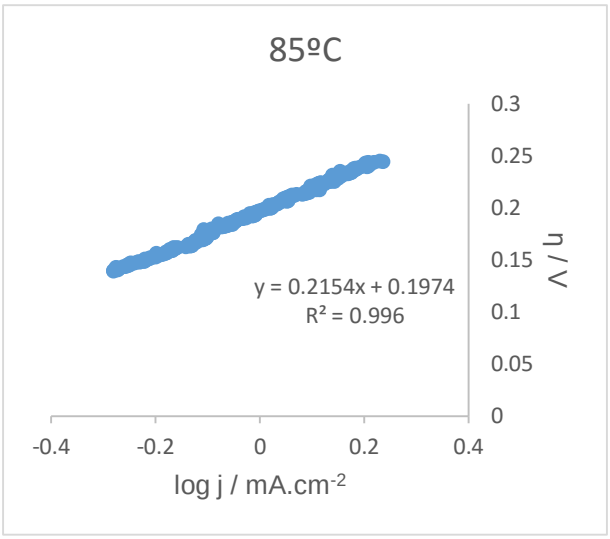

(cont.) Fig. 47 - Tafel plots at different temperatures with Ni electrode of the domestic wastewater effluent after KOH addition.

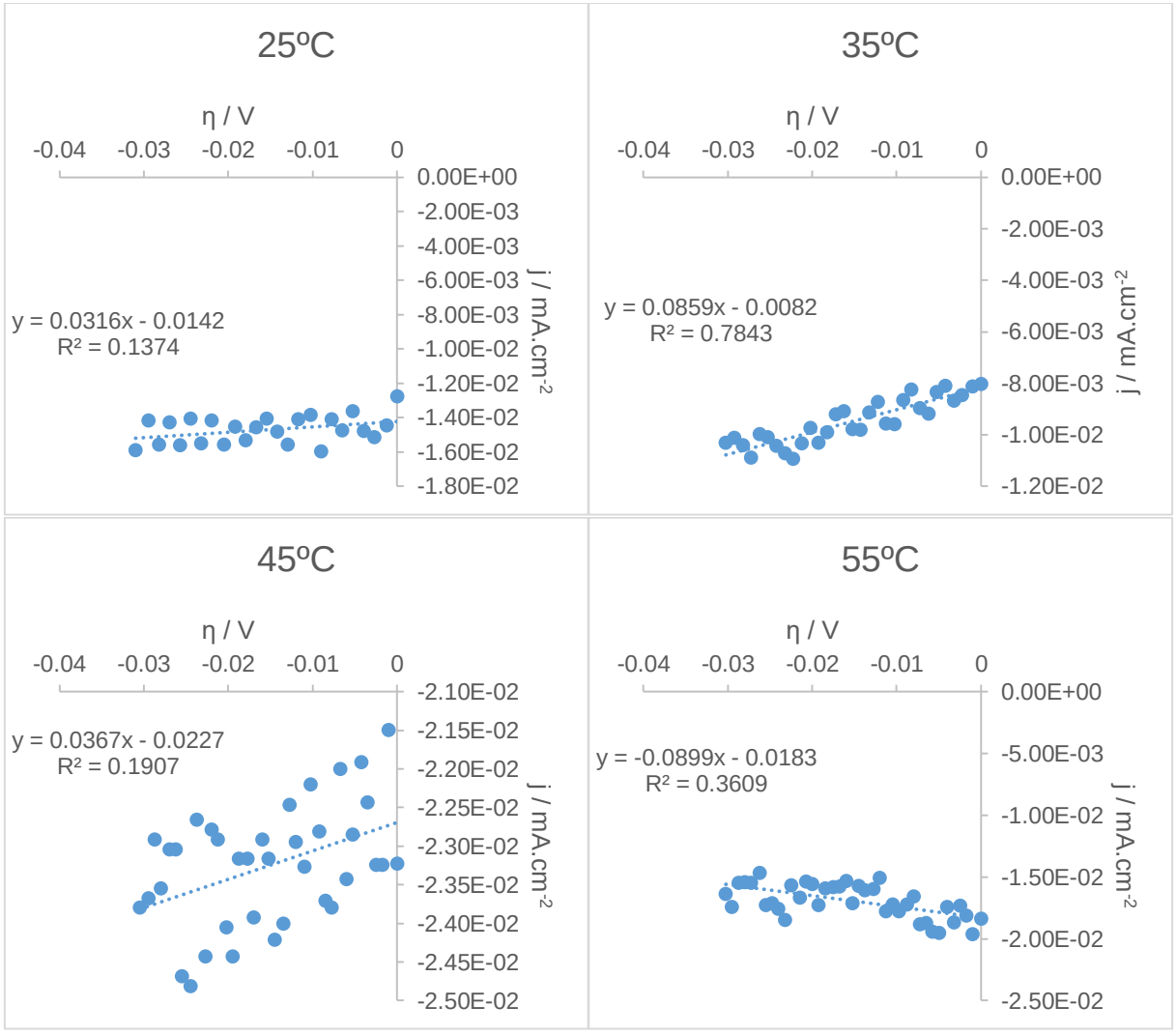

Fig. 48 - Low overvoltage representation with Ni electrode for Butler-Volmer equation of the domestic wastewater effluent after KOH addition.

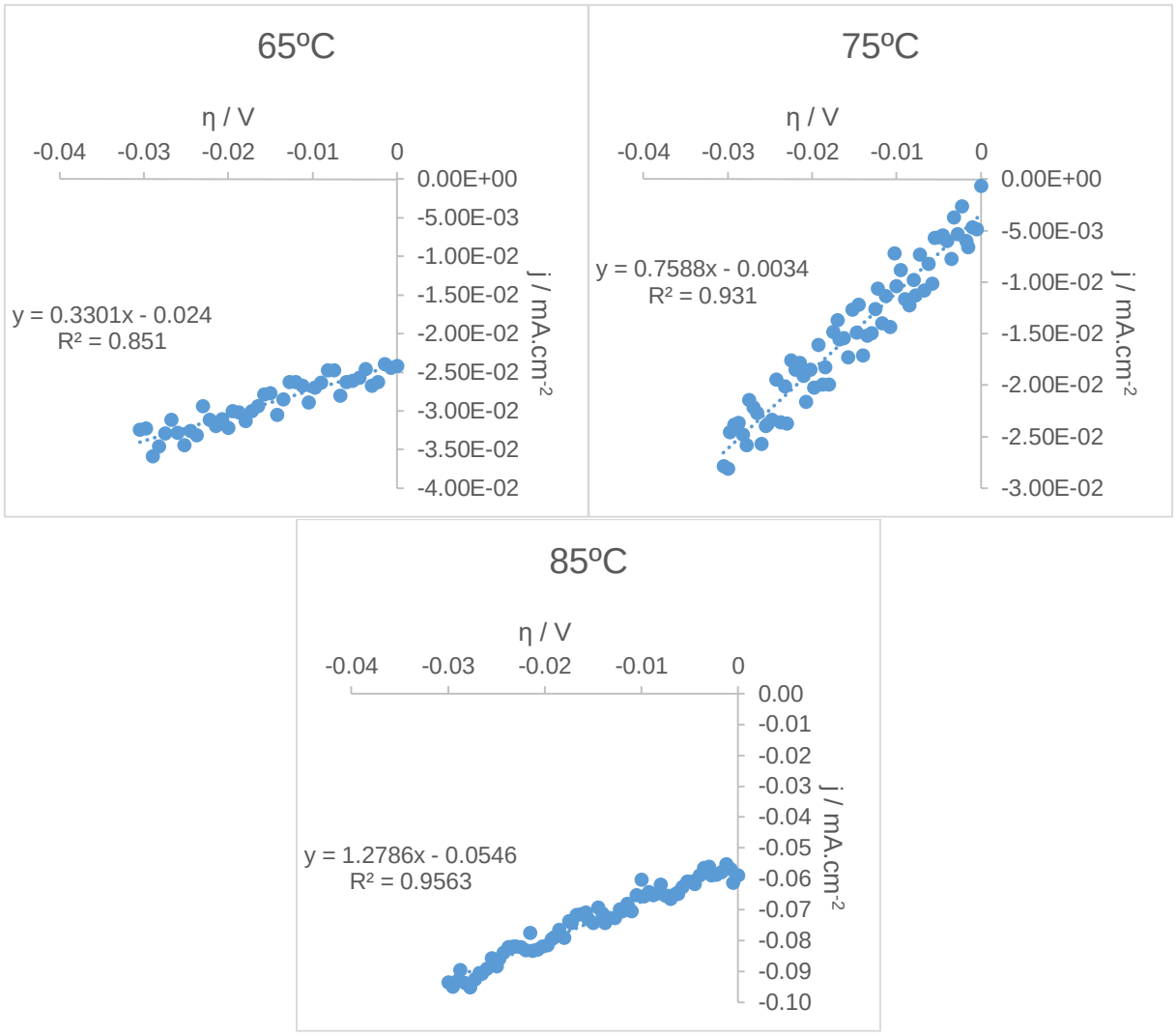

(cont.) Fig. 48 - Low overvoltage representation with Ni electrode for Butler-Volmer equation of the domestic wastewater effluent after KOH addition.

8.2.3. Stainless steel 304

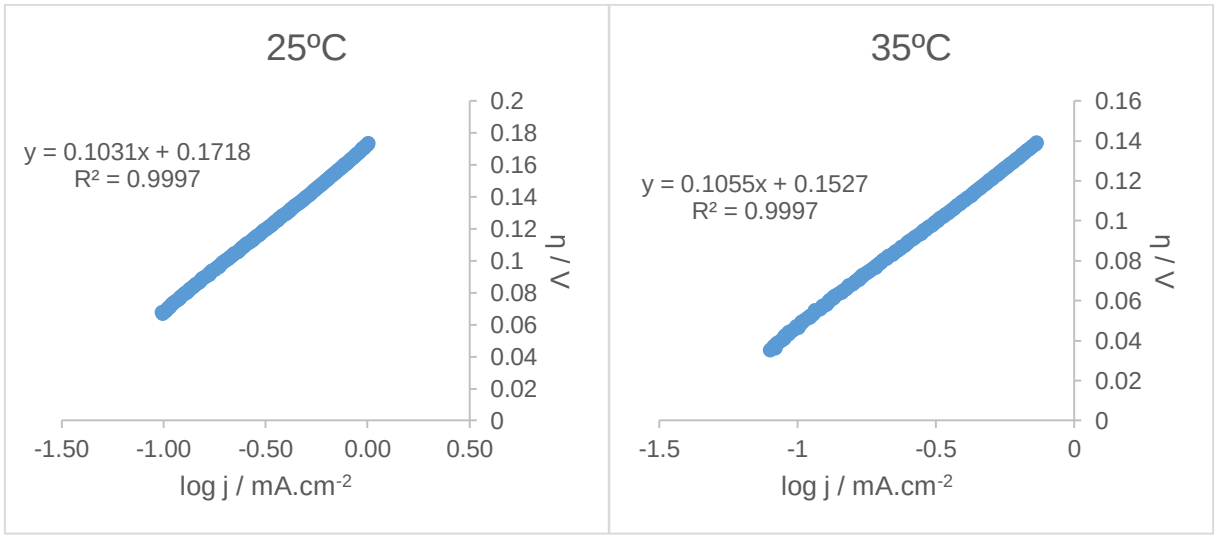

Fig. 49 - Tafel plots at different temperatures with SS 304 electrode of the domestic wastewater effluent after KOH addition.

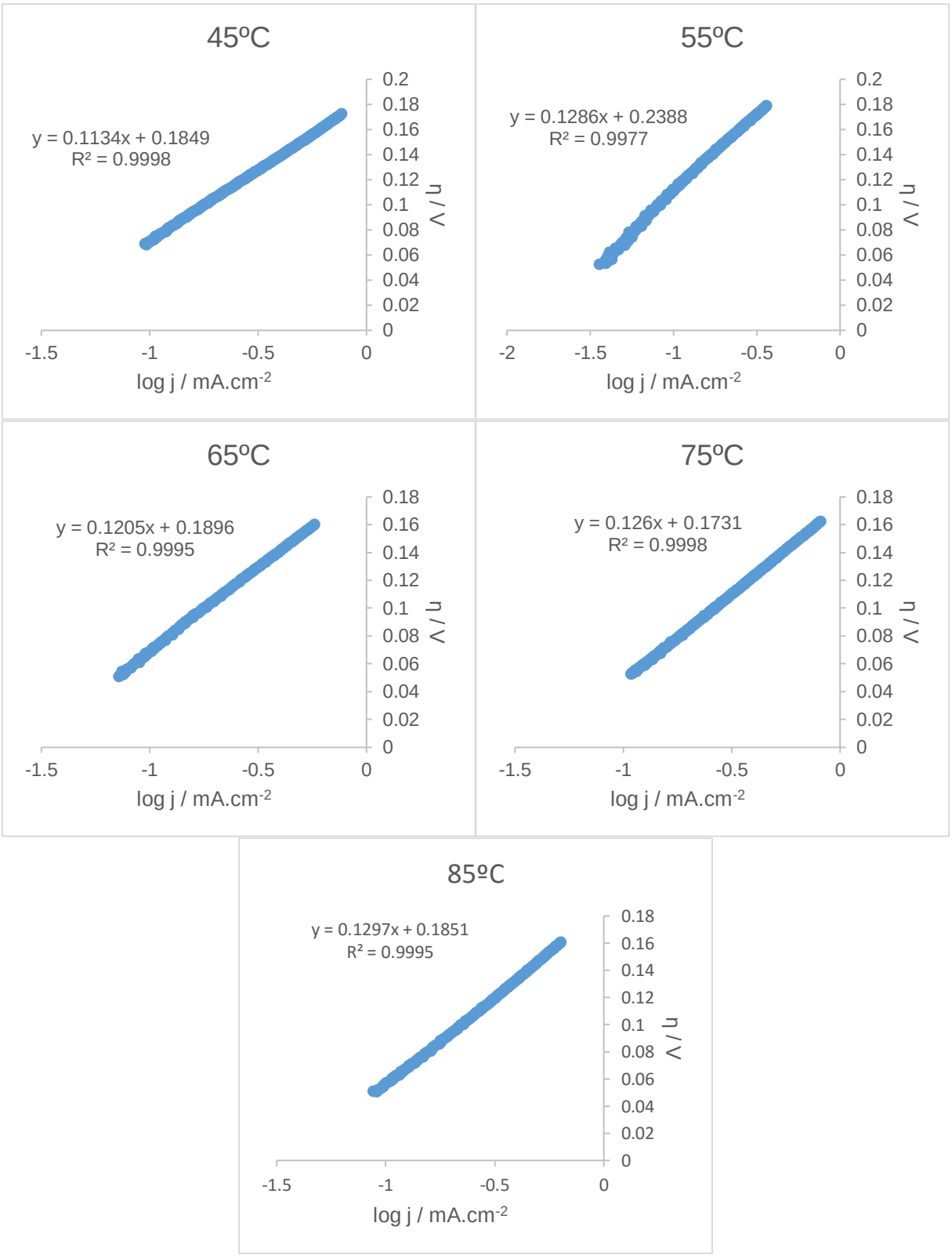

(cont.) Fig. 49 - Tafel plots at different temperatures with SS 304 electrode of the domestic wastewater effluent after KOH addition.

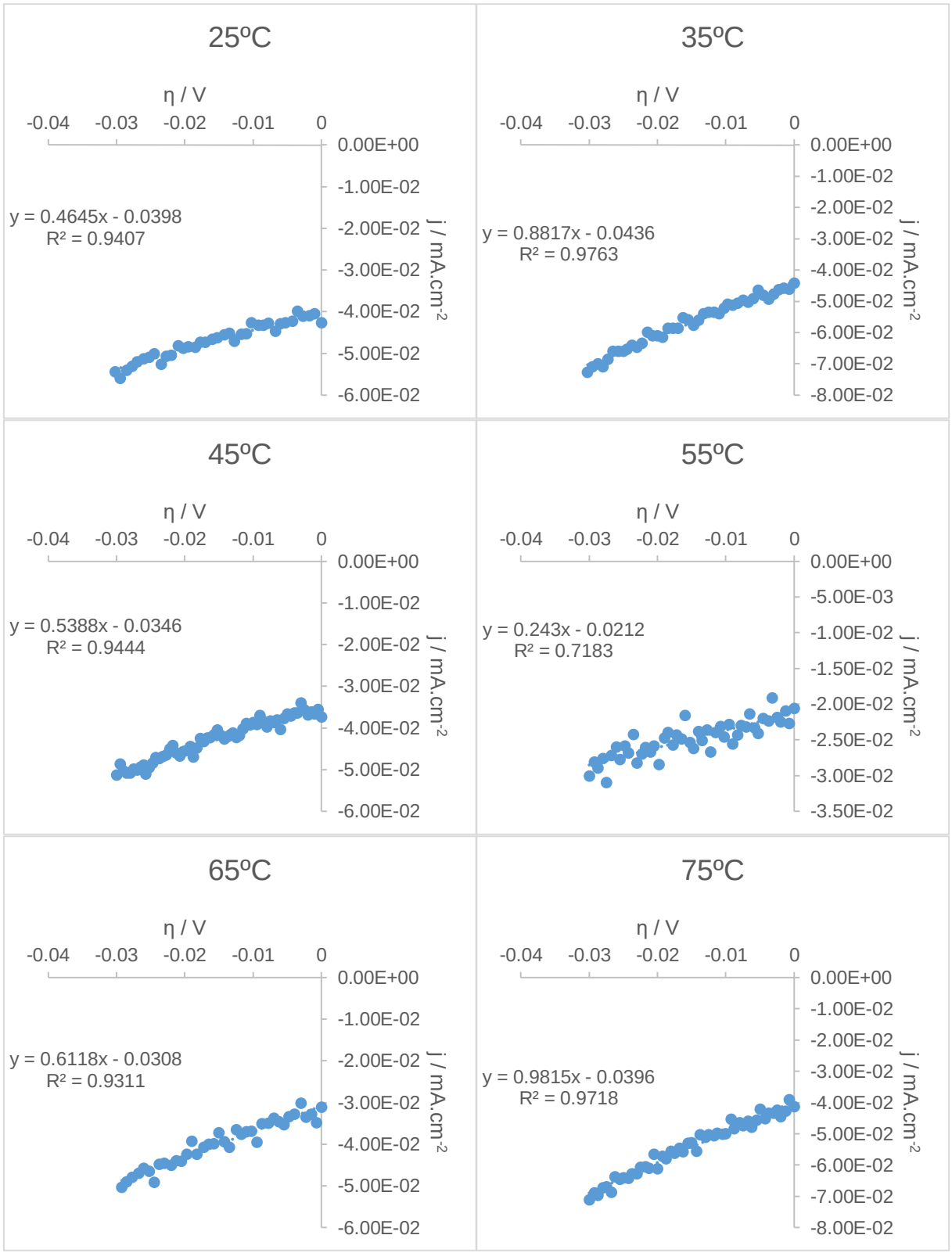

Fig. 50 - Low overvoltage representation with SS 304 electrode for Butler-Volmer equation of the domestic wastewater effluent after KOH addition.

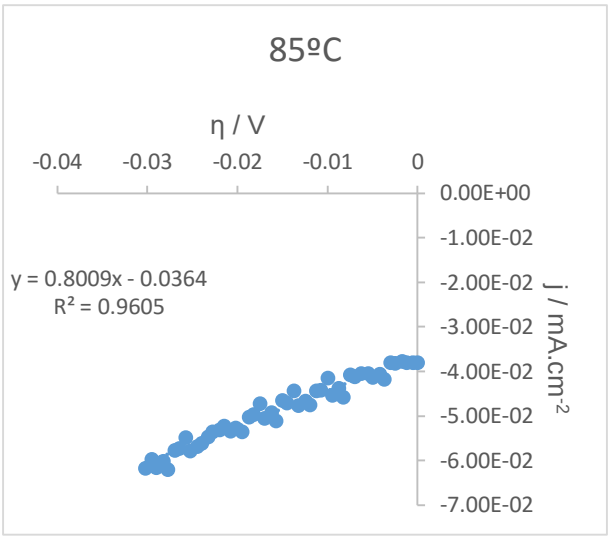

(Cont.) Fig. 50 - Low overvoltage representation with SS 304 electrode for Butler-Volmer equation of the domestic wastewater effluent after KOH addition.

8.2.4. Pt-Ce electrode

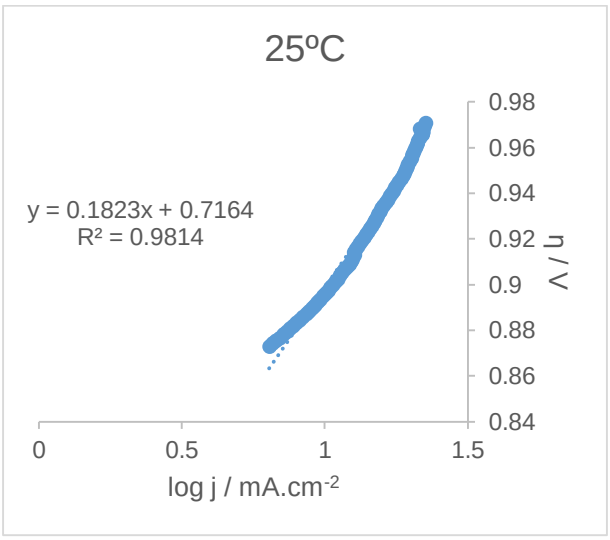

Fig. 51 - Tafel plots at different temperatures with Pt-Ce electrode of the domestic wastewater effluent after KOH addition.

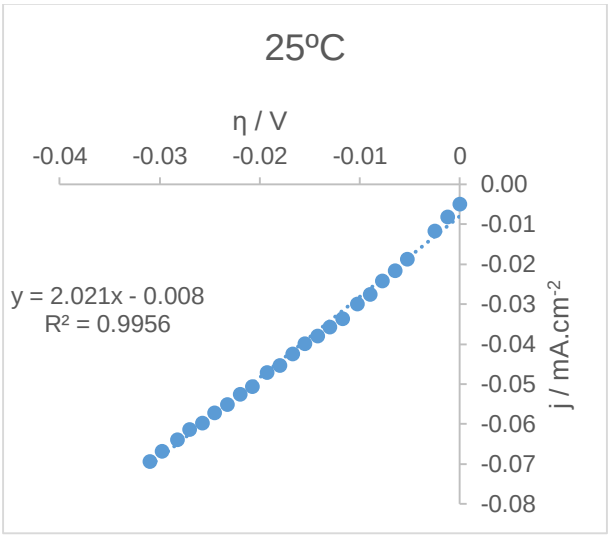

Fig. 52 - Low overvoltage representation with Pt-Ce electrode for Butler-Volmer equation of the domestic wastewater effluent after KOH addition.

8.2.5. Pt-Dy electrode

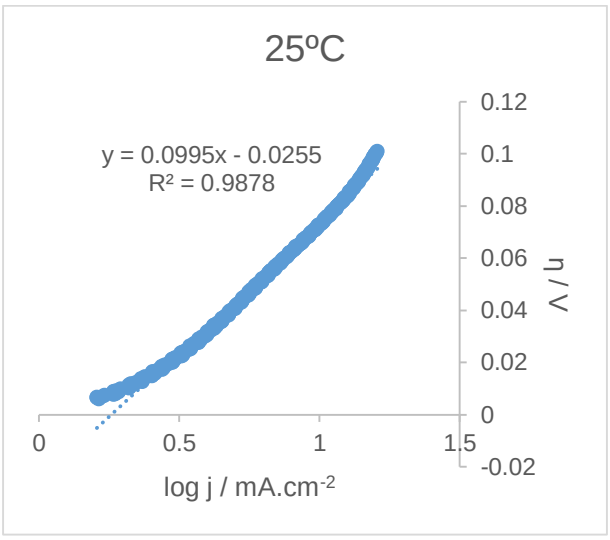

Fig. 53 - Tafel plots at different temperatures with Pt-Dy electrode of the domestic wastewater effluent after KOH addition.

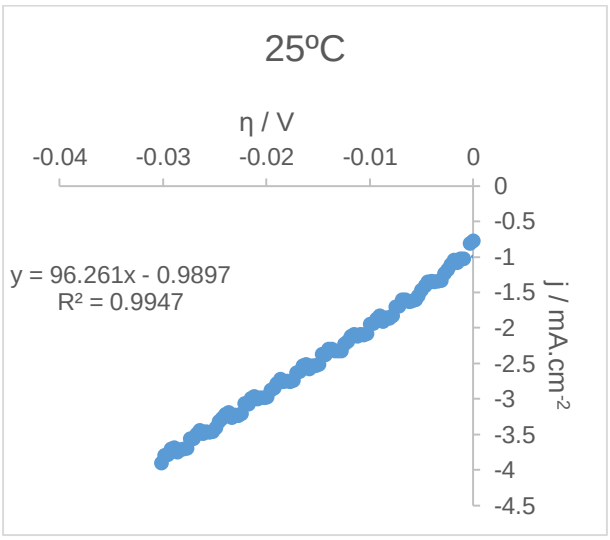

Fig. 54 - Low overvoltage representation with Pt-Dy electrode for Butler-Volmer equation of the domestic wastewater effluent after KOH addition.

8.2.6. Pt-Ho electrode

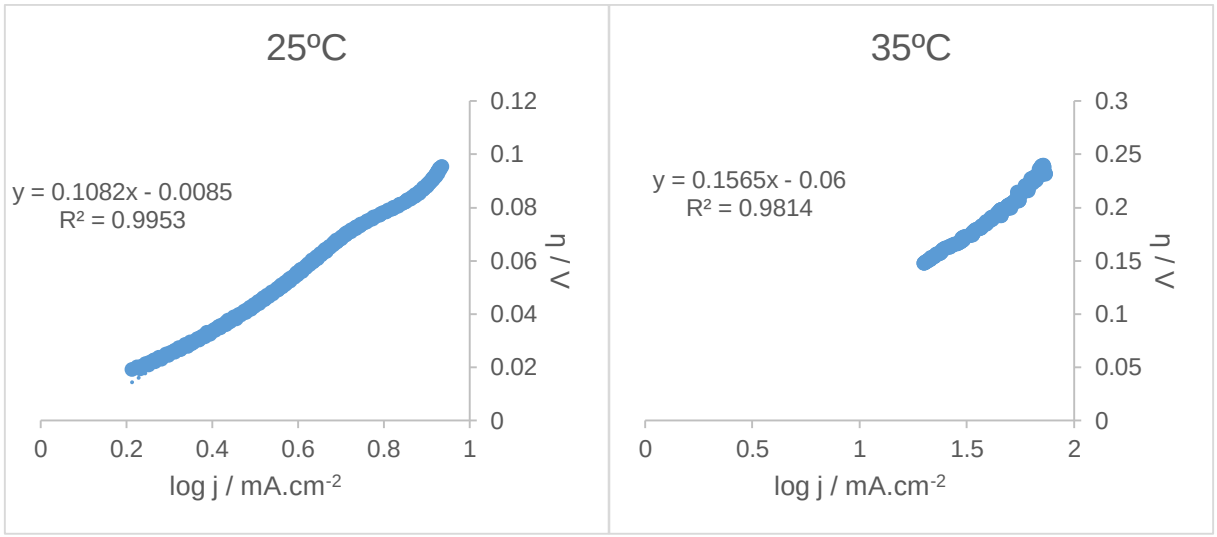

Fig. 55 - Tafel plots at different temperatures with Pt-Ho electrode of the domestic wastewater effluent after KOH addition.

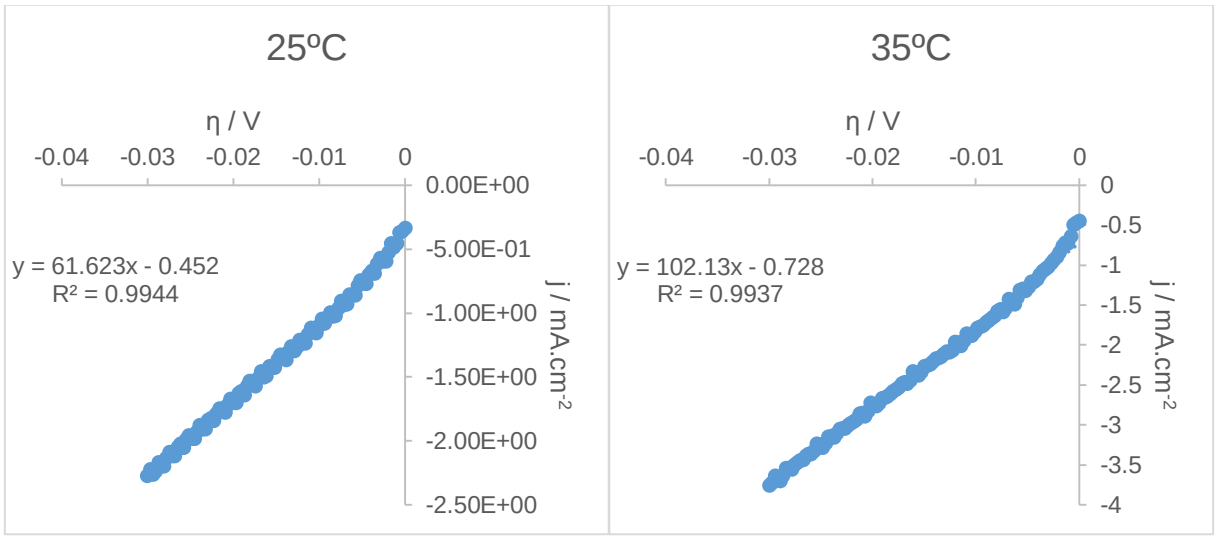

Fig. 56 - Low overvoltage representation with Pt-Ho electrode for Butler-Volmer equation of the domestic wastewater effluent after KOH addition.

8.2.7. Pt-Sm electrode

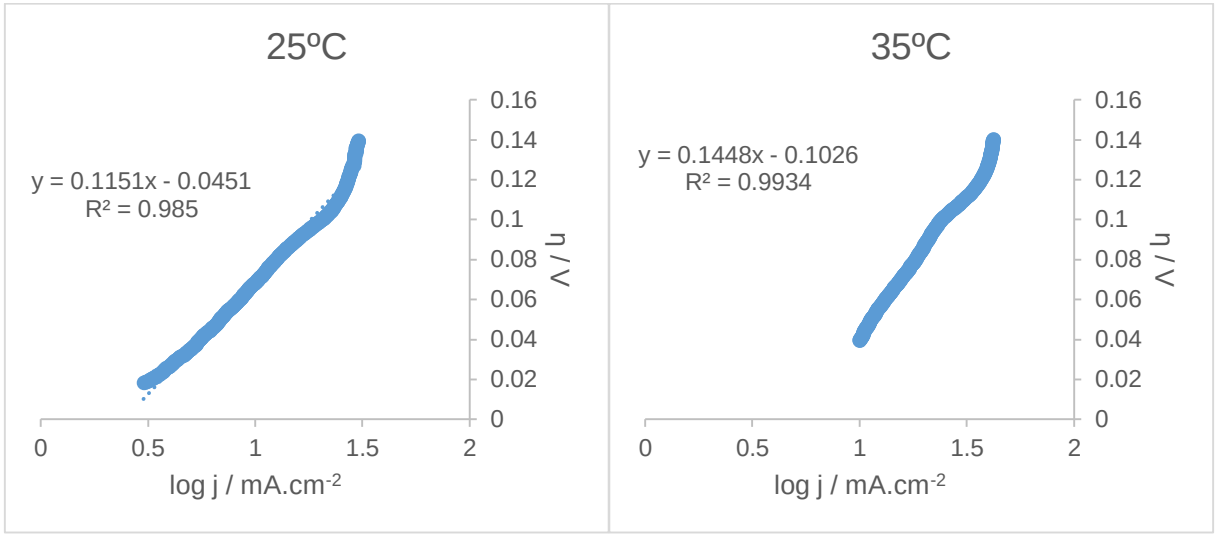

Fig. 57 - Tafel plots at different temperatures with Pt-Sm electrode of the domestic wastewater effluent after KOH addition.

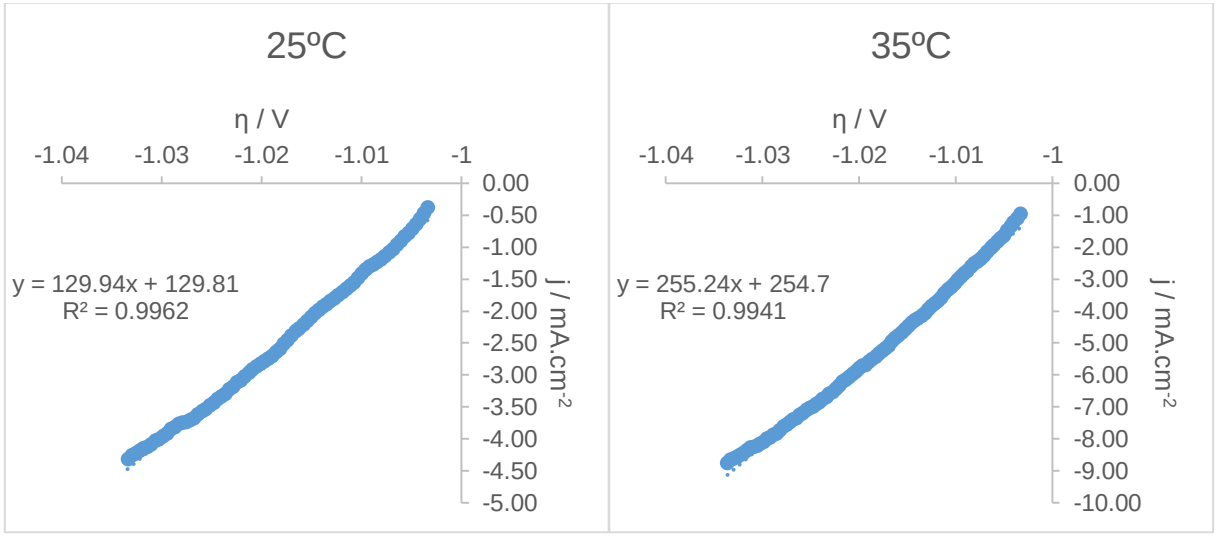

Fig. 58 - Low overvoltage representation with Pt-Sm electrode for Butler-Volmer equation of the domestic wastewater effluent after KOH addition.

8.2.8. Ni-Ce electrode

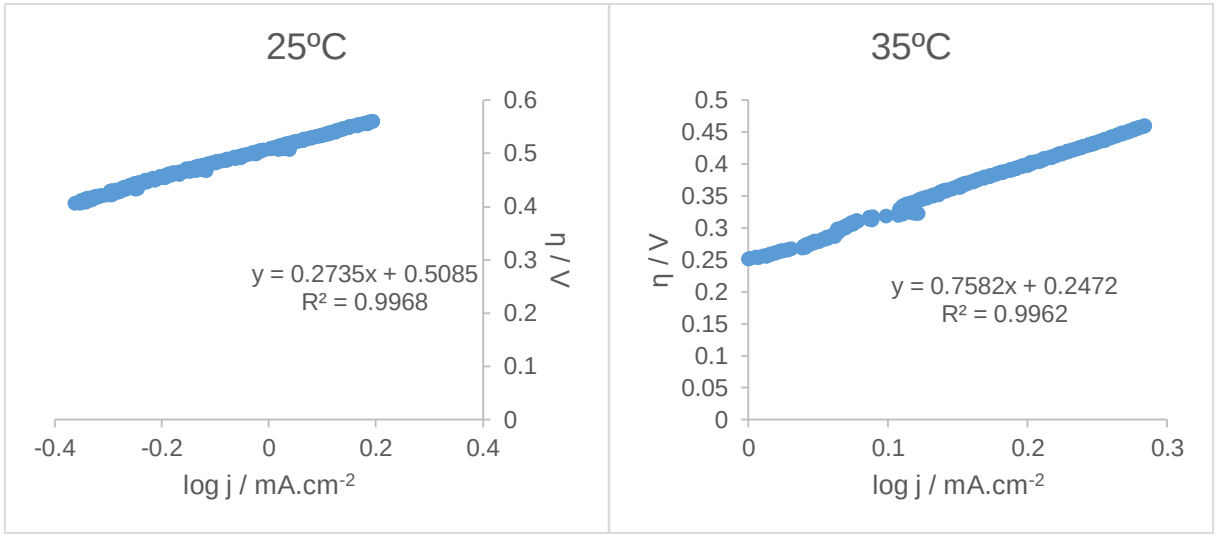

Fig. 59 - Tafel plots at different temperatures with Ni-Ce electrode of the domestic wastewater effluent after KOH addition.

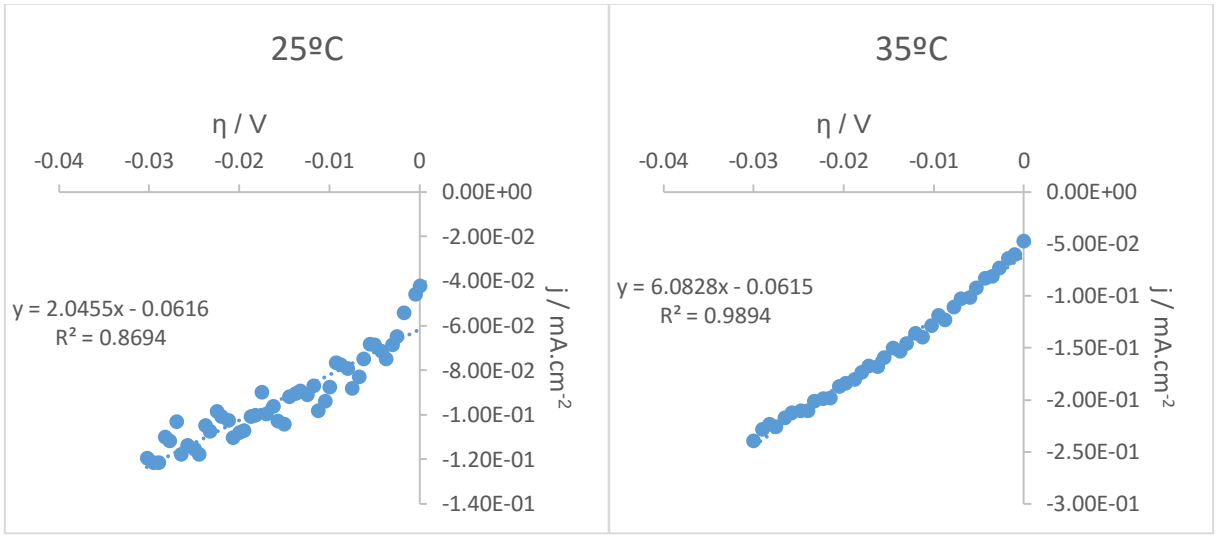

Fig. 60 - Low overvoltage representation with Ni-Ce electrode for Butler-Volmer equation of the domestic wastewater effluent after KOH addition.

8.2.9. Ni-Dy electrode

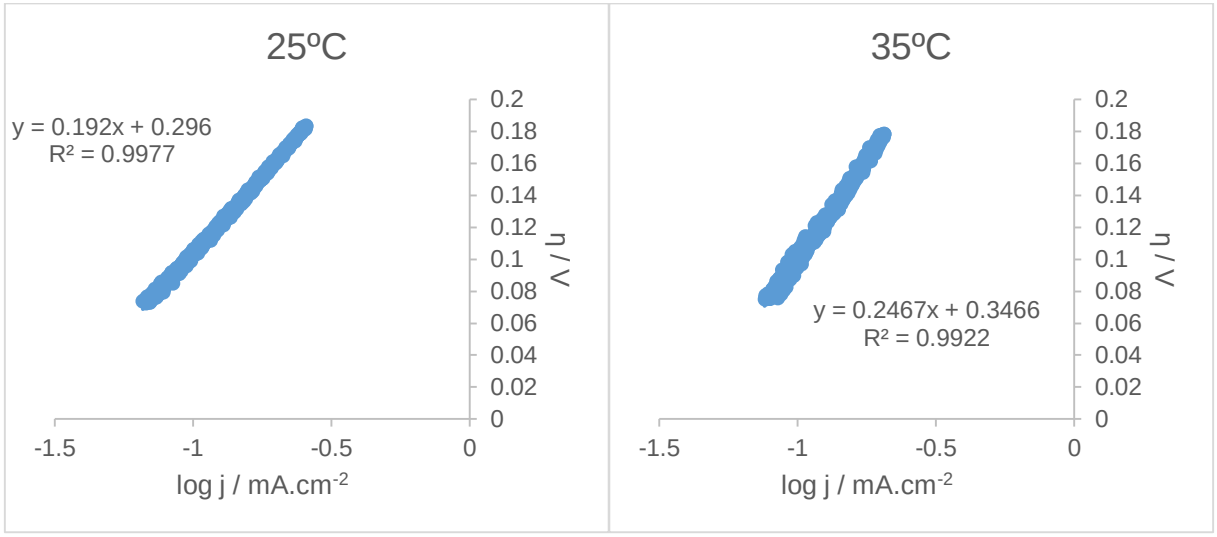

Fig. 61 - Tafel plots at different temperatures with Ni-Dy electrode of the domestic wastewater effluent after KOH addition.

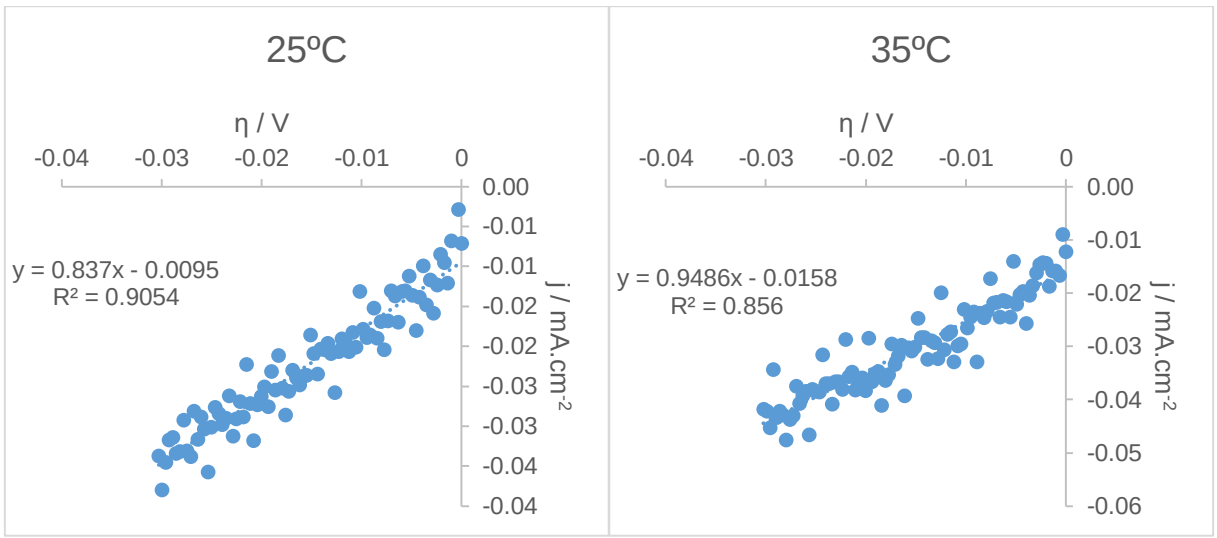

Fig. 62 - Low overvoltage representation with Ni-Dy electrode for Butler-Volmer equation of the domestic wastewater effluent after KOH addition.

8.2.10. Ni-Sm electrode

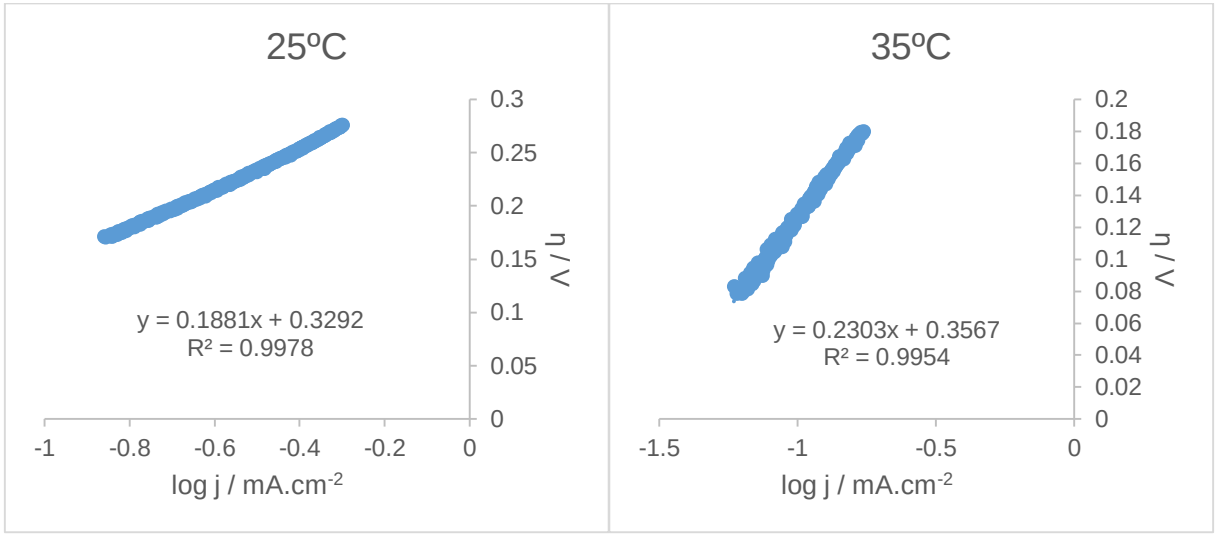

Fig. 63 - Tafel plots at different temperatures with Ni-Sm electrode of the domestic wastewater effluent after KOH addition.

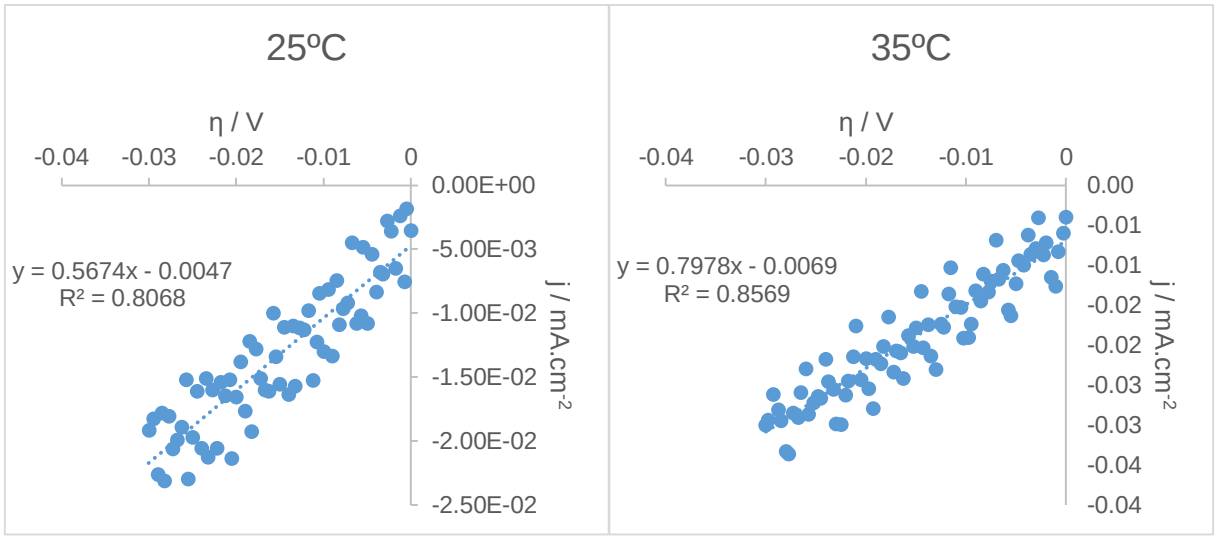

Fig. 64 - Low overvoltage representation with Ni-Sm electrode for Butler-Volmer equation of the domestic wastewater effluent after KOH addition.

Table 19 - Parameters obtained from chronoamperometry

				First peak		Second peak	
ν (mV/s)	ν (V/s)	$\nu^{1/2}$	ln ν	η (V)	j (A/cm^2)	η (V)	j (A/cm^2)
0.5	0.0005	0.022	-7.601	-0.843	-1.63E-04	-1.120	-1.22E-03
1	0.001	0.032	-6.908	-0.801	-2.36E-04	-1.145	-1.81E-03
1.5	0.0015	0.039	-6.502	-0.811	-3.77E-04	-1.137	-1.90E-03
2.5	0.0025	0.050	-5.991	-0.771	-3.97E-04	-1.017	-1.06E-03
5	0.005	0.071	-5.298	-0.812	-6.05E-04	-1.062	-1.85E-03
10	0.01	0.100	-4.605	-0.817	-7.51E-04	-1.072	-2.11E-03
15	0.015	0.122	-4.200	-0.841	-8.84E-04	-1.131	-2.54E-03
25	0.025	0.158	-3.689	-0.843	-9.85E-04	-1.106	-2.60E-03
50	0.05	0.224	-2.996	-0.863	-1.22E-03	-1.152	-3.22E-03

100	0.1	0.316	-2.303	-0.855	-1.43E-03	-1.198	-4.17E-03
150	0.15	0.387	-1.897	-0.862	-1.88E-03	-1.204	-5.26E-03
250	0.25	0.500	-1.386	-0.854	-2.06E-03	-1.211	-5.94E-03
500	0.5	0.707	-0.693	-0.958	-3.35E-03	-1.214	-8.46E-03
1000	1	1.000	0.000	-0.976	-4.26E-03	-1.388	-1.11E-02

Table 20 – Parameters from the CA scan.

Potential	η (V)	OCP	I (mA)	j (mA/cm^2)	Log j
0	-0.237	0.237	1.00E-01	0.1	-1.000
-0.2	-0.428	0.228	1.50E-01	0.15	-0.824
-0.3	-0.532	0.232	1.50E-01	0.15	-0.824
-0.4	-0.614	0.214	1.50E-01	0.15	-0.824
-0.5	-0.722	0.222	1.50E-01	0.15	-0.824
-0.55	-0.776	0.226	1.50E-01	0.15	-0.824
-0.6	-0.809	0.209	1.50E-01	0.15	-0.824
-0.65	-0.872	0.222	2.00E-01	0.2	-0.699
-0.7	-0.928	0.228	3.00E-01	0.3	-0.523
-0.75	-0.972	0.222	3.00E-01	0.3	-0.523
-0.8	-1.02	0.22	3.50E-01	0.35	-0.456
-0.85	-1.067	0.217	3.50E-01	0.35	-0.456
-0.9	-1.115	0.215	5.00E-01	0.5	-0.301
-0.95	-1.168	0.218	9.00E-01	0.9	-0.046
-1	-1.218	0.218	1.20	1.2	0.079
-1.05	-1.265	0.215	1.55	1.55	0.190
-1.1	-1.31	0.21	1.95	1.95	0.290
-1.15	-1.35	0.2	3.05	3.05	0.484
-1.2	-1.399	0.199	3.55	3.55	0.550
-1.25	-1.448	0.198	4.30	4.3	0.633
-1.3	-1.488	0.188	5.20	5.2	0.716
-1.35	-1.529	0.179	6.25	6.25	0.796
-1.4	-1.571	0.171	7.55	7.55	0.878
-1.45	-1.614	0.164	8.80	8.8	0.944
-1.5	-1.652	0.152	10.1	10.1	1.004

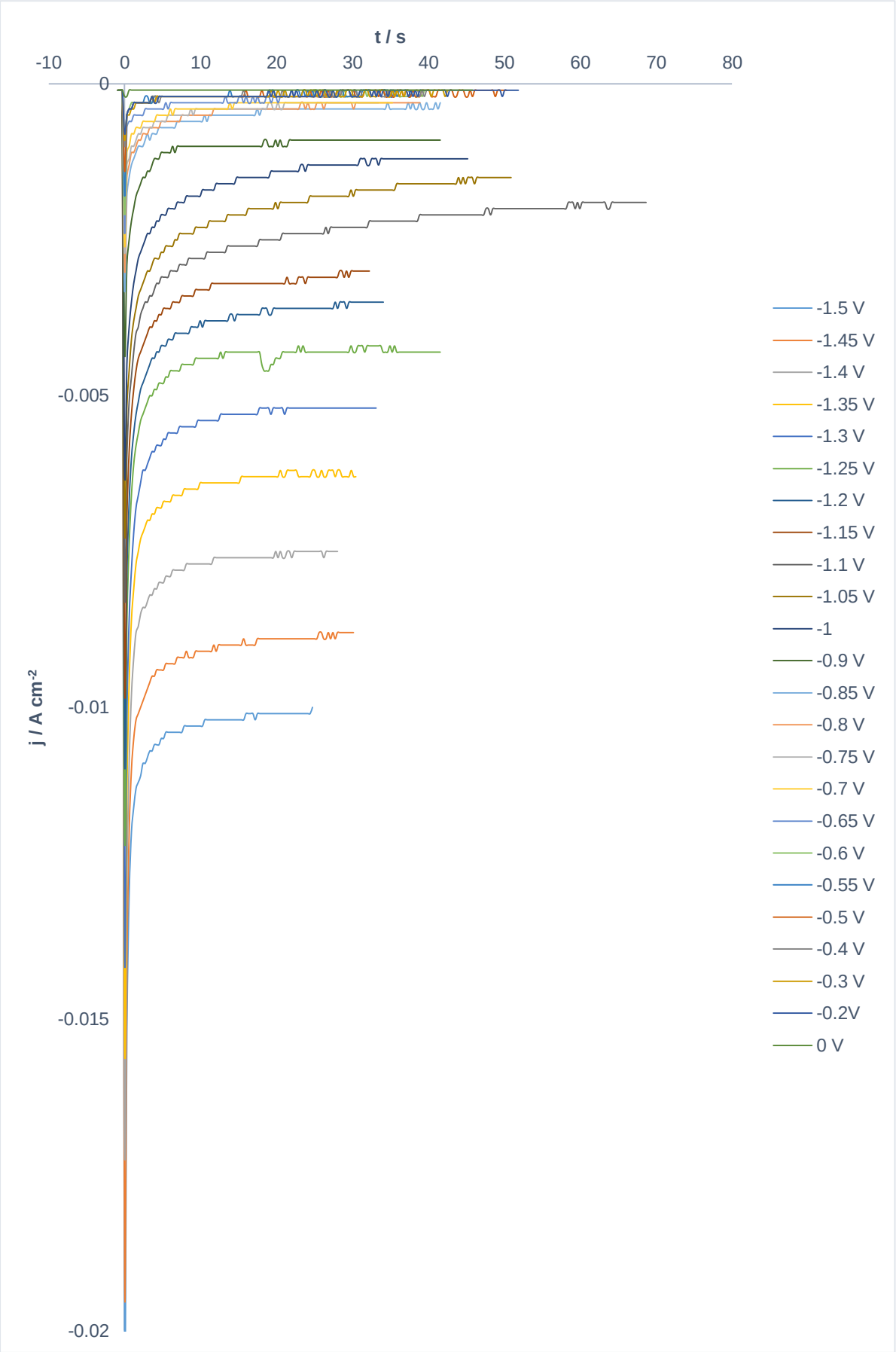

Fig. 65 – Synthetic urine chronoamperometric scans

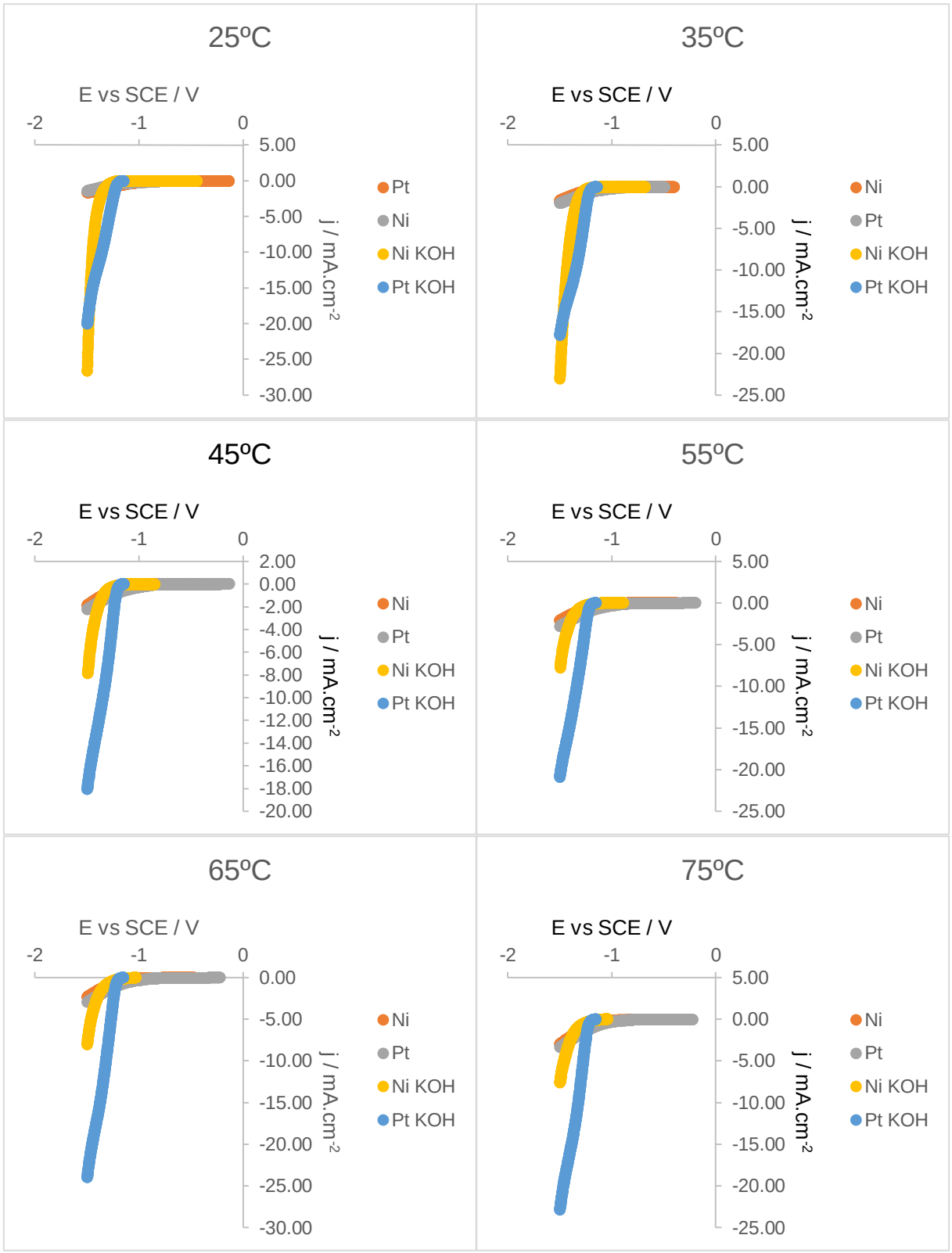

Fig. 66 - Comparison of different effluent's CV scans from different temperatures with a 0.5 mV s^{-1} rate.

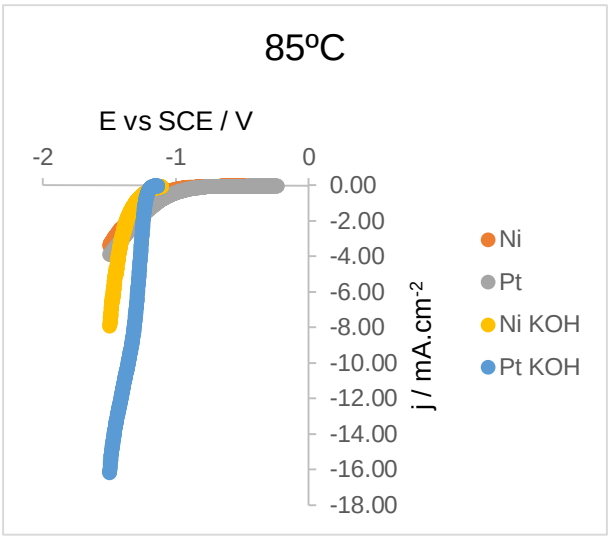

(cont.) Fig. 66 - Comparison of different effluent's CV scans from different temperatures with a 0.5 mV s-1 rate

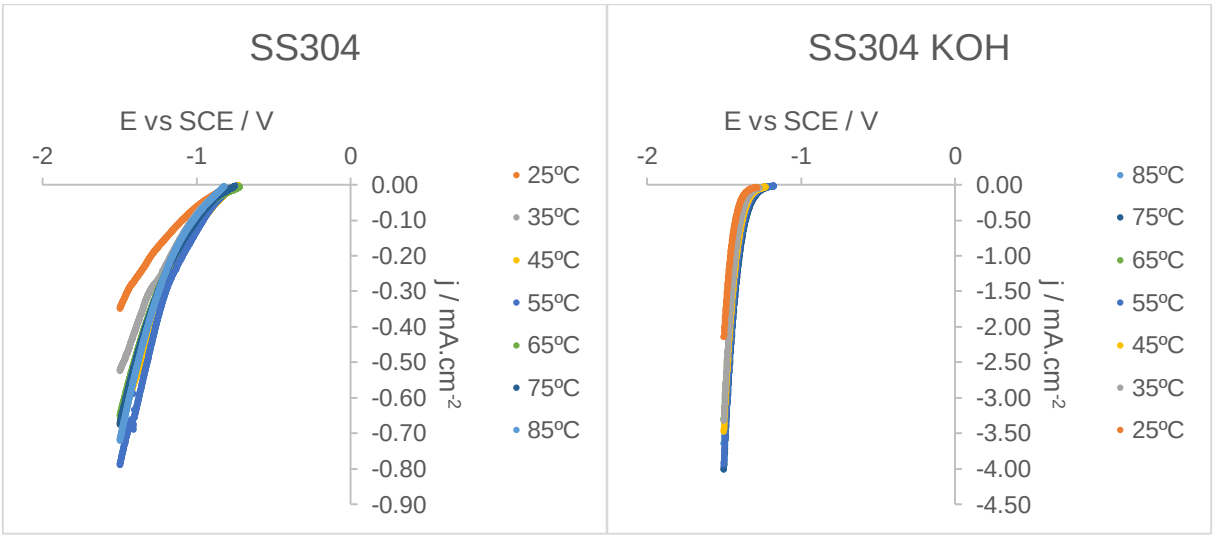

Fig. 67 - Comparison of different effluent's CV scans from different temperatures with a 0.5 mV/s rate of SS304 electrode

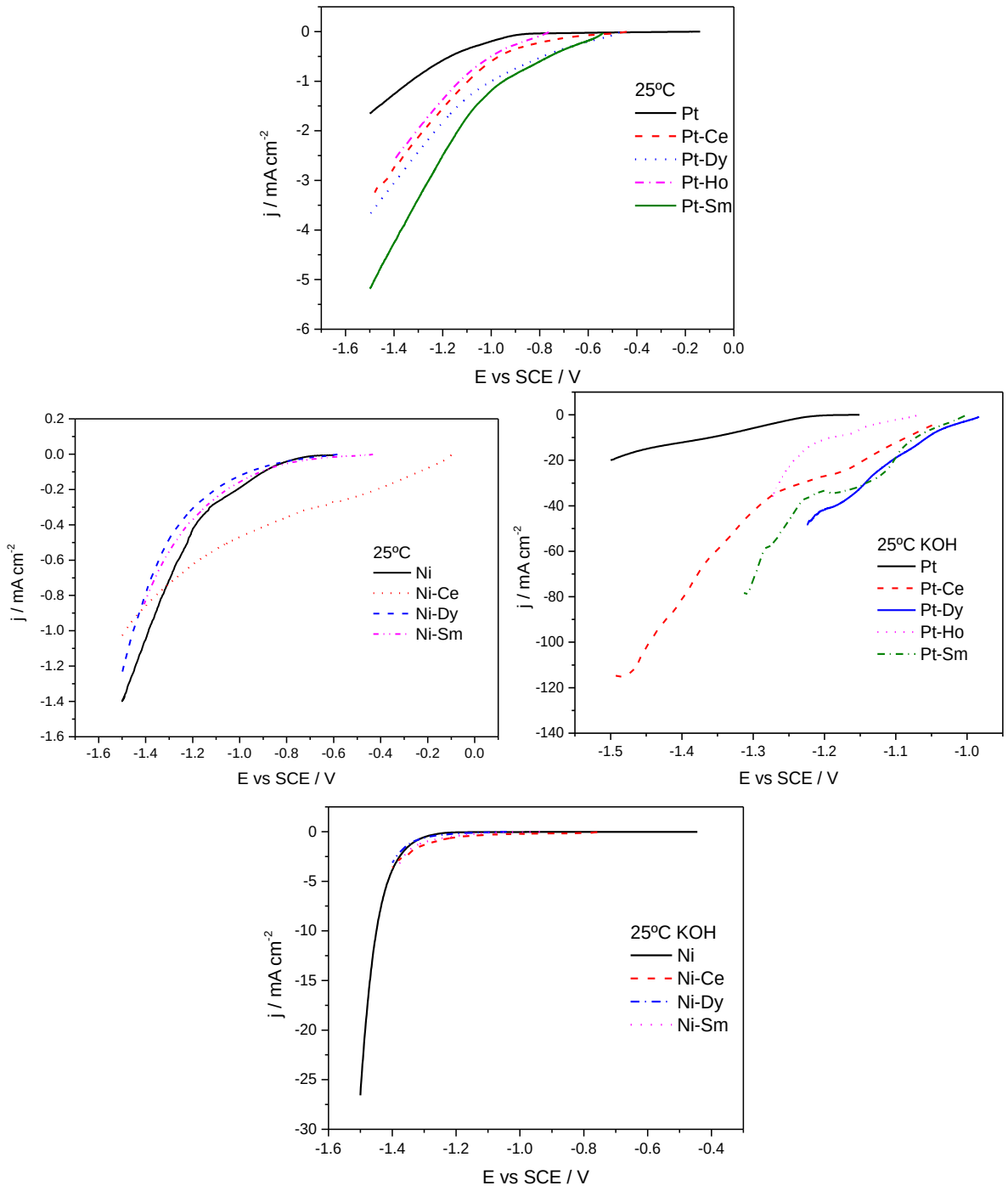

Fig. 68 - Comparison of different effluent's CV scans from different temperatures with a 0.5 mV s^{-1} rate at 25ºC.

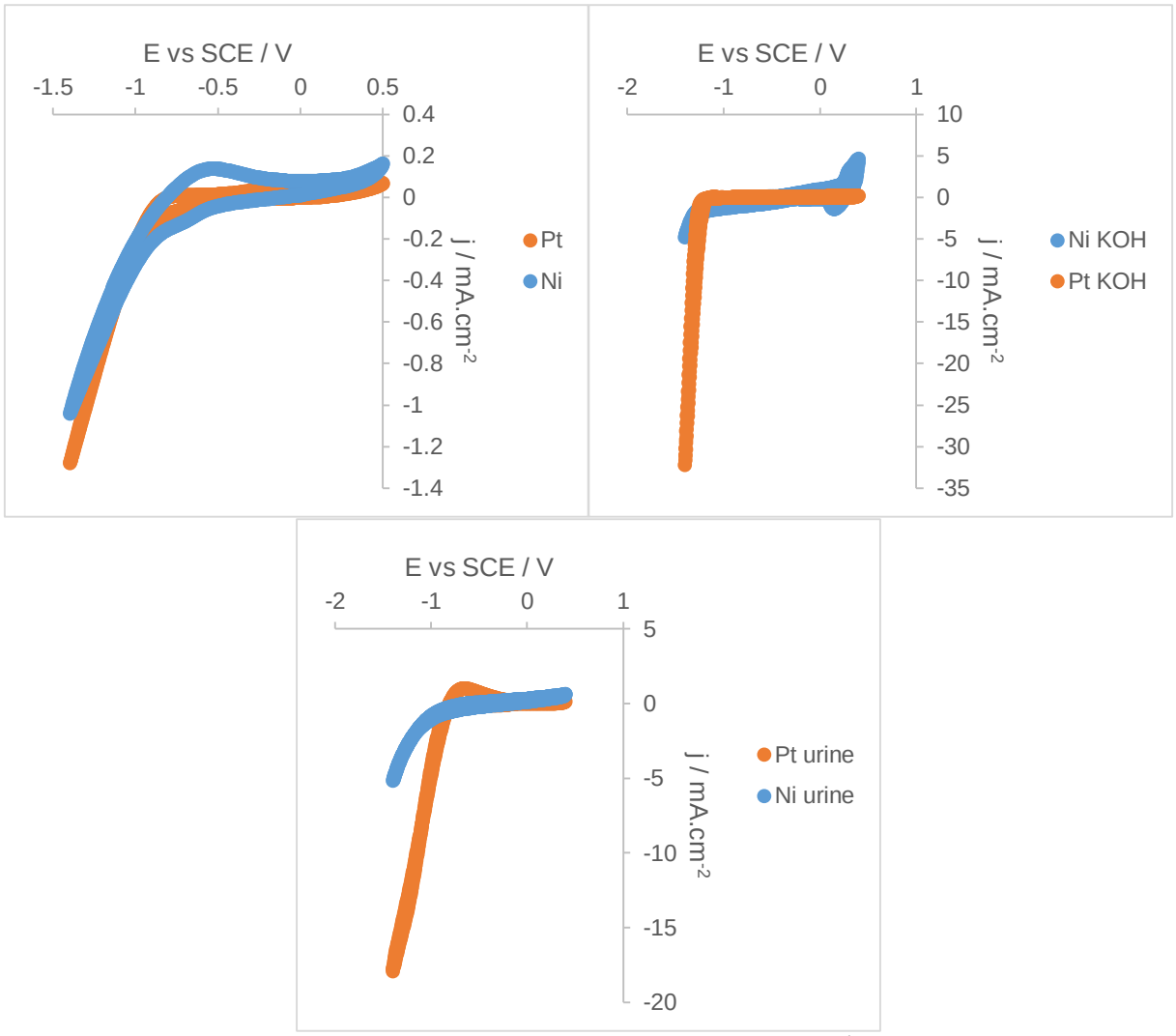

Fig. 69 - Complete CV of the effluent and synthetic urine with 50 mV s^{-1} rate at 25ºC.

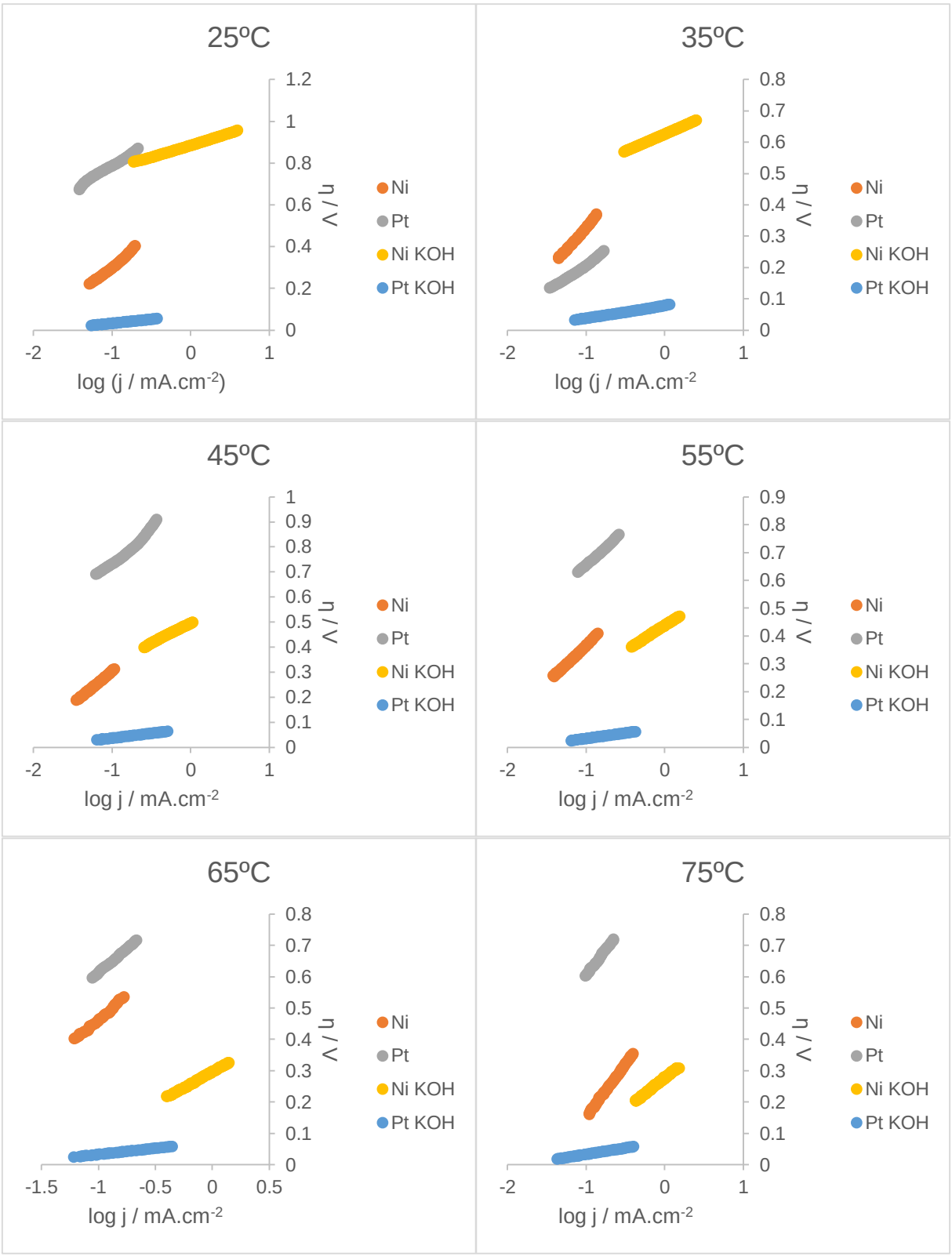

Fig. 70 - Comparison of Tafel plot.

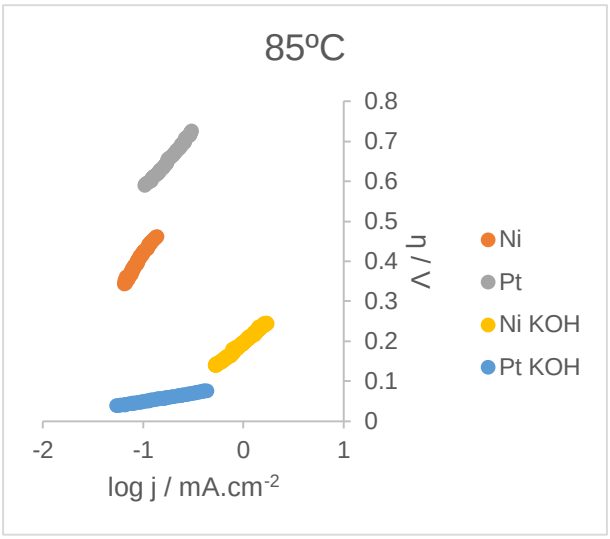

(cont.) Fig. 70 - Comparison of Tafel plot.

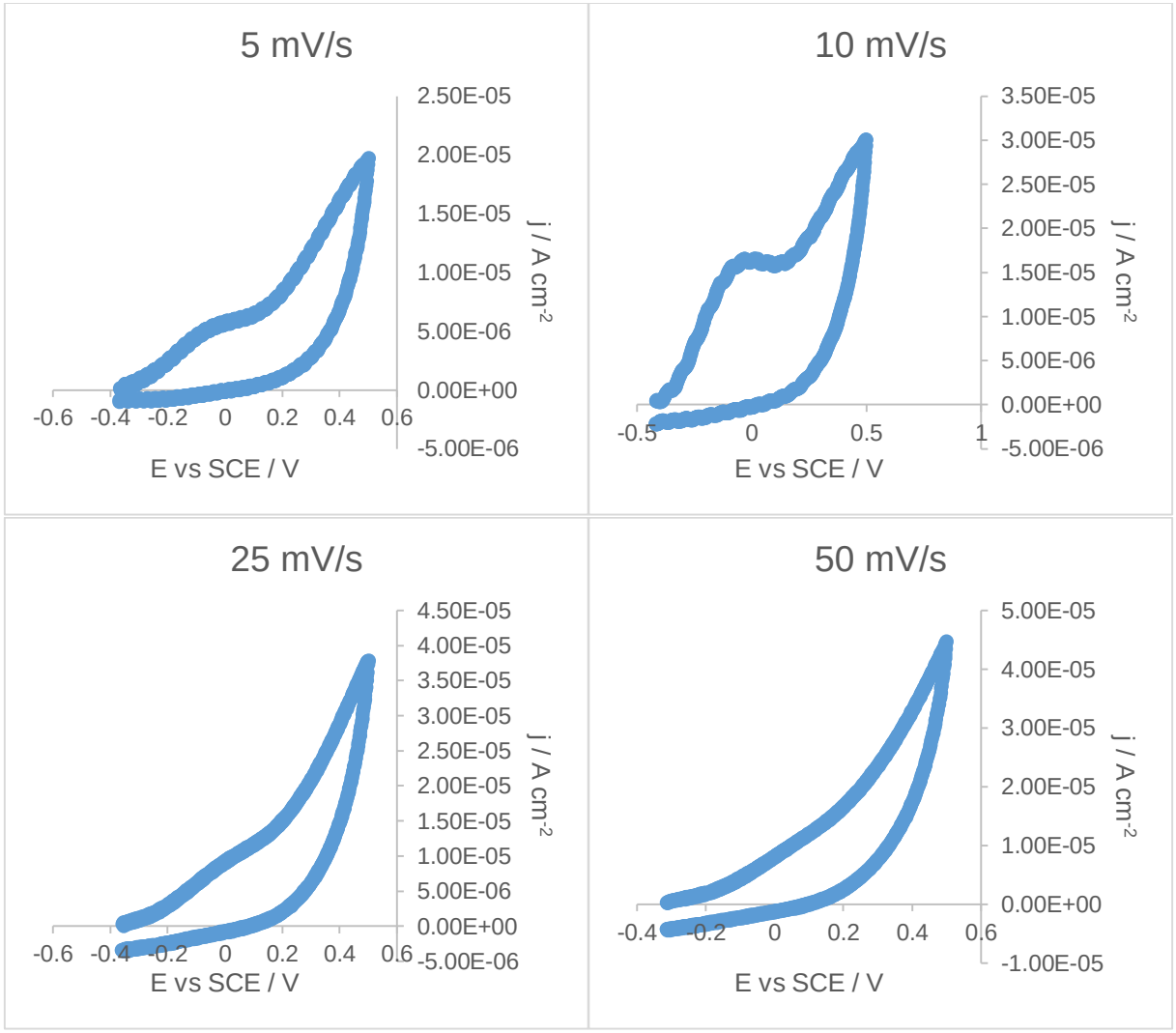

Fig. 71 - Anodic scan of the effluent at 25ºC at different rate with Pt electrode.

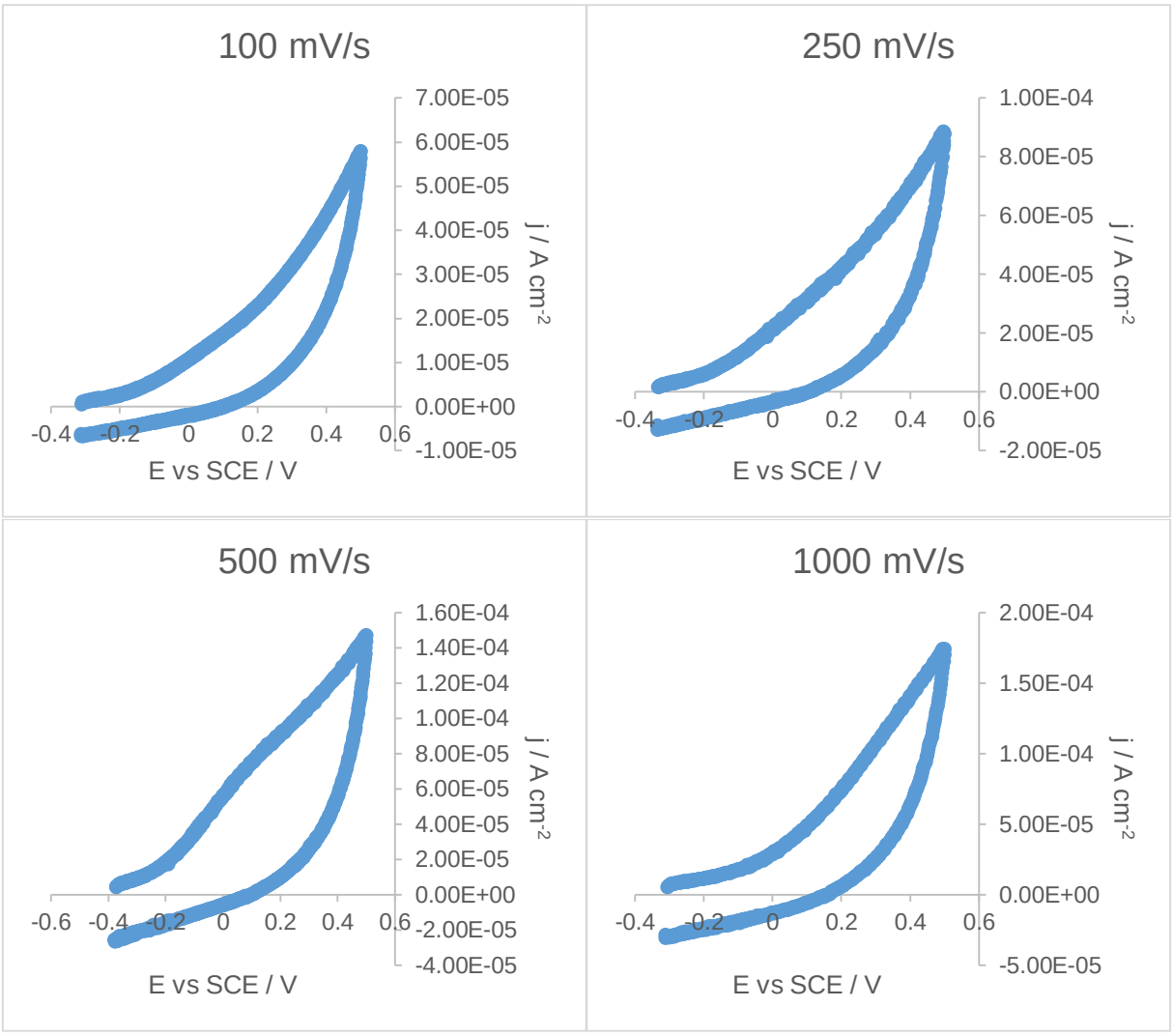

(cont.) Fig. 71 - Anodic scan of the effluent at 25ºC at different rate with Pt electrode.

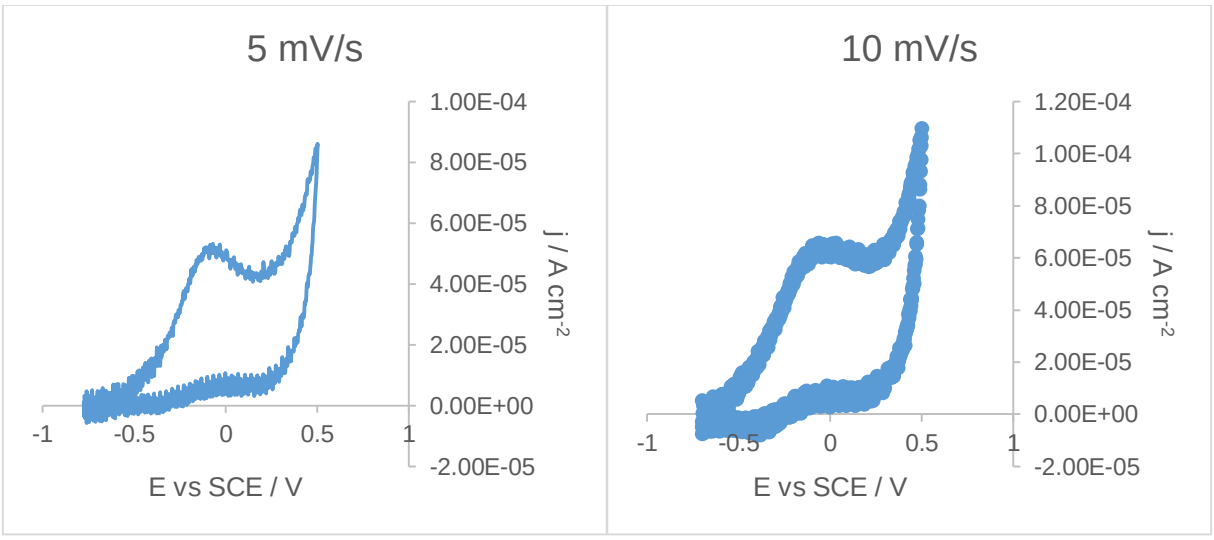

Fig. 72 - Anodic scan of the effluent with KOH at 25ºC at different rate.

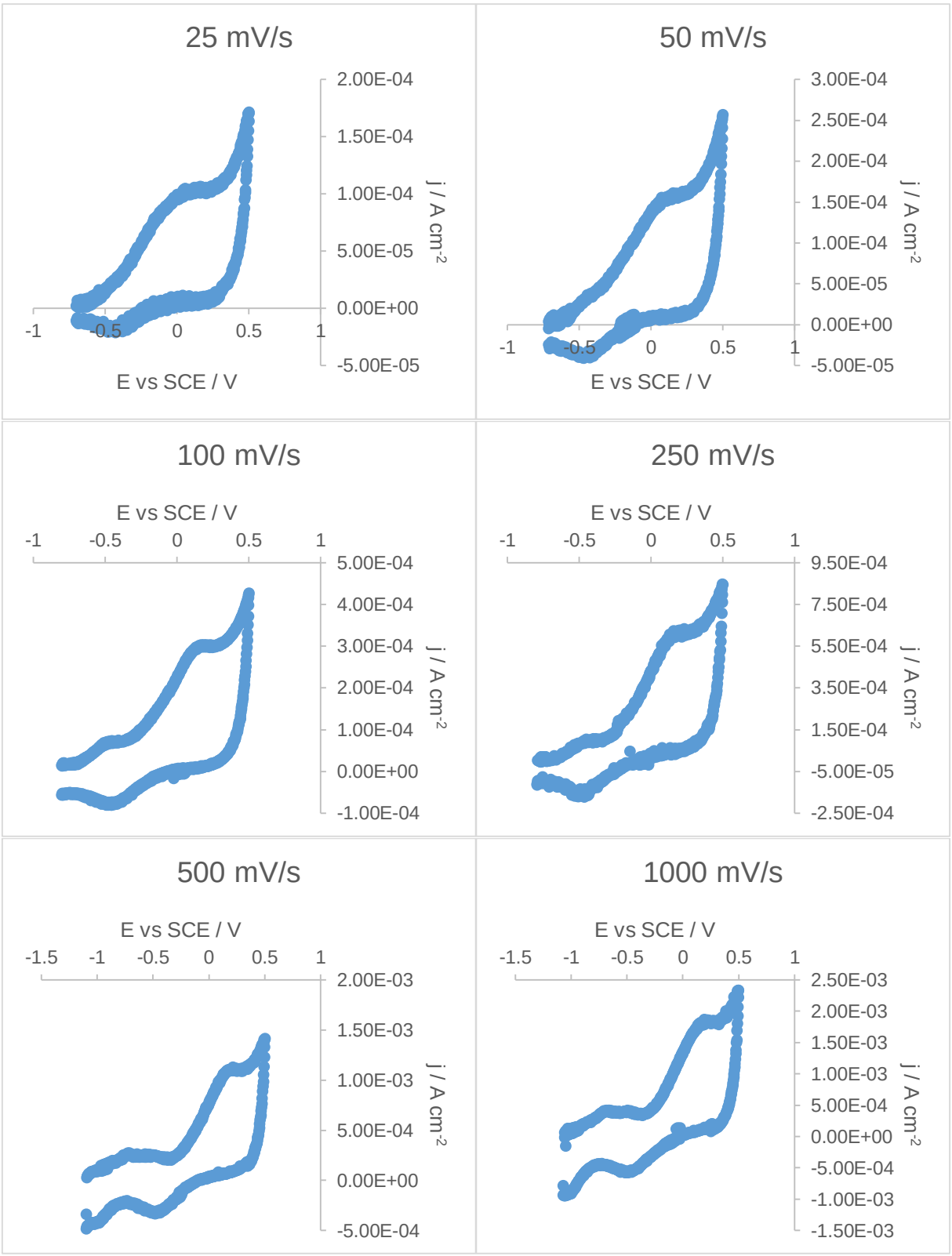

(cont.) Fig. 72 - Anodic scan of the effluent with KOH at 25ºC at different rate.

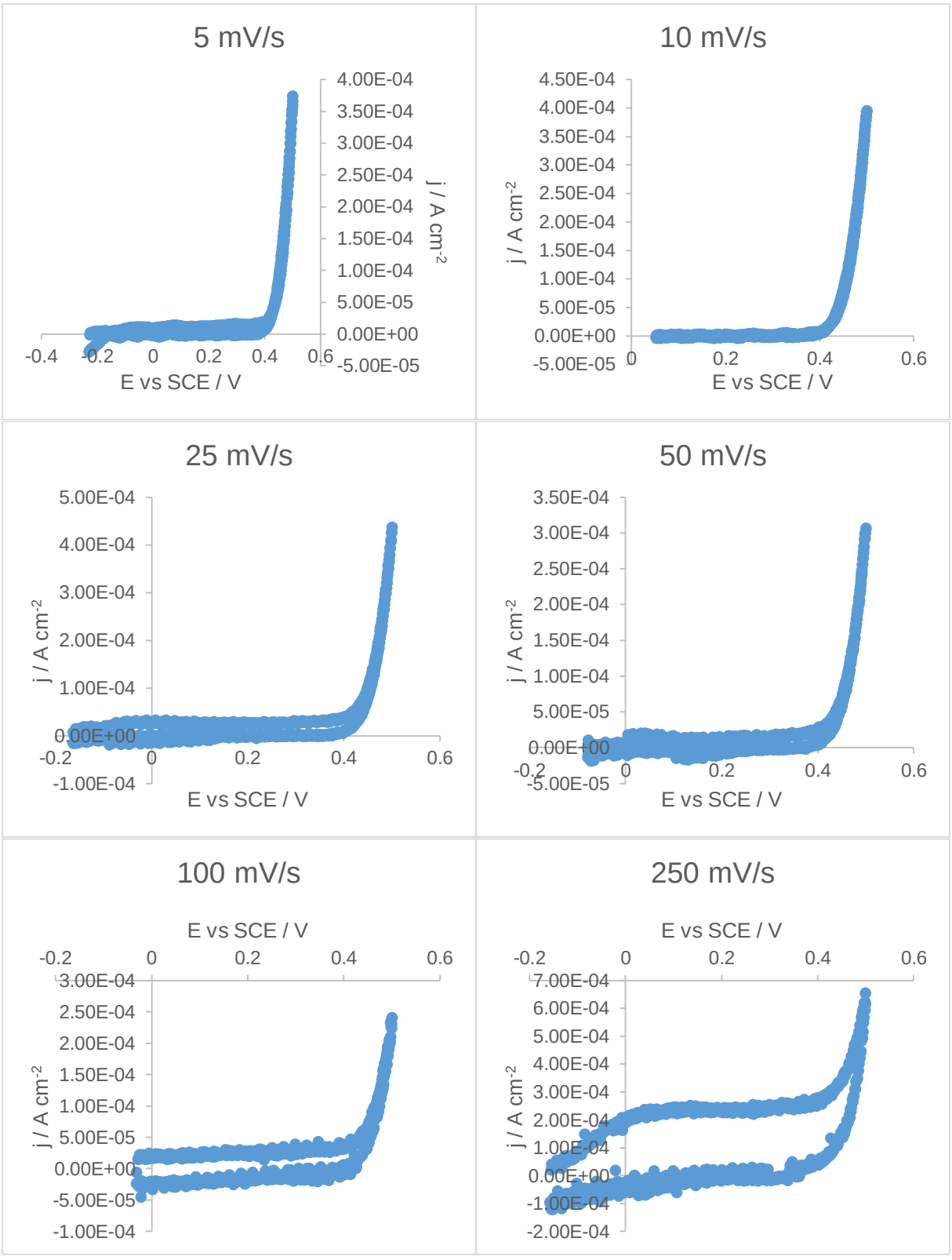

Fig. 73 - Anodic scan of the KOH solution at 25ºC at different rate with Pt electrode.

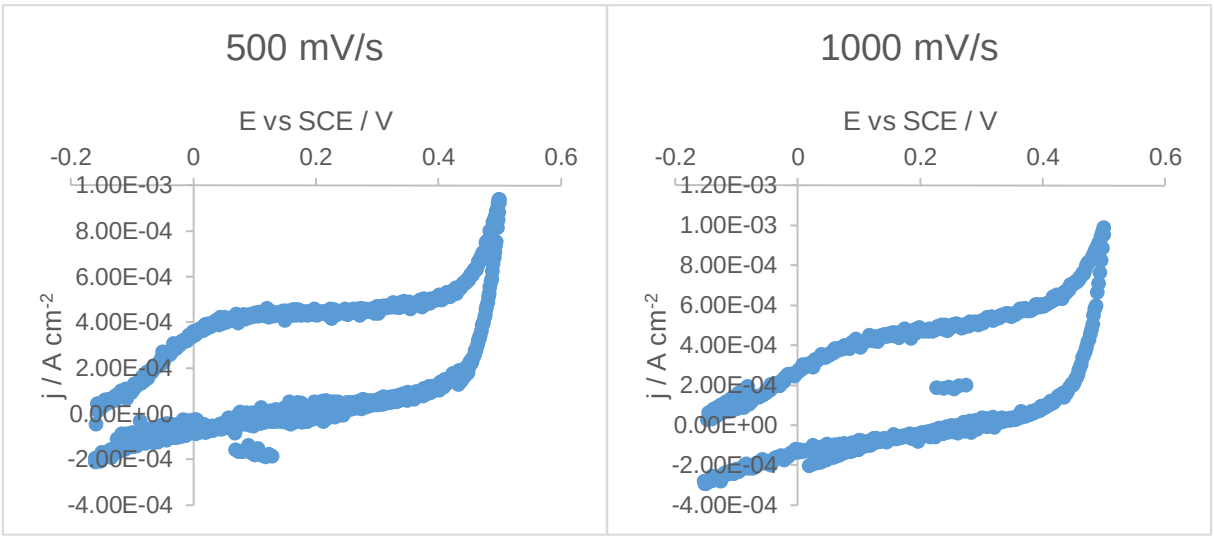

(cont.) Fig. 73 - Anodic scan of the KOH solution at 25ºC at different rate with Pt electrode.

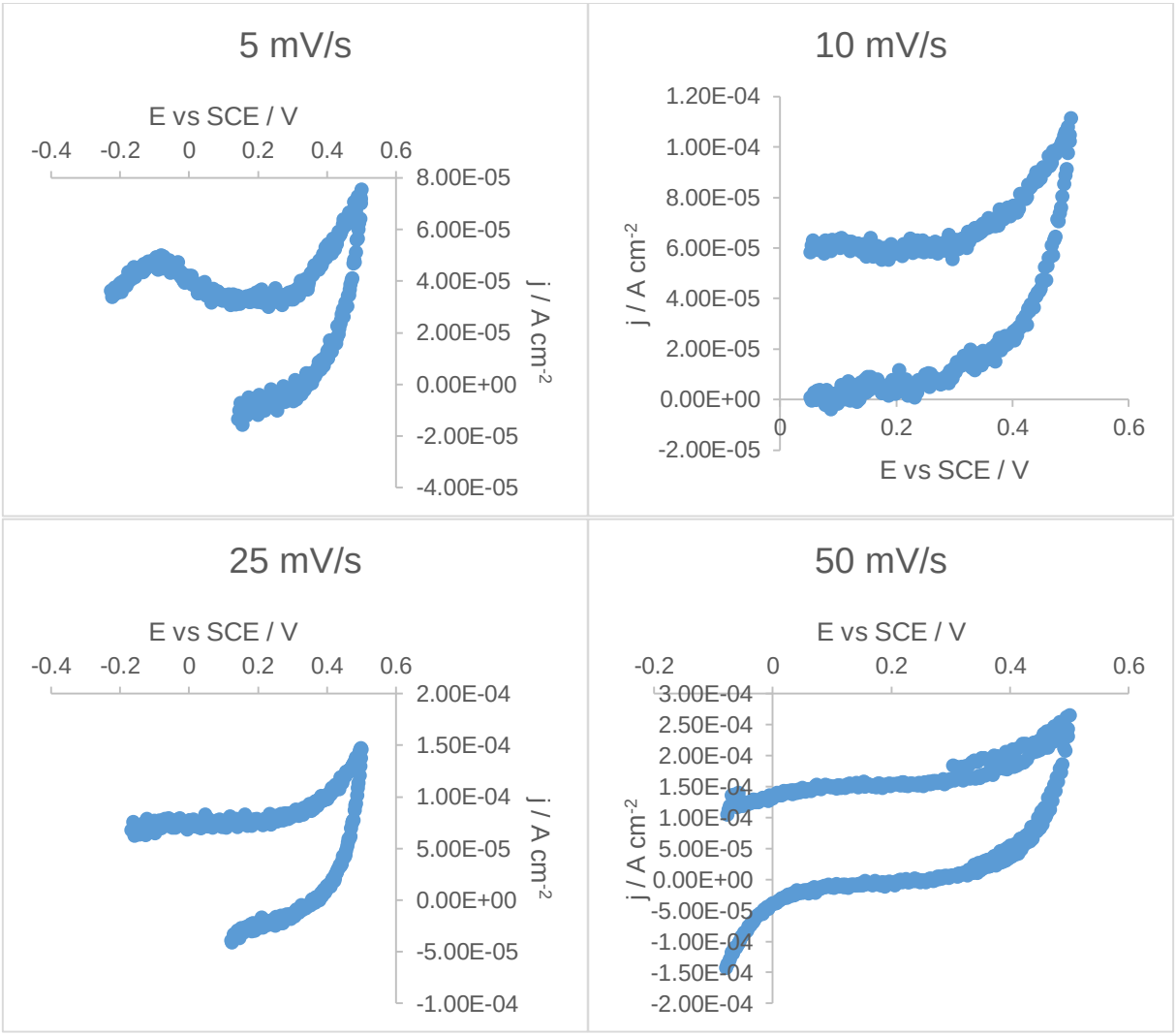

Fig. 74 - Anodic scan difference between effluent with KOH and water with KOH at 25ºC at different rate with Pt electrode.

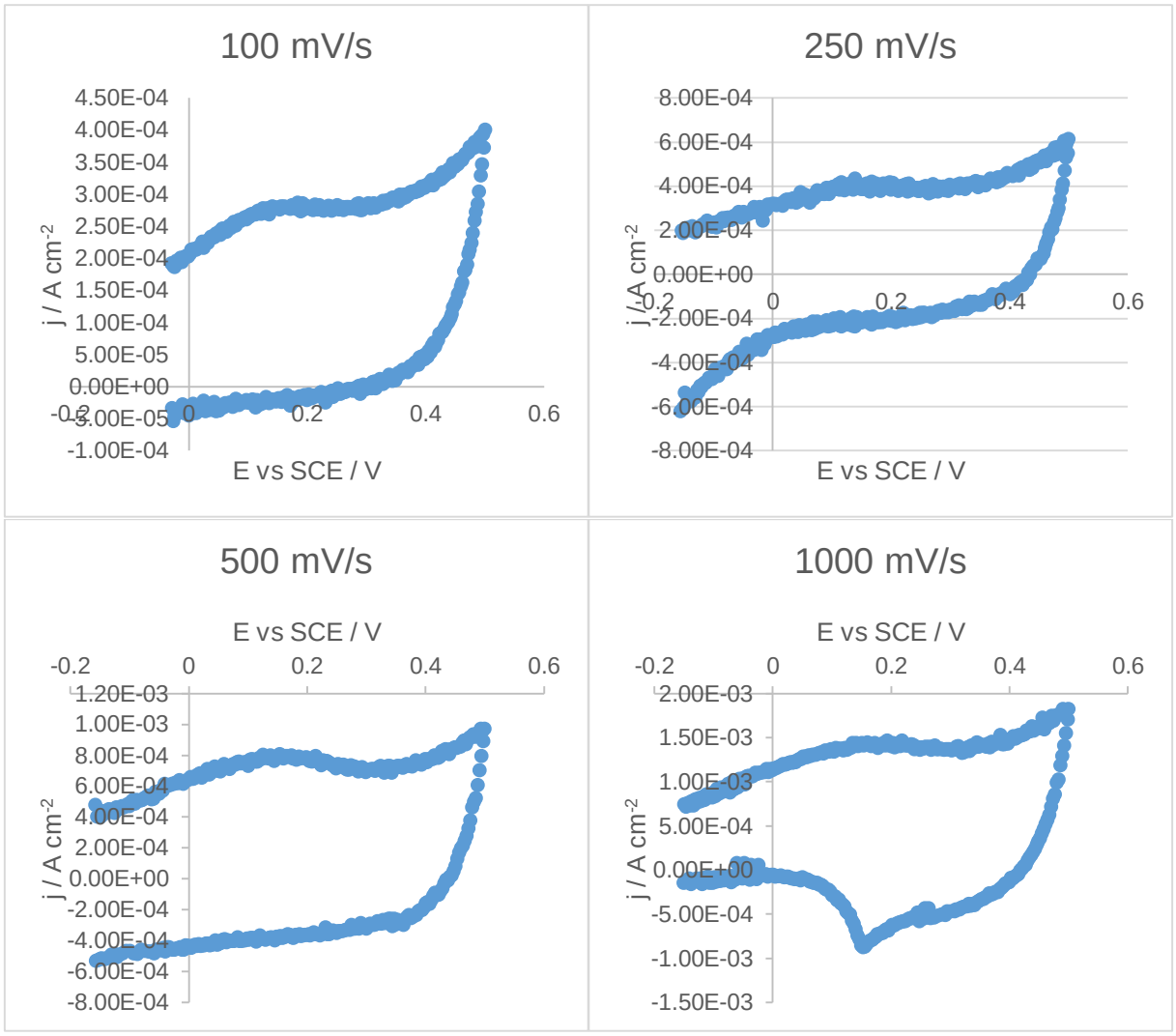

(cont.) Fig. 74 - Anodic scan difference between effluent with KOH and water with KOH at 25ºC at different rate with Pt electrode.

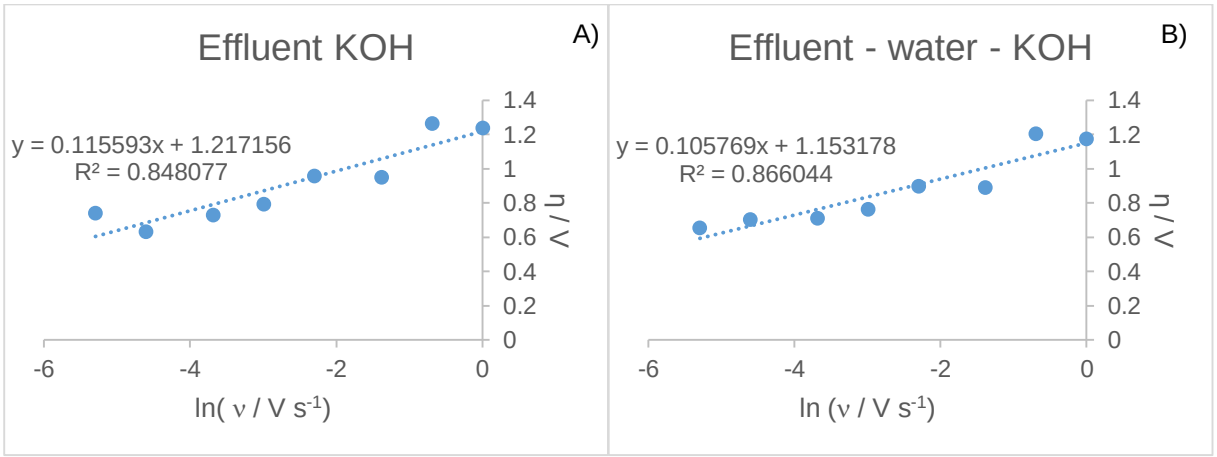

Fig. 75 - Plot of η vs ln ν from just effluent+KOH (A) and effluent+KOH subtracted with water+KOH (B) with Pt electrode